

Publication No. 02-030-056

# RECLAMATION OF PHOSPHATIC CLAY WASTE PONDS BY CAPPING

Volume 1: Centrifugal Model Evaluation of Reclamation Schemes  
for Phosphatic Waste Clay Ponds



Prepared by University of Florida, Department of Civil Engineering,  
under a grant sponsored by the  
Florida Institute of Phosphate Research  
Bartow, Florida

April 1988

**FLORIDA INSTITUTE OF PHOSPHATE RESEARCH**



The Florida Institute of Phosphate Research was created in 1978 by the Florida Legislature (Chapter 378.101, Florida Statutes) and empowered to conduct research supportive to the responsible development of the state's phosphate resources. The Institute has targeted areas of research responsibility. These are: reclamation alternatives in mining and processing, including wetlands reclamation, phosphogypsum storage areas and phosphatic clay containment areas; methods for more efficient, economical and environmentally balanced phosphate recovery and processing; disposal and utilization of phosphatic clay; and environmental effects involving the health and welfare of the people, including those effects related to radiation and water consumption.

FIPR is located in Polk County, in the heart of the central Florida phosphate district. The Institute seeks to serve as an information center on phosphate-related topics and welcomes information requests made in person, by mail, or by telephone.

## **Research Staff**

**Executive Director**  
**Richard F. McFarlin**

### **Research Directors**

G. Michael Lloyd Jr.  
Gordon D. Nifong  
David J. Robertson  
Hassan El-Shall  
Robert S. Akins

-Chemical Processing  
-Environmental Services  
-Reclamation  
-Beneficiation  
-Mining

**Florida Institute of Phosphate Research**  
**1855 West Main Street**  
**Bartow, Florida 33830**  
**(863) 534-7160**

**Reclamation of Phosphatic Clay Waste Ponds by 'Capping'**

**Volume 1: Centrifugal Model Evaluation of Reclamation Schemes for Phosphatic Waste Clay Ponds**

**Research Project: FIPR 82-02-030**

**Prepared by**

**Department of Civil Engineering  
University of Florida  
Gainesville, Florida 32611**

**IMC Bartow, Florida  
AGRICO, Milberry, Florida  
MBIL, Nichols, Florida**

**Principal Investigators**

**F. C. Townsend  
D. G. Bloomquist  
S. A. McClimans  
M. C. McVay**

**Prepared For**

**Florida Institute of Phosphate Research  
1855 West Main Street  
Bartow, Florida 33830**

**FIPR Project Manager: Dr. Henry L. Barwood**

**September 1986**

## **DISCLAIMER**

**The contents of this report are reproduced herein as received from the contractor.**

**The opinions, findings and conclusions expressed herein are not necessarily those of the Florida Institute of Phosphate Research, nor does mention of company names or products constitute endorsement by the Florida Institute of Phosphate Research.**

## **PERSPECTIVE**

**Henry L. Barwood, Ph. D.  
Hassan E. El-Shall, Dr. Eng. Sc.  
Project Managers**

**Florida Institute of Phosphate Research**

**During the phosphate beneficiation process, substantial quantities of water clays are produced which are typically disposed in large impoundment areas. Due to the low permeability and self-weight of these clays, years are required prior to reclamation. There is an increasing concern, both from the phosphate industry and the public in general, to reduce the quantity of phosphatic clays that are stored above ground and to reduce the turnaround time between mining and reclamation. Florida Institute of Phosphate Research shares in this concern. Therefore, FIPR has mobilized great research efforts to find solutions to this problem**

**Fundamental to the design of any reclamation scheme for these areas, be it for industrial, agriculture, or grazing purposes, is the realization that the waste clays must be covered or capped to provide a stable foundation. Furthermore, the application of a 6-10 ft. cap appeared to be (at the time of inception of this project) the only practical method to enhance consolidation rates and increase the final solids content to provide below ground storage. Hence, this research was dedicated to determining feasible methods for capping these waste clay ponds.**

**The research efforts included extensive laboratory investigations and a full-scale field test. Specifically, three capping schemes were evaluated (a) use of geotextiles, (b) vegetative crust for tensile reinforcement, and (c) capping without reinforcement directly on the surface crust. Laboratory evaluation consisted of centrifugal model tests of capped waste clays, permeameter tests on geotextiles and viscosity tests to measure shear strength versus solids content. Obtained data were used to verify and improve existing large strain consolidation predictive models. Results of this investigation are published in six volumes. In addition, two volumes containing detailed data and field test results are placed in an open file at FIPR's library as a reference material for interested parties. Discussion of the subject matter of these volumes is presented below:**

### **Volume I "Centrifugal Model Evaluation of Reclamation Schemes for Phosphatic Waste Clay Ponds"**

**The objective of this part of research was to evaluate reclamation schemes for minimizing the turnaround time between mining and reclamation by enhancing consolidation of these waste clays. Specifically, the schemes evaluated were: (a) no treatment, (b) s/c mix, (c) sand caps over clay, (d) s/c mix caps over clay, and (e) use of flocculating agents coupled with s/c mixes or sand caps.**

Traditionally, 1-g bench tests using graduated cylinders have been used to evaluate clay settling rates and consolidation. Unfortunately, this method is unsatisfactory as (a) the stress levels are lower than field conditions, and (b) excessive testing times are required. Offsetting these limitations is the use of centrifugal modelling techniques by which prototype stress levels are applied and testing times reduced due to shortened drainage paths. Thus, this research involved centrifugal models 8 to 12 cm high accelerated to 60 to 80 g's, thereby replicating waste ponds 4.8 m to 9.6 m deep. A closed form solution was also developed to estimate consolidation magnitudes for clay, s/c mixes, and capped (sand or s/c mix) ponds,

The results of these centrifugal model tests demonstrated that centrifugation is a viable method for examining prototype waste clay disposal schemes, provided modelling of models is used for determining the time scaling exponent, and sand segregation potential in s/c mixes is considered. It was found that the time scaling exponent was a function of the solids content and increased from 1.6 to 2.0 as the solids contents increased from 14 to 20%. Sand segregation was not a problem at 60 g's for solids contents 16%.

The descending order of disposal technique effectiveness in achieving the highest final solids content is: (a) sand capping (staged), (b) s/c mix capping, (c) s/c mix 1:1 to 2:1, (d) flocculants or untreated clay. The time required, however, is in proportion to the solids content; e.g., higher solids content require longer times.

For s/c mixes, the greatest reduction in interface height occurs for a SCR of approximately 1:1. For s/c mixes exceeding 3:1, the final interface height is above that for untreated clays. The grain size of the sand used has little effect on interface height for low (1:1) s/c mixes.

For capped ponds, a threshold solids content exists, below which the clay is incapable of supporting a cap.

Flocculants have a primary benefit of increasing setting rates and can be used to achieve rapidly clay solids contents capable of supporting sand caps. However, flocculated clays and flocculated clay/sand mixes provided final solids contents comparable to untreated clays (but at shorter times).

## Volume II "Centrifugal Modeling of the Consolidation Behavior of Phosphatic Clay Mixed with Lime or Gypsum"

This second part of the research investigates the use of lime and gypsum as additives which might enhance the consolidation of the waste clays. The research was divided into two stages. In the first stage, experimental techniques were used to determine the appropriate quantities of lime and gypsum to be added to the waste clays and assess the strength gains due to these additives. The second stage involved centrifuge modeling of the consolidation of the waste clays with the determined quantities of lime and gypsum added.

The results of this investigation reveal that the pH test provides a rapid method for determining the minimum lime content required for strength producing clay-lime reactions. Lime percentages of approximately 12% were required to achieve the pH level for the clays tested. Miniature vane shear tests showed 28-day strength gains of 3 to 5 times that of untreated clay when 12% lime was added while relatively small strength increases occurred for lower lime contents. Unfortunately, the high concentrations of lime required, and the relatively low 28-day strengths (14 to 25 psf) question the feasibility of lime treatment from the standpoints of economics or surface strength to support equipment. However, sufficient strength to support a sand cap might be feasible, but caution is advised. In the case of gypsum the pH test was unsuitable for determining the target gypsum content. Gypsum/clay ratios as high as 12:1 produced practically no strength improvement.

Centrifugal model tests revealed that addition of lime hindered the consolidation magnitude of the clays. Apparently, the lime strengthens the soil skeleton sufficiently that little self-weight consolidation occurs. Instead, the consolidation behavior of lime treated clay is akin to that of sand. In the case of gypsum addition, the consolidation magnitude was enhanced. Consolidation occurred more quickly, and final effective clay solids contents approached those of untreated clay. The behavior of clay/gypsum mixtures is similar to that for sand/clay mixes.

### Volume III "Evaluation of the Use of Geotextiles for Capping Phosphatic Waste Clays"

The basic objective of this research was to evaluate the use of geotextiles for capping phosphatic clay waste clay ponds and, thus, to enhance the consolidation process of these materials.

A system was designed and constructed for performing the permeability tests such that four geotextiles could be tested simultaneously. Waste clays at initial solids contents ranging from 17 to 19% were placed in the system and allowed to consolidate against the bottom of the geotextiles under the application of an approximate 21 inch water head difference and air pressure ranging from 3 to 4 psi, resulting in total head differences ranging from 8.6 to 10.9 feet of water. Flow rates versus time were determined for each of the geotextiles that were tested. Total heads were measured adjacent to and 1 inch below the bottom of the geotextiles for the final two test groups. The flow rate and clogging indicator (to be defined later) versus time results were plotted to provide an indication of the long-term behavior of each geotextile. Additionally, the thickness and equivalent opening size of the, geotextiles were analyzed to determine the effects on geotextile performance.

At the conclusion of each group of tests, samples of the waste clays were obtained adjacent to each geotextile to determine the final solids content. Additionally, scanning electron microphotographs (SEM S) were obtained of several of the geotextiles before and after testing in order to examine clogging within the geotextiles.

All of the above results were then utilized to compare the long term filtration/permeability characteristics for the tested geotextiles in order to develop a recommendation for selecting a geotextile for use in field testing applications. This, in turn, may lead to large-scale field use for capping phosphatic waste clay ponds.

The following conclusions were developed based on the laboratory results:

1. Nonwoven polypropylene geotextiles with a thickness in the range of 70 to 110 mils exhibited the best long-term permeability/filtration characteristics and should be selected for field testing.
2. Geotextiles manufactured of polypropylene yarns and filaments exhibited better long term flow rate/filtration characteristics than geotextiles manufactured of polyester yarns and filaments.
3. No correlations existed between geotextile EOS and stabilized flow rate or long term filtration performance under the applied laboratory conditions.
4. Some piping of clay particles across the geotextiles occurs with the slurry at an initial solids content of 17-19% until the slurry attains a solids content such that the solid particles will "bridge" the geotextile. However, this piping does not adversely affect the long term performance characteristics for the desired applications.
5. The geotextiles generally prevent significant piping of solid clay particles with the slurry at an initial solids content of 17-19%.
6. With the exception of some thin nonwoven geotextiles, all geotextiles undergo partial clogging/plugging from solid clay particles under the application of approximately 8.7 feet of water head.
7. Economics, construction procedures, and exposure to field conditions should be taken into consideration before a geotextile is utilized in the field to enhance the consolidation of phosphatic waste clay slurries.
8. It appears that the use of geotextiles for capping phosphate waste clay ponds will cause the development of a solids content profile within the clays that will be greatest adjacent to the geotextile and will decrease with depth, which may, after a period of time, prevent water from escaping and, thus, prevent the clays from consolidating further.



#### **Volume IV "Piecewise Linear Computer Modeling of Large Strain Consolidation"**

The major objectives of this study were as follows:

- A. To modify an existing piecewise linear computer program
- B. To compare spatial vs. reduced representation finite strain non-linear consolidation theory,
- C. To predict a series of model ponds to be discussed at the "Symposium on Consolidation and Disposal of Phosphatic and Other Waste Clays," Lakeland, Florida (1987).
- D. To develop a multiple layer piecewise linear large strain consolidation model.

Several consolidation computer programs based on the Gibson, England, and Hussey (GEH) theory (1969), and a piecewise linear program based on a spatial representation of finite strain, have been developed. However, GEH programs cannot model non-homogeneous profiles and the piecewise linear program has difficulty modelling initial filling conditions. Furthermore, no multiple layer large strain consolidation model, either finite strain or piecewise linear, has been developed. These drawbacks limit the applicability of computer modelling. Since piecewise linear theory is simpler than GEH theory, and allows for non-homogeneous profiles, a large strain piecewise linear program was developed which allows for any filling scheme in single layer consolidation (UF-MGS) and a method of solution for piecewise linear multiple layer consolidation model is outlined.

Results indicate that the UF-MGS model has excellent agreement with GEH theory for quiescent consolidation, quiescent consolidation with surcharge, and continuous fill. Also, the UF-MGS model agreed with a closed form solution developed for homogeneous quiescent clays.

#### **Volume V "Centrifugal Model Evaluation of the Consolidation Behavior of Phosphatic Clays and Sand/Clay Mixes"**

This part of study investigates the consolidation behavior of phosphatic clays taken from 19 sites located in central and northern Florida. Three types of centrifuge tests were run on each waste clay -- uncapped tests, capped tests, and sand/clay mix tests. Atterberg limits and x-ray diffraction tests were also conducted on the clays. The research had two main objectives. The first objective was to determine if the Atterberg limits or the mineralogy of the waste clays could be related to their settling behavior in the uncapped tests. The second objective was to examine the effects of sand caps and sand/clay mixes on the settlement characteristics of the clays.

It was found that Atterberg limits predicted the consolidation behavior of the clay fairly well. A relationship was observed between liquidity index and effective stress for the uncapped clays, while no definite trends were observed between clay mineralogy and consolidation

behavior. Both sand/clay mixes and sand caps improved the settlement characteristics of the clays. Sand/clay mixes enhanced the time rate of consolidation more than the sand caps, while the sand caps generated a higher final clay solids content than the sand/clay mixes.

**The final published volume (Volume VI) "Consolidation Properties of Phosphatic Clays from Automated Slurry Consolidometer and Centrifugal Model Tests"**

An automated slurry consolidometer, which is fully controlled by a computer-data acquisition system that monitors load, pore pressure, total stress, and deformation, was developed. The load is applied by a stepping motor. Results from the tests conducted show the effectiveness of the apparatus. The Constant Rate of Deformation test was found to have several advantages over the Controlled Hydraulic Gradient test and is recommended for future applications; the results from both tests were consistent. A "pseudo-preconsolidation" effect, attributed to the initial remolded condition of the specimen, was observed in both constitutive relationships. Thus, the curves are not unique but depend upon the initial solids content. However, different curves approach what seems to be a "virgin zone." The compressibility relationship also was found to be dependent upon the rate of deformation.

The technique using centrifugal modelling is based on the measurement of pore pressure and void ratio profiles with time, and the use of a material representation of the specimen. The compressibility relationship obtained was in good agreement with the results of CRD tests performed at a slow rate of deformation. The permeability relationship plotted parallel to the CRD curves, however, permeability values were approximately a half order of magnitude higher. Further research is required to explain this difference.

The constitutive relationships obtained in the study were used to predict the behavior of hypothetical ponds modelled in the centrifuge. A good agreement between centrifugal and numerical models was found.

Data obtained in the field are tabulated in Volume 7 which will be placed in an open file at FIPR's library. However, it should be mentioned that these tests were not conclusive due to several technical and practical problems encountered during such tests.

At the end of each volume, the authors have listed several recommendations for further research. Most of these recommendations, however, are related to further modifications in test procedures or equipment to obtain more accurate data. Nothing is recommended regarding future and practical aspects of capping techniques of phosphatic clays. Nevertheless, the results of this research are informative regarding the use of centrifugal and computer modeling of the consolidation behavior of phosphatic clays.

## **ACKNOWLEDGEMENTS**

**The support and sponsorship provided by the Florida Institute of Phosphate Research for this investigation is acknowledged. The support of IMC, Bartow, and Dr. J. E. Lawver for the preliminary sand capping models is greatly appreciated. The co-operation and assistance for the project is acknowledged for:**

**Dr. J. E. Lawver, IMC**

**Mr. Steve I. Olson, Agrico**

**Mr. H. H. Miller, Agrico**

**Mr. A. J. Propp, Mbil**

**Portions of this report reflect the Ph.D dissertation of Dr. David Bloomquist and M.S. report of Mr. Stuart A. McClimans; Department of Civil Engineering, University of Florida, Gainesville, Florida 32611.**

## TABLE OF CONTENTS

List of Figures.....	xi
List of Tables.....	xiv
Abstract.....	xv
Chapter 1: Introduction, Objectives and Scope.....	1
Introduction.....	1
Objectives and Scope.....	1
Chapter 2: Literature Review.....	7
Florida Statutes.....	7
Flocculating Agents.....	7
S/C Mix.....	9
Capping.....	14
Centrifugal Modelling Considerations.....	15
Chapter 3: Equipment, Procedures, and Materials.....	39
University of Florida Geotechnical Centrifuge.....	39
Centrifuge Specifications.....	39
Data Acquisition.....	39
The Camera.....	44
Model Container.....	44
Instrumentation.....	47
Testing Procedures.....	50
Materials.....	55
Chapter 4: Presentation and Discussion of Results.....	57
Introduction.....	57
Time Scaling Relationships.....	57
S/C Mix Evaluation.....	64
Consolidation Enhancement by Capping with Sand.....	84
Consolidation Enhancement by Capping with S/C Mix.....	99
Flocculant Treatment of Noralyn Clay.....	127
Chapter 5 Conclusions.....	137
References.....	139
Appendix A: Derivation of Height vs Solids Content.....	A-1
Appendix B: Derivation of S/C Mix and S/C Mix Cap Relationships.....	B-1
Appendix C: Derivation of Unit Weights for Waste Clays and S/C Mixes.....	C-1

## LIST OF FIGURES

1. Relationship between Permeability and Quality of Bentonite Added to SB Backfill (From D'Appolinia, 1980).....	11
2. Stress Similitude in a Centrifuge Model.....	18
3. Plan Views of Rotating Sample.....	25
4. Forces Acting on a Fluid During Centrifugation.....	28
5. Geometric Parameters Used in Model Analysis.....	30
6. Bucket Under Rotation Because of Pivot Friction.....	32
7. Bucket Configurations for Orientation Adjustment.....	34
8. Centrifuge Linear Acceleration Versus Time Start-Up.....	36
9. Schematic of Centrifuge and Camera Set-Up.....	40
10. Calculation of Offset Acceleration for a 10.5 cm Sample.....	49
11. Flow Diagram of Testing Sequence.....	51
12. Example of Photographic Monitoring.....	54
13. Modelling of Models Program Performed on Kingsford Clay.....	60
14. Time Scaling Acceleration Exponent, Computed from Modelling of Models Program Results.....	61
15. Modelling of Models Analysis Performed on Kingsford Waste Clay.....	62
16. Comparison of Centrifuge Model and IMC Tank Test.....	65
17. Grainsize Distribution for Sand Used in Sand/Clay Mix Modelling of Models and Initial Capping Tests.....	68
18. Modelling of Models Analysis Performed on 6:1 Sand/Clay Mix (Effective Clay Solids Content).....	69
19. Time Scaling Exponent Computed from Modelling of Models Analysis, 6:1 Sand/Clay Mix (Effective Clay Solids Content).....	71
20. Prototype Interface vs Model Time for Test Series KC80-0/6 (1:1 and 6:1 Sand/Clay Mix, 40-100 Sand) and KC80-6/0.....	72

21. Percent Reduction in Height $\left(\frac{H_0 - H_F}{H_0} \times 100\right)$ vs Sand/Clays Ratio for Test Series KC80-6/0 and KC80-0/6.....	74
22. Clay Solids Content vs Shear Strength Based on Plastic Viscosity.....	77
23. Maximum Particle Diameter vs Clay Solids Content for both the Cardwell and Weiss Equations (Acceleration = 1g).....	78
24. Maximum Particle Diameter vs Clay Solids Content for both the Cardwell and Weiss Equations (Acceleration = 80g).....	79
25. Acceleration Level vs Maximum Particle Diameter for Both the Cardwell and Weiss Equations.....	80
26. Prototype Interface vs Model Time for Test Series KC80-0/6 (1:1 Sand/Clay Mix).....	81
27. Prototype Interface vs Model Time for the Test Series KC80-0/6 (6:1 Sand/Clay Ratio Mix).....	82
28. Profiles of Total Solids Contents and Sand/Clay Ratios With Depth for the Test Series KC80-0/6 (1:1 Sand/Clay Mix).....	85
29. Profiles of Total Solids Contents and Sand/Clay Ratio with Depth for the Test Series KC80-6/10 (6:1 Sand/Clay Mix).....	86
30. Plot of Solids Content Versus Elapsed Time of Centrifuge Capping Test.....	89
31. Comparison of Three Centrifuge Tests - Capped Versus No Cap.....	90
32. Effect of Capping on the Final Solids Content of Kingsford Waste Clays.....	92
33. Effect of Stage Sand Capping on Final Clay Solids Content.....	93
34. Summary of Bearing Capacity vs Solids Content /or Kingsford Waste Clays.....	98
35. Prototype Interface vs Model Time for the Test Series KC80-6/4.5 (3:1 and 6:1 sand/clay cap) and KC80-10.5/0.....	101
36. Profiles of Total Solids Content and sand/clay ratios with Depth, Test Series KC80-6/4.5 (3:1 and 6:1 sand/clay caps).....	103
37. Prototype Interface vs Model Time for the Test Series KC80-0/10.5 (3:1 and 6:1 sand clay mix) and KC80-10.5/0.....	104

38. Profiles of Total Solids Contents and Sand/Clay Ratio With Depth for the Test Series KC80-0/10.5 (3:1 and 6:1 Sand/Clay Mixes).....	105
39. Prototype Interface vs Model Time for the Test Series KC80-6/4.5 (6:1 Sand/Clay Cap Over Remixed Clay at 25.1% Solids) and KC80-6.6/4.0 (6:1 Sand/Clay Cap Over Undisturbed Clay at 24.0% Solids).....	106
40. Profiles of Total Solids Content and Sand/Clay Ratio With Depth for Test Series KC80-6/4.5 and KC80-6.6/4.0.....	108
41. Grain Size Distribution for Phosphate Sand Tailings.....	110
42. Prototype Interface vs Model Time for 4 cm Cap, Test Series KC80-7.5/4.0.....	112
43. Prototype Interface vs Model Time for 2cm Cap, Test Series KC7.5/4.0 + 2.0.....	113
44. Profiles of Effective Clay and Total Solids Contents With Depth, Test Series KC80-7.5/4.0 + 2.0.....	116
45. Profiles of Sand/Clay Ratios With Depth for KC80-7.5/4.0 Series (1:1, 3:1, and 6:1 Sand/Clay Caps).....	117
46. Prototype Interface vs. Model Time for KC80-7.5/4.0 and KC80-7.5/2.0 + 2.0.....	119
47. Comparison of Effective Stress Profiles for S/C Mix vs Capped 10 ft. Deep Waste Pond .....	123
48. Effect of Dosage on Sedimentation/Consolidation for Noralyn Clay.....	130
49. Average Solids Content Versus Time for Several Flocculated Specimens.....	132
50. Effect of Flocculant on Sedimentation/Consolidation for Noralyn Clay.....	133
51. Results of Flocculants Plus Sand Cap Treatment.....	135
52. Results of Flocculant Plus Sand Mix.....	136

## LIST OF TABLES

1. Potential Dewatering Methods (Bromwell et.al., 1977).....	3
2. Examples From Florida Statutes, Chapter 17 Pertaining to Waste Clay Reclamation.....	8
3. Properties of Noralyn and Kingsford Clays.....	56
4. Summary of Time Scaling Relationship Centrifugal Model Tests of Kingsford Clay.....	59
5. Summary of Sand/Clay Mix Centrifugal Model Tests.....	67
6. Summary of Sand Capped Centrifugal Model Tests On Kingsford Clay.....	87
7. Summary of Bearing Capacity Failures of Capped Models.....	97
8. Summary of Sand/Clay Cap Centrifugal Model Tests.....	100
9. Comparisons of SCR Effects in S/C Caps.....	114
10. Effective Stress Profiles for S/C Mix vs Capped 10 ft. Waste Pond.....	123
11. Comparison of Consolidation Magnitudes for S/C Mix and Capped Waste Ponds.....	126
12. Evaluation of Flocculants by Centrifugal Models.....	128
13. Approximate Optimum Dosages for Reagents Tested.....	129



## **Reclamation of Phosphatic Clay Waste Ponds by 'Capping'**

### **Volume 1: Centrifugal Model Evaluation of Reclamation Schemes for Phosphatic Waste Clay Ponds**

**Research Project FIPR 82-02-030**

#### **Abstract**

**During the phosphate beneficiation process, substantial quantities of waste clays are produced which are typically disposed in large impoundment areas. Due to the low permeability and self-weight of these clays, years are required prior to reclamation. Accordingly, the objective of this research was to evaluate reclamation schemes for minimizing the turnaround time between mining and reclamation by enhancing consolidation of these waste clays. Specifically, the schemes evaluated were: (a) no treatment, (b) sand/clay mix (s/c) (c) sand caps over clay, (d) sand/clay mix (s/c) caps over clay, and (e) use of flocculating agents coupled with s/c mixes or sand caps.**

**Traditionally, bench tests using graduated cylinders have been used to evaluate clay settling rates and final solids contents. Unfortunately, this method is unsatisfactory as (a) the stress levels are lower than field conditions, and (b) excessive testing times are required. Consolidation testing has been used to obtain input parameters for calculating settlement rates and magnitudes, but this also suffers from lengthy test times and theory limitations. Offsetting these limitations is the use of centrifugal modelling techniques by which prototype stress levels are applied and testing times reduced due to shortened drainage paths. Thus this research involved centrifugal**

models 8 to 12 cm high accelerated to 60 to 80 g's, thereby replicating waste ponds 4.8 m to 9.6 m deep. A closed form solution was also developed to estimate consolidation magnitudes for clay, s/c mixes, and capped (sand or s/c mix) ponds.

The results of these centrifugal model tests demonstrated that centrifugation is a viable method for examining prototype waste clay disposal schemes, provided modelling of models is used for determining the time scaling exponent, and sand segregation potential in s/c mixes is considered. It was found that the time scaling exponent was a function of the solids content and increased from 1.6 to 2.0 as the solids contents increased from 14 to 20%. Sand segregation was not a problem at 60 g's for solids contents > 16%.

The descending order of disposal technique effectiveness in achieving the highest final solids content is: (a) sand capping (staged), (b) s/c mix capping, (c) s/c mix 1:1 to 2:1, (d) flocculants or untreated clay. The time required, however, is in proportion to the solids content; e.g., higher solids contents require longer times.

For s/c mixes, the greatest reduction in interface height occurs for a Sand:Clay Ratio (SCR) of approximately 1:1. For s/c mixes exceeding 3:1, the final interface height is above that for untreated clays. The grain size of the sand used has little effect on interface height for low (1:1) s/c mixes.

For capped ponds, a threshold solids content exists, below which the clay is incapable of supporting a cap.

**Flocculants have a primary benefit of increasing setting rates and can be used to achieve rapidly clay solids contents capable of supporting sand caps. However, flocculated clays and flocculated clay/sand mixes provided final solids contents comparable to untreated clays (but at shorter times).**

## **CHAPTER I: INTRODUCTION, OBJECTIVES AND SCOPE**

### **INTRODUCTION**

**Phosphate has neither substitute nor replacement and hence, is used extensively by the fertilizer industry. Unfortunately, during the phosphate beneficiation process, several types of waste material are produced, specifically waste clays and sand tailings. It is the adequate disposal of these waste clays, that are one of the industry's most pressing problems.**

### **Waste Clay Disposal**

**At present, the only economically feasible method of disposal has been the retention of the waste clays in large impoundment areas surrounded by earthen dikes. When introduced into these impoundment areas, the waste clays are in a form of slurry with a solids content of only three to six percent by weight. Due to the very low permeability and self-weight of this material, it may take tens of years to reach a solids content of 20-25 percent. Because of this low solids content, the volume of the slurried waste clay far exceeds the volume of phosphate, sand, and clay originally removed from the mined area. As a result, large above-ground impoundment areas are required.**

**When considering the waste clay disposal problem, a handful of relevant facts should be kept in mind. These include:**

- 40 million tons (dry weight) of clay are produced per year in Florida**
- For each ton of clay solid produced, four to five tons of interstitial water remains permanently entrapped**

- More than 50,000 acres of settling areas are now in existence with 4,000 acres added every year
- More than 300 miles of earth dams with heights up to 40 feet are surrounding the settling areas
- 12-15 percent of the available phosphate remains in the waste slurry
- All mined lands must now be reclaimed according to Florida Statutes Chapter 16 and DNR Regulations

Considerable research has been directed toward minimizing the above-ground storage areas. Generally speaking, if the average clay solids content could be increased to approximately 30 percent then the waste clay would occupy a volume equal to the ore mined. Mined areas could then be fully reclaimed and above-ground storage could be minimized.

A wide variety of dewatering methods have been proposed since the mid-1970's (see Table 1). Preliminary investigations of these methods indicate several economically viable methods for increasing the solids content of waste clays. These are:

- (1) chemical flocculation of clay slimes
- (2) desiccated surface crusts
- (3) addition of sand tailings (through either sand caps, sand/clay caps, or sand/clay mixes)

While chemical flocculation can be studied in the laboratory using graduated cylinders, no laboratory method exists for evaluating desiccated crusts or addition of sand tailing to clays.

**Table 1:**

**Potential Dewatering Methods (Bromwell et.al., 1977)**

<b>ADMIXING WITH COARSE MATERIAL</b>	<b>EVAPO- TRANSPIRATION</b>
<b>ADSORPTION</b>	<b>FILTRATION</b>
<b>BIOLOGICAL AGGREGATION</b>	<b>FLOCCULATION</b>
<b>CENTRIFUGATION</b>	<b>FREEZE- THAW</b>
<b>CHEMICAL COAGULATION</b>	<b>HEAT</b>
<b>CHEMICAL SOLIDIFICATION</b>	<b>MAGNETIC SEPARATION</b>
<b>DEEP- WELL INJECTION</b>	<b>MECHANICAL THICKENERS</b>
<b>DRAINAGE SYSTEMS</b>	<b>RADIOACTIVE IRRADIATION</b>
<b>DYNAMIC VIBRATION</b>	<b>REVERSE OSMOSIS</b>
<b>ELECTRIC FIELD</b>	<b>SPHERICAL AGGLOMERATION</b>
<b>ELECTROOSMOSIS</b>	

## Stress Levels

Consolidation is defined as the time dependent settlement of a soil mass due to the squeezing out of water under an excess pore water pressure gradient. In most cases, the driving force causing consolidation is a surcharge applied to the soil e.g., a structure foundation. In the phosphatic clay retention pond, since a surcharge is not normally applied, it is the self-weight body forces of the clay particles which generate the excess pore pressures. With a 50 foot high dam, even though the solids concentration is low, there is sufficient material to induce appreciable self-weight consolidation.

In a typical laboratory bench test, however, this is not the case. For example, a 1,500 ml container filled with a 4% solids content slurry contains approximately 60 grams of clay. After some time the solids content will approach 15%. This translates into an effective stress of 12 psf at the bottom of the container. Clearly, this does not approach the magnitude of stress levels encountered in a field environment, and is not sufficient to induce any significant consolidation.

## Time

The second factor involves the substantial time required to complete primary consolidation. Several researchers have used large pipe columns to simulate field stress (e.g., Martin et. al., 1977) While the boundary conditions approach those of actual slime ponds, in some cases, the maximum duration of the tests were only 69 days. In terms of consolidation, this is not a sufficient time to allow complete primary settlement to occur.

**Offsetting these limitations is the application of centrifugal modelling techniques in which a 1/Nth scale model is constructed using identical materials and geometry. Stress similitude is accomplished by increasing the gravitational unit weight N times via centrifugal acceleration.**

#### **OBJECTIVE AND SCOPE**

**From the preceding considerations, the research objectives of this study were to evaluate various reclamation schemes to enhance consolidation rates and magnitudes and thus reclamation efforts. Specifically, the use of (a) flocculants, (b) sand/clay mixes, and (c) capping as waste clay pond treatments were investigated.**

**These objectives were investigated using centrifugal modelling techniques as applied to various reclamation schemes using waste clay from IMC's Kingsford mine.**



## **CHAPTER II LITERATURE REVIEW**

### **FLORIDA STATUTES**

**Table 2 presents excerpts from Chapter 16C-16 Mine Reclamation pertaining to waste clay reclamation. As stated (Para. 9-a-2) avoidance of long-term existence of above ground disposal areas is recommended, which suggests consolidating the clays to solids contents greater than 30-40%. Paragraph 9-b-1 suggests using the sand tailings for accelerating the thickening (i.e., consolidation) or mixing the sand with the clays. Paragraphs 12-b-1 and 13-a suggest using a sand/clay mix and/or innovative techniques which will hasten reclamation. Accordingly, Florida legislature has acknowledged waste clay reclamation and mandated the use of innovative techniques, It is the evaluation of some of these potential reclamation techniques, that is the subject of this report.**

### **FLOCCULATING AGENTS**

**Since initial USBM flocculating agent studies on phosphatic clays in 1972, literally hundreds of flocculating agents have been screened and tested. The concept being that by adding chemical agents to the clays, flocculation and rapid settlement are promoted, thereby increasing solids contents. Flocculation costs and the residual effects on future beneficiation has greatly reduced the number of viable flocculants. Onoda (1977) examined the settling characteristics on waste montmorillonitic clays treated with organic and inorganic flocculants and concluded the most effective reagents were: non-ionic polyacrylamide (PAM), followed by cationic and anionic PAMs. Smalley**

**Table 2 Excerpts From Florida Statutes Chapter 17  
Pertaining to Waste Clay Reclamation**

(9) Waste Storage.

(a) Clay wastes.

1. Retention areas shall be reclaimed as expeditiously as possible. Experimental methods which speed reclamation which are consistent with these rules are encouraged.

2. To the greatest extent practical, all waste clays shall be disposed of below grade, in a manner that avoids the long-term existence of elevated clay disposal areas. The Board may grant exceptions to this general requirement if it determines that such exceptions are in the public interest.

3. Above ground retention areas shall be reclaimed in a manner so that long-term stabilization of retention dikes and dams is assured.

4. Where appropriate to the land use in the general area and the restoration of surface drainage patterns, reclamation of retention areas as wetlands is encouraged.

(b) Sand tailings.

1. Sand tailings should not be permanently spoiled above natural grade unless needed to meet regulatory or environmental requirements.

2. The operator shall give highest priority to the use of sand tailings for backfilling mine cuts, for accelerating the thickening of waste clays, or as a soil enhancement by mixing the sand with the surface clays on clay storage areas. Sand tailings may be used in the construction of dams or other construction uses.

(c) Subsection (9) does not apply to the temporary storage awaiting sale of clay or sand which is the ore material being mined.

(12) Timetable.

(a) Each operator shall develop a timetable for completion of the reclamation process in the area covered by the application. The timetable shall include:

1. When removal of ore in the area will be completed.

2. A schedule for the completion of any other mining operations in the area.

3. When the reclamation process will be initiated.

4. When the grading and contouring will be started and when completed.

5. When revegetation will be started and completed.

6. When the growing season requirement will be met.

(b) Completion date.

1. Reclamation and restoration shall be completed within two (2) years of the completion of mining operations, exclusive of the required growing season to ensure the growth of vegetation except that where sand-clay mix or other innovative technologies are used, the department may specify a later date for completion. The required completion date may vary within a mining unit depending upon the specific type of mining operation conducted.

2. The length of the necessary growing season shall be determined as part of the approval of the application.

(c) Changes in timetable.

1. Changes in the approved timetable beyond 30 days shall be reported to the bureau.

2. Changes in the approved timetable beyond 90 days shall be submitted to the department as an amendment to the program.

(13) Exceptions and Innovations. In order to encourage the development of new technology which will hasten reclamation or improve the quality of restored lands, the Board may grant exceptions to any of the requirements of Rule 16C-16.051 at the time of approval of a reclamation program for the following circumstances:

(a) Experimental or innovative techniques where the technology is not proven.

(b) Methods which will increase the overall quality of the reclamation program through the creation of particular landforms or habitats.

(14) Reclamation Advisory Committee. The department will submit each application for approval of a reclamation program to the Reclamation Advisory Committee for their advice concerning the criteria set forth in this Rule. The recommendations of the Committee shall be considered by the staff in making their final recommendations to the Board.

*Specific Authority 211.32, 370.021 FS. Law Implemented 211.32 FS. History—New 10-6-80, Amended 7-19-81.*

and Field (1979) evaluated various organic and inorganic flocculating reagents and concluded that hydrofluoric acid and polyethylene oxide (PEO) were the most effective, with PEO being the most promising. However, Barwood (1982) points out that PEO is mineral specific, i.e., good performance is obtained with smectite rich clays, but very poor performance is obtained with polygorskite clays. Apparently, consideration must be given to presence of sulfide materials and exchange ions other than calcium

Several pilot full-scale processes involving flocculants have been used; specifically, Gardinier's process, Occidental's rotary screen process, and Estech's enviro-clear process. Gardinier's process is a two-stage flocculating system using proprietary flocculants and achieves a reported 27-32 percent clay solids. Occidental's rotary screen is based upon the USBR's PEO concept. PEO forms very strong stable flocs, which can be partially dewatered on a static screen and further dewatered on a rotary screen (tromel). The Estech's "Enviro-clear" process is a technique utilizing a combination of flocculant and sand tailings. A proprietary anionic polymer is used to flocculate the clay to which sand is subsequently added. (Mtendon, et. al., 1983)

The optimum dosage to obtain the most beneficial settling rate and final solids content for these processes is usually evaluated via bench tests, with typical values less than 1.25 kg/MT (2.5 lbs/Ton).

#### **SAND/CLAY MIX**

The concept of a sand/clay mix disposal scheme arises from the obvious need to dispose of both waste clays and tailings from the beneficiation process. Accordingly, combining these two materials for

simultaneous disposal has additional suggested advantages of increased unit weight and permeability of the mix, both which enhance consolidation magnitude and rate. However, it should be cautioned that, the increase in unit weight created by adding sand to waste clays will be quite modest; i.e., assuming  $G_{s\text{clay}} = G_{s\text{sand}}$ , then for sand/clay mix

$$\gamma_t = \frac{(1 + S_o \times \text{SCR}) \gamma_w G}{G(1 - S_o) + S_o(1 + \text{SCR})}$$

where  $\gamma_t$  = total unit weight and  $\gamma_w$  = unit weight of water

$G$  = specific gravity

$S_o$  = Solids content of clay

SCR = sand:clay ratio

and for untreated clays  $\gamma_t = \frac{\gamma_w S_o (G_s - 1)}{G_s (1 - S_o) + S_o}$

For example, a 2:1 sand/clay mix of 16% clay solids using  $G=2.65$  will have a buoyant unit weight of 18.3 pcf as compared to 6.9 pcf for the unmixed clays. Although a 268% increase in unit weight is obtained, a buoyant unit weight of 18.3 pcf is quite low. The suggested increase in permeability benefit is tempered by investigations involving the effect of fines content on the permeability of sands which reveal that very small quantities of montmorillonitic clays; i.e., 4-5% are required to render sand impermeable; i.e.  $k \approx 10^{-7}$  to  $10^{-8}$  cm/sec as illustrated in Figure 1.

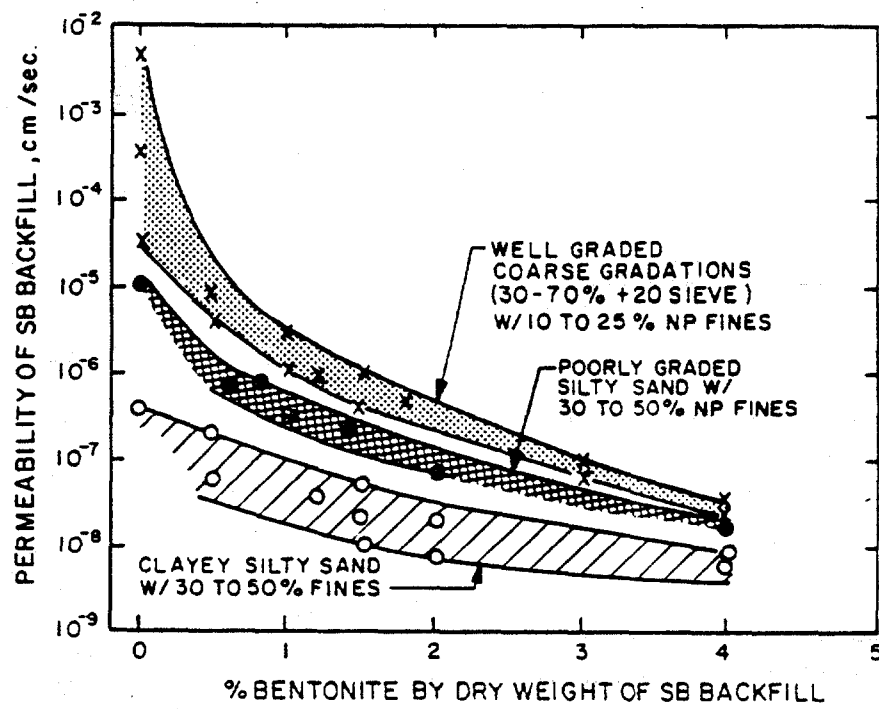


Figure 1. Relationship between Permeability and Quantity of Bentonite Added to SB Backfill (From D'Appolonia, 1980)

**Sand/clay mixes are currently used by CF Industries (Hardee) (Keen, 1982) and Brewster Phosphates (Leitzman, 1982). The CF operation involves discharging waste clays from the beneficiation plant to an initial settling area where they thicken naturally to about 12% to 18% solids. A dredge is then used to excavate the thickened clay and pump it to a mixing station where a 2:1 mix is prepared and pumped to previously mined cuts for reclamation. Field data show that from an initial average clay solids content of ~ 20%, the average clay solids content has increased to ~ 32 to 36% over a 1.5 year period in a waste pond approximately 35 ft. deep.**

**Estech's "Enviro-clear" process also involves sand/clay mixes, however, in this case a flocculant (PAM) is added to the beneficiation clays ( $\approx 3 - 5\%$ ) to achieve rapidly a solids content capable of maintaining the sand tailings in the mix. The clay, flocculant and sand tailings are mixed simultaneously to produce a 1:1 to 2:1 s/c mix and subsequently pumped to a waste storage pond.**

**IMC experimented with sand/clay mixes in which a 1.5:1 mix was placed in an 18 ft. deep pit. Unfortunately, their observations concluded that the ultimate clay density of the sand/clay mix would be insufficient to allow the clays to be disposed at or below ground level.**

**In 1977-78, IMC performed tank tests to compare a 1:1 sand/clay mix with clay only. Two tanks 9' x 14' x 22' were filled, one with Kingsford clay ( $S_o = 12.6\%$ ) and the other with a 1:1 s/c with the clay at 15.4%. After 403 days the clay had increased from 12.6% to 21.1% or an increase of 8.5% solid content units. Correspondingly, the clay**

fraction of the s/c mix increased from 15.4% to 24.6% or a net change of 9.2% solid content units; as summarized below:

	<u>Waste Clay</u>	<u>S/C Mix</u>
Initial Solids Content, %	12.6	15.4
Clay Solids after 403 days, %	21.2	24.0
Initial height in tank, ft.	20.75	21.4
Final height, ft.	12.2	12.5
% Settlement, $\Delta H/H_0$	41.2	41.6

From these results, it was concluded that the value of a s/c mix is detectable, but of limited benefit.

Lawver (1982) using Somogyi's (1979) computer model, which had been calibrated using the IMC tank tests, compared simulated consolidation rates of clays only vs s/c mixes. For identical 34.5 ft. deep ponds with 0:1, 1:1 and 3:1 s/c mixes using a filling rate of  $3 \times 10^6$  tons/yr, the following results were obtained:

	<u>0:1 s/c</u>	<u>1:1 s/c</u>	<u>3:1 s/c</u>
Fill Time, days	748	785	748
% clay solids when filled	22.2	25.6	29.4
Ultimate Settlement, ft.	9.2	8.4	6.6
% clay solids ultimately	28.7	33.1	37.4
Ultimate clay storage cap. T of clay/Acre-ft.	476.1	491	428

These results show that an optimum s/c ratio exists (i.e., 1:1) for ultimate clay storage capacity, and that a net loss could occur if the s/c ratio is too high.

## **CAPPING**

**An alternative method to sand/clay mixes for simultaneous disposal of sand tailings and waste clays is to cap the waste clay settling ponds with the sand tailings. Capping has the advantage of applying a greater effective stress than the increased unit weight of a sand/clay mix. Unfortunately, the major impediment to sand capping is; how does one place a 2.5 ft. sand cap over very soft clays without having the cap merely displace the clays and settle to the pit bottom? In this context, IMC-Agrico-Mobil during 1978-1982 experimented with sand capping (Lawver and Olson, 1982).**

**Their first large scale experiment evaluated methods for capping a 1.5 s/c mix in test pit; specifically, (a) sand sprays (as used by Brewster, Lietzman, 1982), (b) flowing tailings from a side delivery system (c) tensile reinforcement of the surface using geotextiles, (d) geotextile plus s/c mix cap.**

**a) Sand sprays - the use of sand sprays resulted in a very uneven tailings distribution with sand piles forming conically around the spray nozzles. Ultimately, these piles lead to localized heaving of the clays and unacceptable results.**

**b) Side delivery pumping - attempts to "flow" the sand tailings across the test pit produced beaches along the pit sides with considerable heaving of the clays at the pit center. Obviously continual disposition along the sides would only produce surface failure of the clays.**

**c) Geotextile reinforcement - An initial experiment placed non-woven fabric (Tynar) over a small test pit consisting of 16% solids**



clay. An attempt to flow sand tailings over geotextile resulted in side beaches and heaving of the clays at the center producing unacceptable results. Subsequently, a larger test pit of 1.5:1 s/c was successfully capped using small bulldozers to push the sand tailings onto the geotextile covering the pit. Although this latter method was technically successful, the use of geotextiles and bulldozers was deemed unfeasible economically.

d) Geotextile reinforcement plus s/c mix cap - Subsequent to the tests described in (c), flowing a high (5:1) sand/clay mix over the geotextile was attempted, with successful results.

Brewster Phosphates utilized a sand spray technique with the objective of creating a sand/clay mix, however, the method could be used to create a cap (Lietzman, 1982). In this procedure, the clays are thickened to approximately 12 to 18% and the sand sprayed onto the clays through nozzles mounted on a floating pipeline. At these solids content the sand settles through the clays creating a s/c mix. If solids contents less than 12% are used the sand merely flows through the clay to the pit bottom while solids higher than 18% result in a cap being formed. Following the spraying operation, bulldozers are then used to spread the final sand with overburden being added.

## **CENTRIFUGAL MODELLING CONSIDERATIONS**

### **Introduction**

Physical modelling is a popular technique in many engineering disciplines and consists of constructing a scale model of prototype dimensions and then subjecting it to actual operating or field conditions. For the model to be a faithful representation of the

prototype, it must be subjected to the same stresses which the prototype might experience. This requirement is often difficult to satisfy.

If a model of reduced scale is constructed, it is reasonable to expect that the model will have identical geometric properties as the prototype. If constructed with the same materials, then material properties will also be identical. It is also possible to subject this scale model to surface or boundary forces similar to those experienced by the prototype. However, when dealing with soils, there is one important condition which cannot be duplicated in a simple scale model. Stresses at corresponding points in the model and prototype are not equal. Although both are subjected to the same gravitational field, stresses at any given point are a function of the height of overlying material and its unit weight. Since these heights differ between model and prototype, the stress levels will also differ. This dissimilarity of body forces restricts the uses of conventional modelling in geotechnical engineering.

Since stress levels in the soil are a function of the height and unit weights of the overlying material, equivalent stress levels can be achieved by increasing either height or unit weight. Since the obvious advantage of modelling is reduced scale, the unit weight of the material needs to be increased. This can be achieved by either changing material (higher specific gravity) or by increasing the gravitational force. Since we wish to model material as well as geometric properties, the obvious choice is to increase the gravitational force. Increased gravitational forces can be modelled by subjecting the model to high centrifugal forces. By increasing the acceleration of gravity  $n$  times

and by decreasing the linear dimensions of the model by the same  $n$  factor, equal stress levels at similar points will be produced.

### Scaling Relationships

The scaling relationships pertinent to modelling waste clay disposal are those involving: (a) geometry, (b) stress, (c) consolidation, and (d) sedimentation.

Geometric scaling. Is simply a scaling factor  $n = L_p/L_m$

Consequently, area:  $A_p = n^2 A_m$  and volume:  $V_p = n^3 V_m$

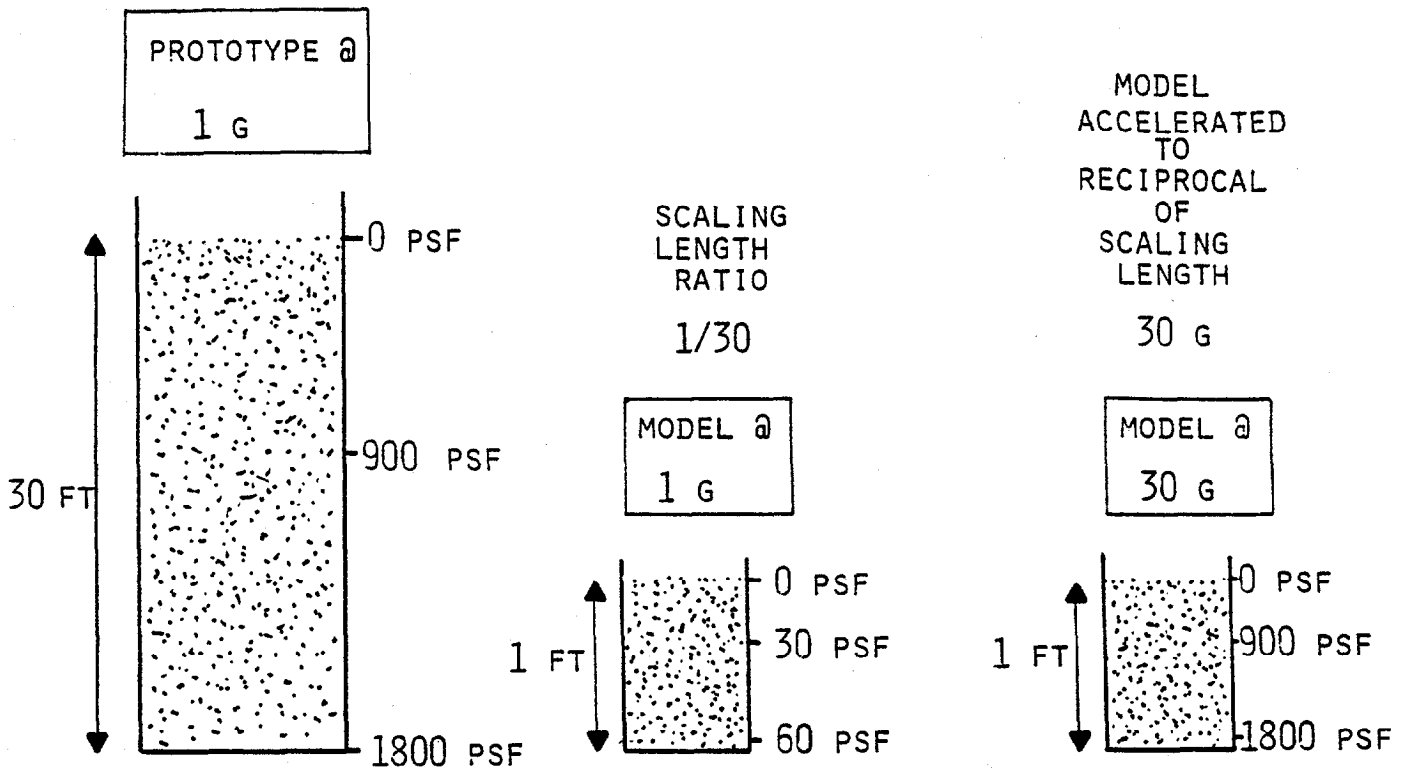
where  $L_p$   $A_p$  &  $V_p$  = length, area, and volume of prototype

$L_m$   $A_m$  &  $V_m$  = length, area and volume of model

Stress. Similitude cannot be achieved in scale models without increasing the unit weight, since stress =  $\gamma Z$ , where  $\gamma$  = unit weight of material, and  $Z$  = depth. However similitude can be achieved by increased accelerations as  $= .g$  (unit wt. = mass density gravitational acceleration). Accordingly, the stress in a scaled model will be in similitude if the gravitation acceleration is increased correspondingly as illustrated in Figure 2.

$$\frac{\sigma_p}{\sigma_m} = \frac{\rho \cdot g \cdot Z}{\rho \cdot n g Z / n} = 1.$$

Consolidation. As sedimentation ends, consolidation begins, with consolidation being characterized by the compression of the sedimented solid particles through the dissipation of pore water pressures within the soil mass. During this phase, the effective stresses are greater than zero. Since the slurry is made up of two constituents, solids and liquids, the modelling requirement of



UNIT WEIGHT OF  
SLURRY - 60 PCF

STRESSES =  $Z \gamma G$

STRESSES	STRESSES	STRESSES
@ SURFACE = 0 PSF	@ SURFACE = 0 PSF	@ SURFACE = 0 PSF
@ MIDPOINT = 900 PSF (15 FT X 60 PCF X 1g)	@ MIDPOINT = 30 PSF (.5 X 60 X 1)	@ MIDPOINT = 900 PSF (.5 X 60 X 30 g)
@ BOTTOM = 1800 PSF (30 X 60 X 1)	@ BOTTOM = 60 PSF (1 X 60 X 1)	@ BOTTOM = 1800 PSF (1 X 60 X 30)

↑ STRESS SIMILITUDE ACHIEVED ↓

Figure 2: Stress similitude in a centrifuge model.

equal stress levels at corresponding points must apply to both materials. Since the model slurry is identical to the prototype, and assuming that the initial state of agitation of the slurry is similar, then the permeability distributions in the model and prototype will be equal.

The dissipation of excess pore water pressures due to self weight consolidation may be analyzed using the general equation governing seepage due to compression of the soil mass. This is given as

$$\frac{\partial u}{\partial t} = \left( \frac{k}{a_v(1+e)\gamma_w} \right) \left[ \frac{\partial^2 u}{\partial x^2} + \frac{\partial^2 u}{\partial y^2} + \frac{\partial^2 u}{\partial z^2} \right]$$

where  $u$  = pore water pressure

$e$  = void ratio

$a_v$  = coefficient of compressibility

$k$  = coefficient of permeability

If the dimensional scaling factor between prototype and model is again taken as  $n$ , then

$$x_p = nx_m, y_p = ny_m, z_p = nz_m$$

$$u_p = \alpha_u u_m$$

$$\gamma_p = \alpha_\gamma \gamma_m$$

$$t_p = \alpha_t t_m$$

$$k_p = \alpha_k k_m$$

where subscripts p and m indicate prototype and model, and the alpha's are as yet unknown scaling factor quantities.

$$\text{Since } u_p = \alpha_u u_m$$

$$\text{and } t_p = \alpha_t t_m$$

$$\text{then } \frac{\partial u_p}{\partial t_p} = \frac{\partial t_m}{\partial t_p} \cdot \frac{\partial u_m}{\partial t_m} \cdot \frac{\partial u_p}{\partial u_m}$$

$$\text{and } \frac{\partial u_p}{\partial t_p} = \frac{1}{\alpha_t} \cdot \alpha_u \cdot \frac{\partial u_m}{\partial t_m}$$

Rewriting the consolidation equation in terms of model dimensions results.

$$\frac{\partial u_p}{\partial t_p} = \frac{k_p}{a_v(1+e)\gamma_p} \left[ \frac{\partial^2 u_p}{\partial x_p^2} + \frac{\partial^2 u_p}{\partial y_p^2} + \frac{\partial^2 u_p}{\partial z_p^2} \right] \text{ for the prototype, and}$$

$$\frac{\alpha_u}{\alpha_t} \cdot \frac{\partial u_m}{\partial t_m} = \frac{\alpha_t k_m}{a_v(1+e)\alpha_\gamma \gamma_m} \left[ \frac{\alpha_u}{n^2} \left[ \frac{\partial^2 u_m}{\partial x_m^2} + \frac{\partial^2 u_m}{\partial y_m^2} + \frac{\partial^2 u_m}{\partial z_m^2} \right] \right] \text{ for the model}$$

$$\text{Simplifying } \frac{\partial u_m}{\partial t_m} = \frac{\alpha_t}{\alpha_u} \left[ \frac{\alpha_u \alpha_k}{n^2 \alpha_\gamma} \right] \left[ \frac{\partial^2 u_m}{\partial x_m^2} + \frac{\partial^2 u_m}{\partial y_m^2} + \frac{\partial^2 u_m}{\partial z_m^2} \right] \text{ and}$$

$$\text{Similitude will be achieved when } \frac{\alpha_t \alpha_x}{n^2 \alpha_\gamma} = 1$$

If the pore fluid used in the model is the same as that in the prototype, then

$$\alpha_\gamma = 1$$

In addition, since the initial solid concentrations and particle characteristics are the same, the subsequent soil structure should

develop in the model as in the prototype. This then indicates that the permeabilities should be equal, and thus

$$\alpha_K = 1$$

These assumptions lead to

$$\alpha_t = n^2$$

and substituting this relation back into  $t_p = t_m \alpha_t$

$$\frac{t_p}{t_m} = n^2 \quad \text{or} \quad t_p = n^2 t_m$$

This means that the time rate of consolidation in the model is speeded up by the square of the scaling factor. Since  $n$  is also the acceleration of the model, the rate varies as the square of acceleration. Thus, at 85 g., a one year time span in the field will take

$$\frac{(365)(24)}{85^2} = 1.2 \text{ hours}$$

in the centrifuge.

Herein lies the major benefit of centrifugal testing. Using this modelling relationship provides a methodology of modelling consolidation most efficiently, thereby allowing evaluation various disposal schemes to completion.

Sedimentation. The initial settling of the waste clay particles is a sedimentation process, and the rate can be approximated by Stoke's Law. During this process, the effective stresses are initially zero,  $\sigma' = 0$ . While it is impossible to separate precisely sedimentation and consolidation phases, it has been suggested that sedimentation ends at solids contents of approximately 8 percent.

Newton's mechanical similarity definition suggests that the proportionality of all the forces acting in a system is explicitly

required, i.e., a common scale factor should be applied to all the forces that governs the modelled phenomenon. Often it is not possible to satisfy this condition (Croce, et. al., 1984). In discrete settling; gravitational forces,  $F_w$ , viscous (drag) forces;  $F_d$ , and buoyant forces,  $F_b$ , govern the phenomena. Ideally,

$$\frac{F_{wp}}{F_{wm}} = \frac{F_{dp}}{F_{dm}} = \frac{F_{bp}}{F_{bm}}$$

Using geometric scaling  $l_p/l_m = \alpha$ , and centrifugal acceleration is

$$\omega_p/\omega_m = n, \text{ the } F_w = \frac{F_{wp}}{F_{wm}} = \frac{M_p \cdot A_p}{M_m \cdot A_m} = \frac{\rho_p \cdot \text{vol}_p \cdot a_p}{\rho_m \cdot \text{vol}_m \cdot a_m} = (1)(1) \frac{1}{n} = \frac{1}{n}$$

Note that the volume of the clay particle is not scaled; i.e.,  $\text{vol}_p = \text{vol}_m$ .

For Stokian settlement of a sphere the viscous (drag) force is

$$F_d = 6\pi R v \eta, \text{ where } R = \text{radius of sphere}$$

$v = \text{velocity}$

and  $\eta = \text{viscosity of the fluid.}$

which in turn leads to:

$$F_d = \frac{F_{dp}}{F_{dm}} = \frac{6\pi R_p l_p t_p \eta_p}{6\pi R_m l_m t_m \eta_m} = (1)(\alpha t_m)(1) = \frac{\alpha t_m}{t_p}$$

Examining the buoyant force,  $F_b = \rho \text{ Vol. } g$ , hence

$$F_b = \frac{F_{bp}}{F_{bm}} = \frac{\rho_p V_p G_p}{\rho_m V_m G_m} = (1)(1) \frac{1}{n} \text{ (actually } F_w = F_b)$$

Note that the particle volume,  $\text{Vol}$ , is not scaled, i.e.,  $\text{Vol}_p = \text{Vol}_m$



Summarizing

$$F_w = 1/n$$

$$F_d = \alpha t_m/t_p$$

$$F_b = 1/n$$

$$\text{Setting } F_w = F_d \rightarrow 1/n = \frac{\alpha t_m}{t_p} \text{ or } t_p = \alpha n t_m$$

$$\text{Note for } F_w = F_d = F_b \text{ then } \alpha = 1 \text{ and } t_m/t_p = 1/n.$$

**Under conditions of discrete settling, there are no restrictions on . However, as settling becomes hindered and pressures become significant, is eventually set equal to n for similitude. The result being:**

A) For low solids contents,  $t_p/t_m = n$

B) For intermediate concentrations,  $n < t_p/t_m < n^2$

and C) For high concentrations  $t_p/t_m = n^2$

A similar conclusion is reached by merely examining Stokes Law

$$v = \frac{2 (\gamma_s - \gamma_f) R^2}{9 \eta} \quad \text{where } v = \text{velocity}$$

R = radius of sphere

$\gamma_s$  and  $\gamma_f$  = unit weight of sphere and fluid

and  $\eta$  = viscosity

$$\alpha_v = \frac{v_p}{v_m} = \frac{(\rho_s - \rho_f)_p \cdot g_p \cdot R_p^2 \cdot \eta_m}{(\rho_s - \rho_f)_m \cdot g_m \cdot R_m^2 \cdot \eta_p} = (1)(1/n)(1)(1)$$

$$v = 1/t \text{ and } (l_p/l_m)(t_m/t_p) = 1/n$$

$$\text{so } \frac{t_m}{t_p} = \frac{l_m}{l_p} \cdot \frac{1}{n} \rightarrow t_p = \alpha n t_m$$

Thus the time scaling relationship is a function of the solids contents, and must be determined experimentally by "modelling of models".

### Boundary Conditions

As in any laboratory experiment the influence of laboratory imposed boundary conditions must be evaluated to ascertain the magnitude of experimental errors on test results. Accordingly, the model deviations from prototype of (a) stress distribution, (b) liquid surface geometry, (c) platform orientation and (d) start-up-time (SUT) during centrifugation are discussed:

Stress Distribution. Inasmuch as the centripetal acceleration is a function of the centrifuge arm length ( $a = \omega^2 R$ ), unlike prototype conditions, the acceleration level varies across the model height. If the vertical stress is given as

$$\sigma_v = \int \rho a dz$$

where

$\rho$  = mass density

$a$  = acceleration

and

$z$  = depth below the model's surface

Following the geometry of Figure 3,  $z = R - R_s$  and the radial stress induced is

$$\sigma_R = \sigma_v = \int_{R_s}^R \rho a dR$$

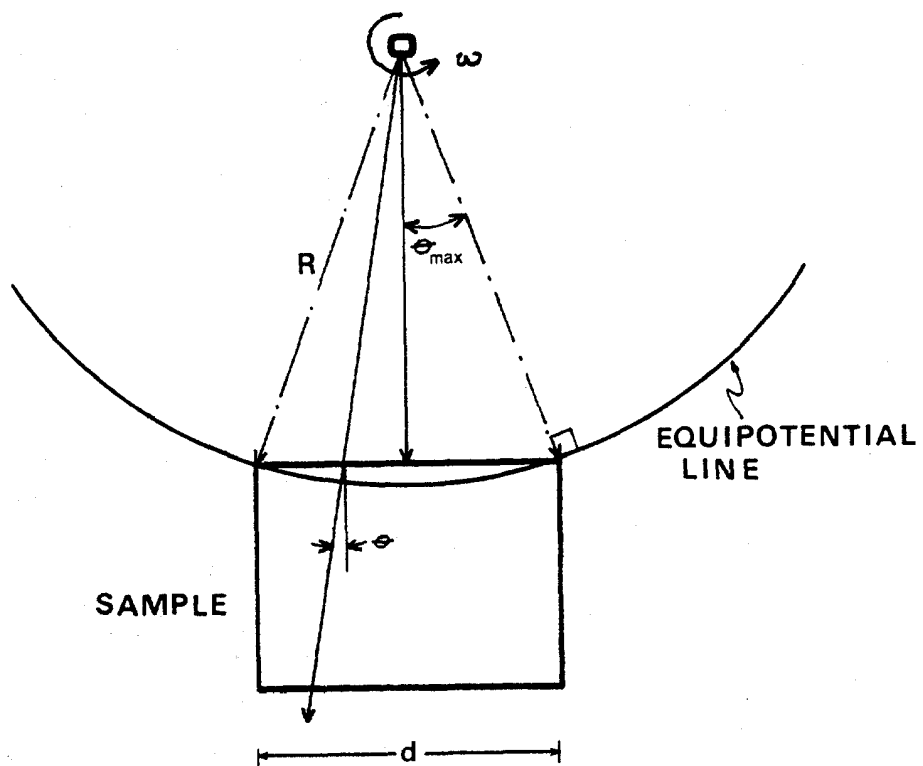
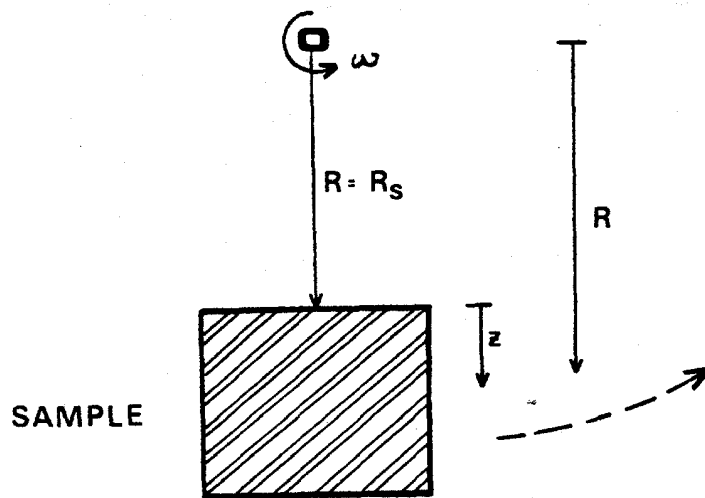


Figure 3: Plan Views of Rotating Sample

these limits are used since the stress is zero at the model's surface.

By multiplying and dividing by  $g$ , this expression becomes

$$\sigma_R = \int_{R_s}^R \rho \cdot g \cdot a / g \, dR$$

Since  $\rho g$  equals the prototype unit weight,  $\gamma$ , and  $a = \omega^2 R$ ,

upon substitution we obtain

$$\sigma_R = \int_{R_s}^R \frac{\gamma \omega^2 R dR}{g}$$

Integrating yields

$$\sigma_R = \sigma_V = \frac{\gamma \omega^2}{g} \left( \frac{R^2 - R_s^2}{2} \right)$$

Hence this equation allows calculation of the stress level at any depth within a centrifugal model. Rearranging and noting the  $z = R - R_s$ , yields

$$\sigma_R = \frac{\gamma \omega^2}{g} z \frac{R + R_s}{2}$$

Since  $\sigma_R = 0$  when  $R = R_s$  and  $\sigma_R$  is a maximum when  $R = R_s + z$  or

$$\sigma_{R_{\max}} = \frac{\gamma \omega^2}{2g} z (2R_s + z)$$

then the stress error,  $\frac{\Delta \sigma_R}{\sigma_R}$ , is given by

$$\frac{\Delta \sigma_R}{\sigma_R} = \frac{\frac{\gamma \omega^2}{2g} z (2R_s + z) - \frac{\gamma \omega^2}{2g} z (2R_s)}{\frac{\gamma \omega^2}{2g} (2R_s)}$$

Cancelling terms,

$$\frac{2R_s + z - 2R_s}{2R_s}$$

which becomes

$$\frac{\Delta\sigma_R}{\sigma_R} = \frac{z}{2R_s}$$

Considering a 10 cm deep model ( $z = 10$  cm) on a 1 meter radius centrifuge, reveals a stress error,

$$\Delta\sigma_R/\sigma_R = 10/2 (100) = 5\%.$$

Liquid Surface Geometry. Figure 4 illustrates the forces acting on a fluid during centrifugation in a vertical plane, specifically, (a) weight = mass x earth's gravity ( $1g$ ) or  $MG$ , (b) centripetal force = mass x centripetal acceleration ( $\omega^2 R$ ) or  $M \omega^2 R$  and (c) the resultant of (a) and (b) =  $MP$  inclined at  $\theta$ . By definition, an equipotential curve is one for which the total head remains surface will be an equipotential curve. For Figure 4, then

$$F_R dr + F_z dz = 0$$

where  $F_R = M\omega^2 R$

and  $F_z = -MG.$

By substitution,  $M \omega^2 R dr - MG dz = 0$

and integration yields  $\frac{R\omega^2}{2} - Gz + C = 0.$

This is the equation of a parabola. That is to say, the liquid surface in a centrifugal model is parabolic, whereas in the prototype it is considered level.

By imposing the boundary conditions that  $D$  represents the model bucket diameter than the boundary conditions of  $z$  are 0 and  $D$ . Accordingly, rearranging the equation in terms of  $z$  and eliminating  $C$ , provides

$$D = \frac{\omega^2 R_D^2}{2G} - \frac{\omega^2 R_0^2}{2G} \quad \text{or} \quad D = \frac{\omega^2}{2G} (R_D^2 - R_0^2)$$

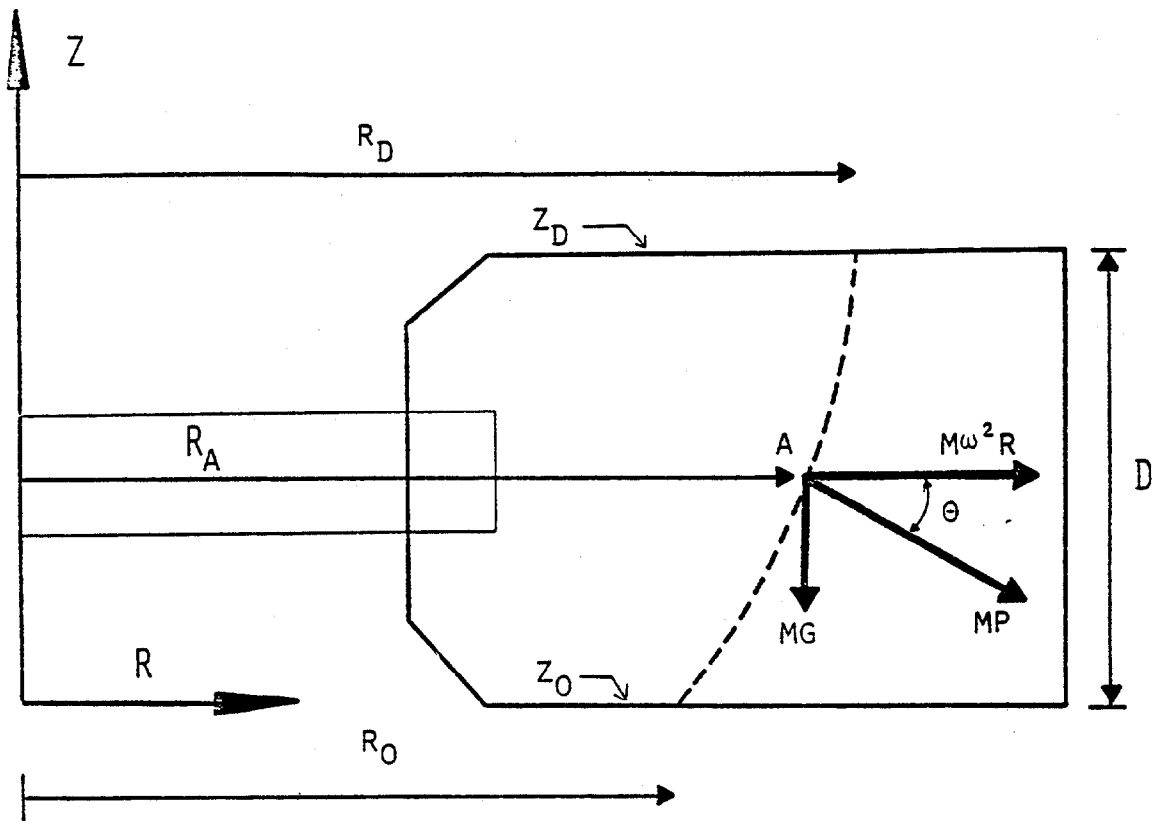


**Figure 4: Forces Acting on a Fluid During Centrifugation**

If we factor  $(R_D^2 - R_O^2)$  to  $(R_D + R_O)(R_D - R_O)$  and note that  $R_D + R_O = 2R_m$ , where  $R_m$  is the distance to the mid-point of the model liquid surface then:

$$R_D - R_O = \frac{GD}{\omega^2 R_m}$$

Since  $\omega^2 R_m$  is the acceleration level of a centrifugal model test, then the difference in fluid surface level,  $R_D - R_O = \frac{D}{\text{Acc Level}}$

For typical 60 g tests using a 14 cm diameter bucket, this will be a total difference of  $\frac{14}{60} = 0.23$  cm, or considering the mid-point, 0.11 cm.

Having considered the liquid surface shape in a vertical plane, it is now appropriate to observe what effect the centrifuge rotation has on the liquid surface slope in a horizontal plane. Since the model follows a circular path as illustrated in Figure 5 the equipotential lines across the model are curved. If the angle  $\theta$  denotes the angle between the model centerline's radius and any other equal radius at another point as the model, then  $0 < \theta < \theta_{\max}$ , where  $\theta_{\max}$  = the subtended angle to the model boundary.

Since acceleration is a vector, it will be parallel to the centerline of any  $\theta$ . To determine the difference in acceleration between midpoint of the model and its boundary at the container edge, it is simply

$$R - R \cos \theta_{\max} = \Delta R$$

For a 1 meter centrifuge and model bucket of  $D = 14$  cm, from geometry

$$\sin \theta_{\max} = D/2R = 0.07, \text{ and}$$

$$\theta_{\max} = 4.0 \text{ deg}$$

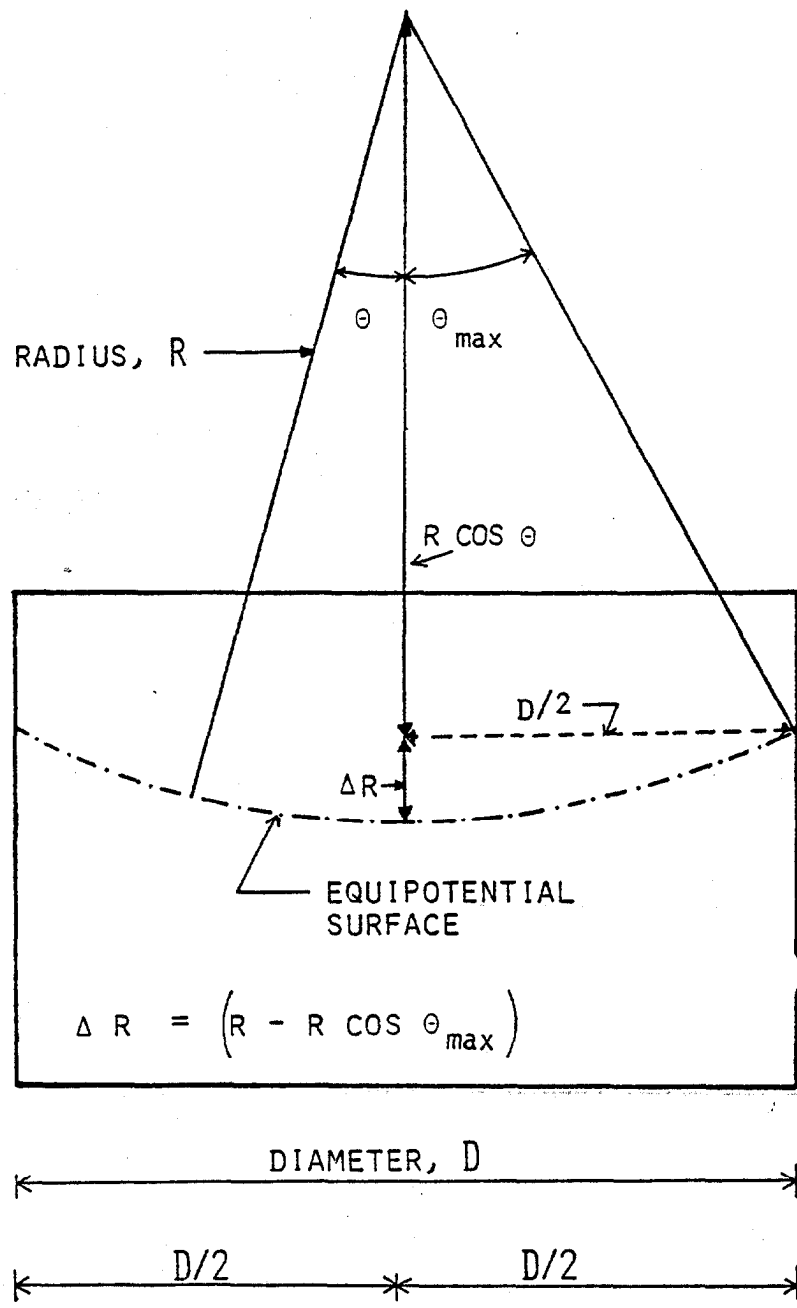


**Figure 5: Geometric Parameters Used in Model Analysis.**



thus the difference will be  $100 - 100 \cos 4.0 = 0.25$  cm. This difference between the edge and the centerline of the model, will correspond to a difference in acceleration level of (for a 60 g test)

$$60 - \frac{100 - 0.25 \times (60)}{100} = 0.15 \text{ g}$$

thus, a difference of 0.15 g is a maxima at the shortest radius and decreases as the interface settles (since D is a constant,  $\theta$  decreases).

Platform Orientation. Most geotechnical centrifuges are now constructed with a pivoting or swing-up bucket. This allows the model to be conveniently placed or constructed in the container under 1-g, earth gravity, conditions. Theoretically, during acceleration, the bucket should rotate upward such that the resultant acceleration field remains exactly perpendicular to the platform's surface. The resultant acceleration is simply the vector sum of the 1-g acceleration acting vertically downward and the chosen horizontal or radial centrifugal acceleration. In practice, unavoidable friction in the pivot bolts will result in an under rotation of the bucket. This is shown to an exaggerated degree in Figure 6. Such an under rotation in the phosphatic slurry tests can result in a significant error. The solids-supernatant interface will be displaced at the viewing windows, and the height of solids will be over predicted. A 4 mm error in this height translates into an error of about 4% in the initial water content and as high as 21% towards the end of consolidation.

Parabolic Liquid Surface and Platform Orientation Adjustments To provide adjustments to the parabolic liquid surface and platform

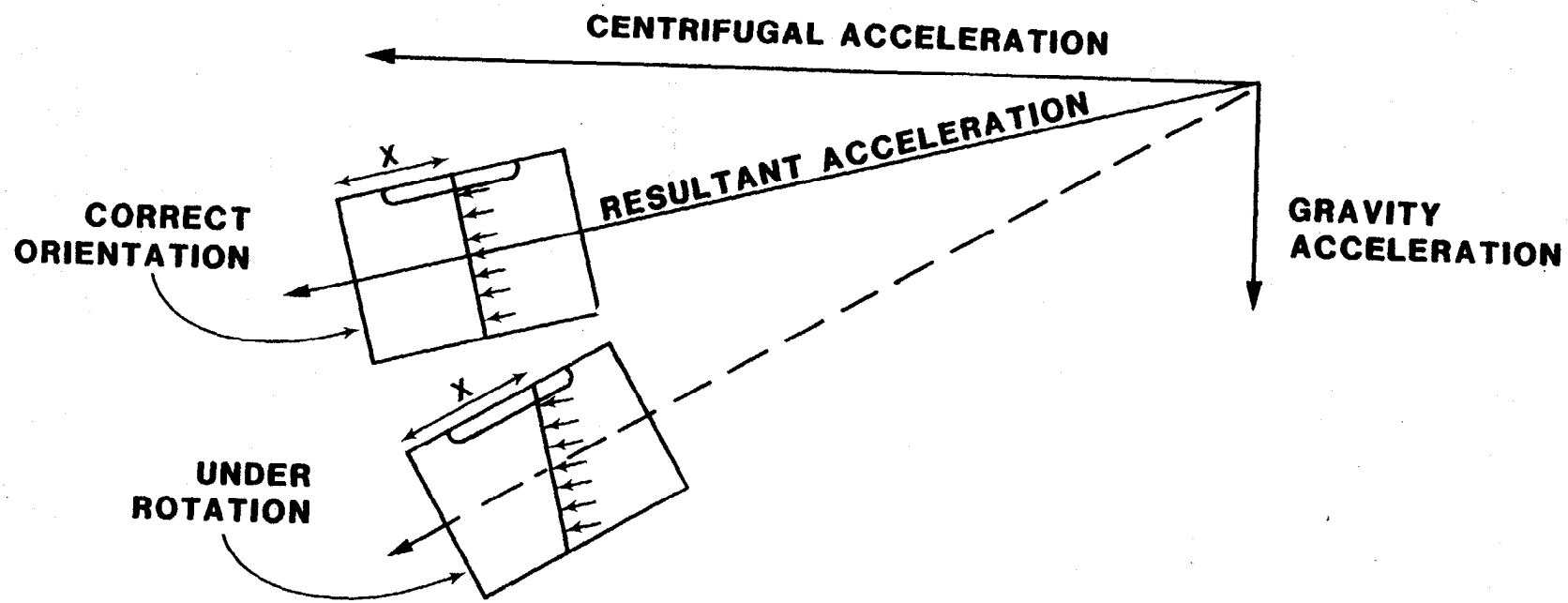
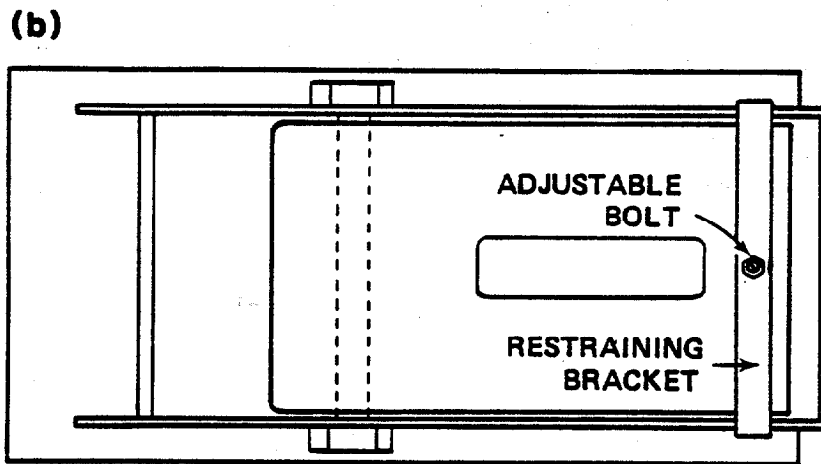
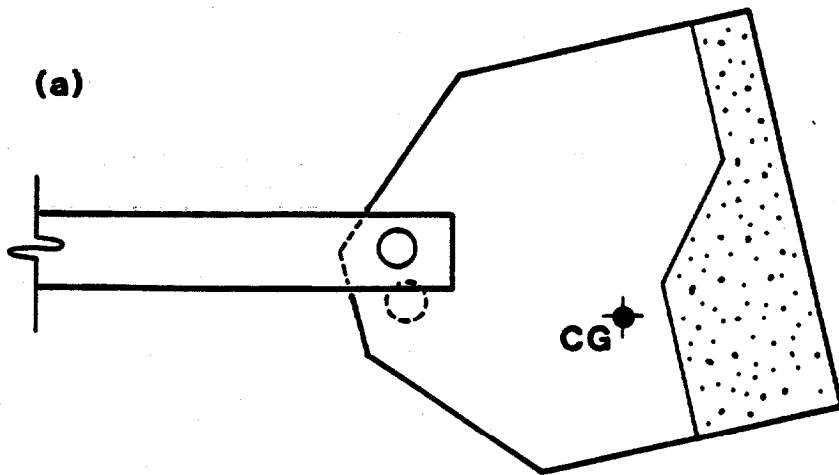


Figure 6: Bucket Under Rotation Because of Pivot Friction

orientation problems, Bloomquist, et. al., (1984) devised a method of allowing the model container buckets to over rotate and then restrain the over rotation, so a calibration can be performed. Over rotation is provided by offsetting the pivot as illustrated in Figures 7a. and b. Once the over rotation is achieved, some method is needed to restrain the bucket at its correct position. This restraint is provided by a restraining bucket and adjustable bolt as illustrated in Figure 7b. The principal disadvantage to this method is that the centrifuge must be stopped each time to adjust the bolt. However, once properly set, no additional adjustment is required for the test deviation. Of course a different model or different acceleration, will require readjustment. In the case of a consolidating waste clay, the center of gravity translates towards the end of the bucket, increasing the upturning moment. Consequently, the initial bolt adjustment is the only one required.

The calibration proceeded to account for the parabolic liquid surface and restraining bolt adjustment is accomplished by placing a known volume of water in the centrifuge plexiglass bucket and adjusting a marking scale on the container side to read the appropriate height of water; i. e., 10 cm. The plexiglass bucket is then accelerated to the proposed test acceleration. If the water level as measured from a Polaroid<sup>®</sup> photograph is too high, the bucket was under rotated, if too low it has over rotated. By repetitive trials, the restraining bolt can be properly adjusted.

Start-up Time. The start-up time (SUT) in centrifuge testing is the elapsed time between start of rotation and achieving the desired



**Figure 7: Bucket Configurations for Orientation Adjustment**

test acceleration. This may vary from 30 seconds to 10 minutes, depending on the magnitude of the acceleration and on the available power supply. For nontime-dependent geotechnical modelling problems, such as bearing capacity and slope stability for drained conditions, the start-up time does not affect the results. However, for such processes as sedimentation, large strain consolidation, and seepage analyses, neglecting this period may substantially affect the results.

Figure 8 shows a plot of acceleration versus time. In this and subsequent figures it has been assumed that the test acceleration of 10 g is reached in 1 minute and that the run-up slope is linear. Note the ordinate axis is labeled from zero rather than from the 1 g. This is common practice and does not introduce appreciable error in the analysis.

Frequently the recording of model elapsed time is started at Point P, with the start of centrifuge rotation. After some length of centrifuging, T minutes, it would be in error to claim that the prototype would be in an identical state after  $(T) (A)^\alpha$  minute (where A is the test acceleration and  $\alpha$  the scaling exponent). This is, of course, because during the model start-up time the acceleration level was not equal to A but was less. Alternatively, some researchers begin recording the model elapsed time after the test acceleration level has been reached, Point Q. This would result in an error in the opposite direction.

The model elapsed time at which recording should be initiated lies between Points P and Q and is a function of the exponent by which the process being tested is governed. Bloomquist, et. al., (1984) have

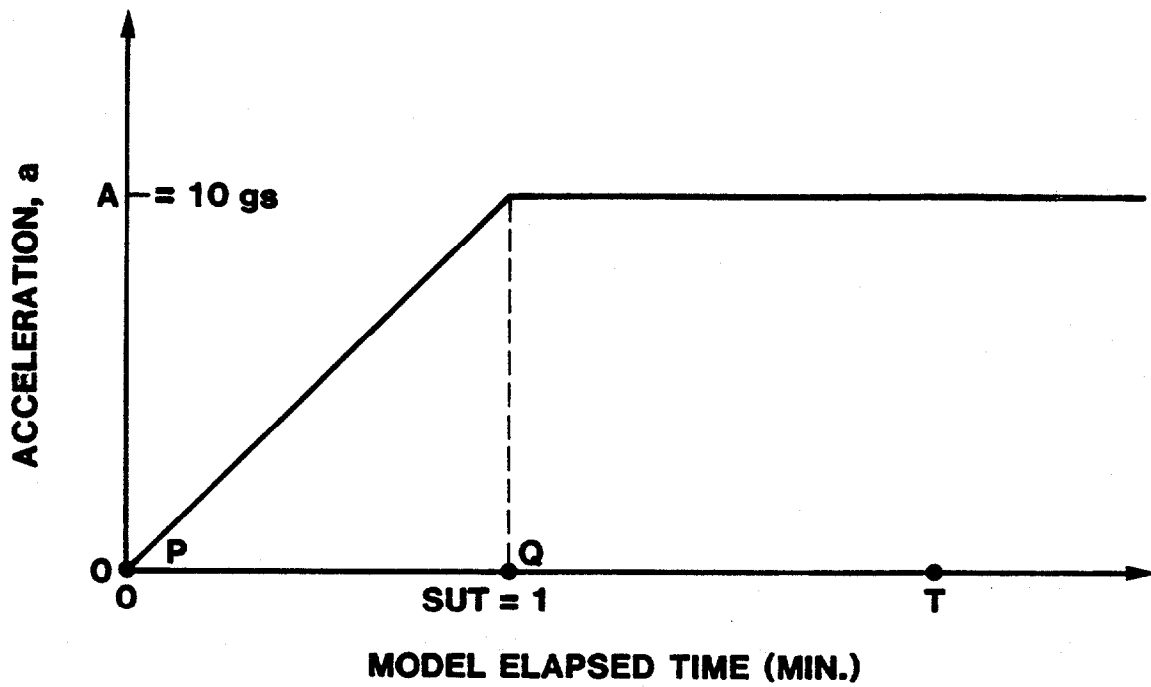


Figure 8: Centrifuge Linear Acceleration Versus Time Start-Up

found that in general for an acceleration level A for a process where the time exponent is  $\alpha$  , then recording of the elapsed time should begin after a time equal to  $[\alpha / (\alpha + 1)]$  (SUT).

In the case of consolidation phenomena where  $\alpha = 2$ , if we assume SUT = 120 sec, then the elapsed time should begin at  $0.667 (120) = 80$  sec. In the case of sedimentation phenomena, where  $\alpha = 1$ , then the elapsed time should begin at  $0.5 (120) = 60$  sec. In practice, application of these correct elapsed times depend upon the centrifugal model test; for consolidation models lasting 1,000<sup>+</sup> minutes corrections are trivial. Conversely, for sedimentation models lasting 10 minutes, correct elapsed times are important.

## **CHAPTER III: EQUIPMENT, PROCEDURES, AND MATERIALS**

### **UNIVERSITY OF FLORIDA GEOTECHNICAL CENTRIFUGE**

The University of Florida geotechnical centrifuge has a one-meter radius and 2,125 g - kg capacity; that is; a capacity of approximately 80 lbs. can be accelerated to 100 g's. For these centrifugal model tests, the waste clays are placed inside a 14 cm diameter by 15.25 cm high plexiglass container, which in turn is housed inside a swinging aluminum bucket. A vertical slot in the aluminum bucket permits visual observation of the model during flight. A photo-electric pick-off and flash delay augment the system for photographic monitoring of the clay surface interface. Figure 9 presents a schematic drawing of the centrifuge.

### **CENTRIFUGE SPECIFICATIONS**

The centrifuge used is a Rucker Model 57-2380 powered by via a 2-horsepower, electric motor. Two rotating arms, 180 degrees apart, each support a platform on which two samples may be mounted, thus permitting simultaneous testing of four specimens. The distance from the axis of rotation to the centroid of a platform is 34 1/2 inches ( $\approx 1$  meter).

A protective metal housing encloses the entire assembly. Access to the platforms is possible through a swinging side door and hinged top panel. A 14 by 16 inch removable, plexiglass viewport is located on the left top-panel, which allows access to the sample, and provides the window through which photographic records are made.

### **DATA ACQUISITION**

Data acquisition is a photographic record obtained using a stroboscope and Polaroid® camera. A strobe was selected over a high speed camera and flash as in a typical test (257 rpm and 42 1/2 inches



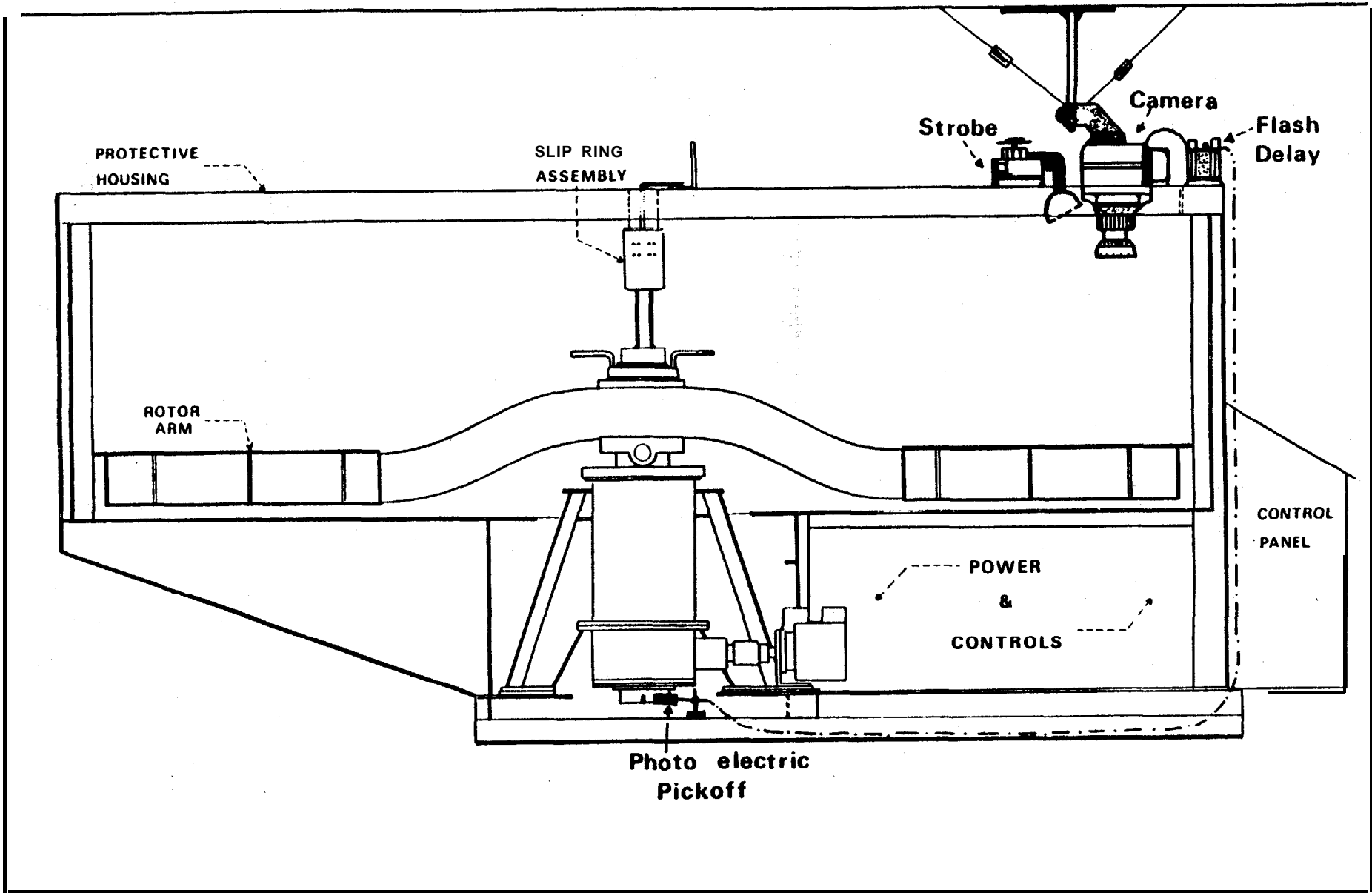


Figure 9: Schematic of Centrifuge and Camera Set-Up

radius, equaling 80 g units), a point on the periphery of the centrifuge moves 1.14 inches in 1/1,000 of a second. This movement is too great for an ordinary mechanical shutter to "stop." Electronic shutters will work, but are extremely expensive and do not provide visual observation of the sample in motion. However, a strobe light can deliver high intensity light flashes of extremely short duration. For example, a standard strobe can produce flash durations of one to three microseconds. Hence, a Stoboslave Model 1539-A manufactured by General Radio Company was used. By aiming the reflector at the sample and manually adjusting the flash rate, the specimen can be made to appear stationary, allowing observation and photographic recording.

Initially it was thought that a manual procedure for adjusting the flash rate to correspond to the arm speed would be adequate. However, the centrifuge does not maintain an exact speed setting. Instead, it varies continuously. Factors that contribute to the minor fluctuations included line voltage surges, mechanical play in the gears and belt, air turbulence and harmonic vibrations. This means that the strobe has to be continuously adjusted to maintain the sample at a particular location. A second problem concerns the flash rate. At 257 rpm the strobe flashes 4.3 times per second. In order to prevent double exposures, the camera shutter must be set at a speed which will open, allow one flash and then close before the next flash occurs. While this is possible, it means that only a few centrifuge speeds are usable, since most cameras have only five to seven available shutter speeds. In addition, the fluctuation of the rotating arm would make photographing the specimen a hit or miss proposition.

It was therefore necessary to make use of the strobe's external trigger which bypasses the internal oscillator and flashes upon reception of an external signal. One possible solution was to install a mechanical triggering device and attach this to the rotating arm. With this arrangement, the strobe would flash when the circuit was completed by the trigger. The sample would therefore remain optically stationary regardless of any speed fluctuations. Several microswitch setups were considered. However, since mechanical closure of contact points triggers the flash, wear, adjustment, and alignment, problems are foreseen. In addition, a new adjustment would have to be made for different speeds; as the delay-time would be different.

A final decision was made to use a photo-electric pickoff (Model 1536-A), a Gen Rad accessory designed for the strobe. It obtains trigger pulses from the moving object by reflected light and thus avoids mechanical closure devices. The pickoff head contains a small lamp, a light sensitive photocell and a lens. These convert abrupt changes in the reflectivity of a moving surface into electrical impulses. The signals are then amplified and received by the strobe unit. In order to provide consistent triggering, a sharp discontinuity in reflectivity must be used as a trigger point. A black (highly light absorbent) tape was used as a background surface, and a small piece (2 mm wide) of Scotch silver polyester film tape (No. 850) applied over it. When the tape passes across the pickoff head, its internal light source is reflected back into the unit to the photoelectric cell, and a one-volt pulse is transmitted to the strobe. The pickoff was located on top of

the centrifuge adjacent to the main spindle. Here, the spindle consists of a 1 1/2 inch diameter shaft extending about four inches above the centrifuge housing. Both tapes were applied to this shaft and the pickoff head was directed towards this area from a distance of several inches.

While this set up provides excellent results, the problem concerning multiple flashes and camera synchronization remained. One other feature was also desired. Since four buckets, and thus four samples may be tested simultaneously, both sets of samples should be observable during operation. However, the pickoff is set to illuminate only one arm a time. The pickoff can be manually moved until the other arm's sample is in view but this is both time consuming and very difficult to adjust accurately during machine operation.

A model 1531-P2 Flash Delay was acquired to solve these problems. This accessory is designed to accept the pickoff impulse, and insert a controlled amount of time delay between trigger pulses and the resulting strobe flashes. Thus, while the pickoff remains stationary, the strobe can be adjusted to flash at different times. This allows for very accurate orientation of the illuminated sample. A second photo-electric pickoff was installed to illuminate the opposite arm. For photographing the sample, a manually operated single flash switch is provided. Once the sample is aligned with the camera lens, the switch can be set to this mode. The strobe will now flash only when the trigger button is pressed. This feature completely eliminates the multiple exposure problem

## **THE CAMERA**

The ability to obtain close-up, instant photographs during a test sequence is the primary reason a Polaroid<sup>®</sup> camera was used. In addition, much versatility is required in order to obtain accurate photographs while the subject is moving at high speeds. For these reasons, a Polaroid<sup>®</sup> model 600 SE camera was selected. The film used, Type 667, is extremely fast (ASA 3,000), and thus provides excellent photographs when used in conjunction with a strobe. The standard camera comes with a 127 mm lens which has a minimum focusing distance of 3.5 feet. For the type of measurements to be made from the photograph (reading to the nearest 1/2 mm), a close-up lens set was added.

Since the centrifuge vibrates during operation, the camera cannot be mounted directly to the protective housing. A platform was anchored to the ceiling joists directly over the viewport. Guy wires and turnbuckles provided platform rigidity. A close-up camera mount was inverted and attached to the platform using C-clamps. This allowed the base to be easily adjusted as needed. A four foot long tube extends to within one inch of the centrifuge housing. The camera attaches to an adjustable mechanism which slides along the tube. This allows the camera to be raised and lowered or moved horizontally three inches.

## **MODEL CONTAINER**

Like most centrifuges, the University of Florida machine rotates in a horizontal plane. The resulting centrifugal force, for all practical purposes, radiates in a horizontal direction. If a prototype is to be scaled down in size and then subjected to an accelerated force field, it is important to maintain the proper orientation of the model during

**flight. For example, if a 50 foot pipe column of slurry is to be scaled to a one-foot model, then accelerated to 50 g's, the model must be placed such that the one-foot dimension is horizontal or within the plane of rotation. If this is not done, then equal stresses within the model and the prototype will not be produced.**

**The University of Florida Centrifuge uses pivoted mounting platforms. This design ensures that the acceleration field will only change in magnitude, but not direction. The resultant acceleration vector is always directed through the bottom of the sample. When the slurry is introduced into the upright container, gravity is the only body force acting. As the machine speed increases, the container swings outward until it reaches a near horizontal position. There, with centrifugal forces predominant, the sample may be observed and its response recorded. The advantage of such a set-up is that the centrifuge may be stopped and restarted without disturbing the sample.**

**The model container assembly designed consists of four individual components:**

- 1. Plexiglas Container**
- 2. Aluminum Bucket**
- 3. Pivot Bolt**
- 4. Aluminum Bucket Housing**

#### **Plexiglas Container**

**The Plexiglas container; which contains the waste clay slurry, was constructed from 6 in. OD, 1/4 in. thick, 6.0 in. lengths of tubular Plexiglas. A 1/4 in. Plexiglas plate bonded to one end forms the container. A metric scale, with millimeter divisions attached to the**

outside of the container, provides visual monitoring of clay slurry interface heights. The empty containers weigh approximately 1.4 lbs. (0.64 kg).

#### Aluminum Bucket

Since high stresses are developed in the centrifuge, the plexiglass container alone would not be strong enough and some means of support and protection was required. Accordingly, a tight fitting aluminum bucket was selected; it would carry most of the in-flight stresses. An aluminum pipe with an outside diameter of 6.563 inches and an inside diameter of 6.063 inches was cut to a 10 inch length, and a 1/4 inch plate heliarc welded to one end. A 1 x 4 inch cutout was made in the lower side, such that the slurry and metric scale would be visible when assembled. Two 3/4 inch diameter holes were drilled to accept the pivot bolt. The aluminum bucket alone weighs six pounds.

#### Pivot Bolt

The aluminum bucket rotates upward into a horizontal position under centrifugal loading. This vertical motion occurs only during starting and stopping, the assembly remaining stationary with respect to the pivot bolt during most of the test. It was felt that roller bearings or bushings were not necessary. Instead, a 3/4 inch high strength steel bolt, nine inches long, was used to provide the pivotable support.

Container pivot bolts are offset slightly from the center of the aluminum buckets to insure that the buckets will always over rotate. A restraining bracket attached to the bucket housing and an adjustable bolt maintain the bucket in a position pre-determined for each acceleration level. This design insures that the resultant acceleration

vector is always perpendicular to the model's ground surface. If the pivot bolt passed through the center of the aluminum bucket, the changing center of gravity of the sample (due to consolidation) would cause bucket orientation, and hence, the acceleration vector, to change (Bloomquist, et. al., 1984).

### Aluminum Bucket Housing

The final component required for testing was the support structure for the buckets. During initial centrifugal testing programs, a single housing with accompanying bucket was mounted on each arm. To increase the efficiency of future testing programs, a dual housing was mounted on each arm; this permits four samples to be tested simultaneously. The housings are built of 1/4 inch aluminum alloy plate with heliarc welded joints. These are bolted directly to the mounting platform. As an added safety consideration, 1 inch X 3/8 inch rectangular steel bars connect opposing bucket housings.

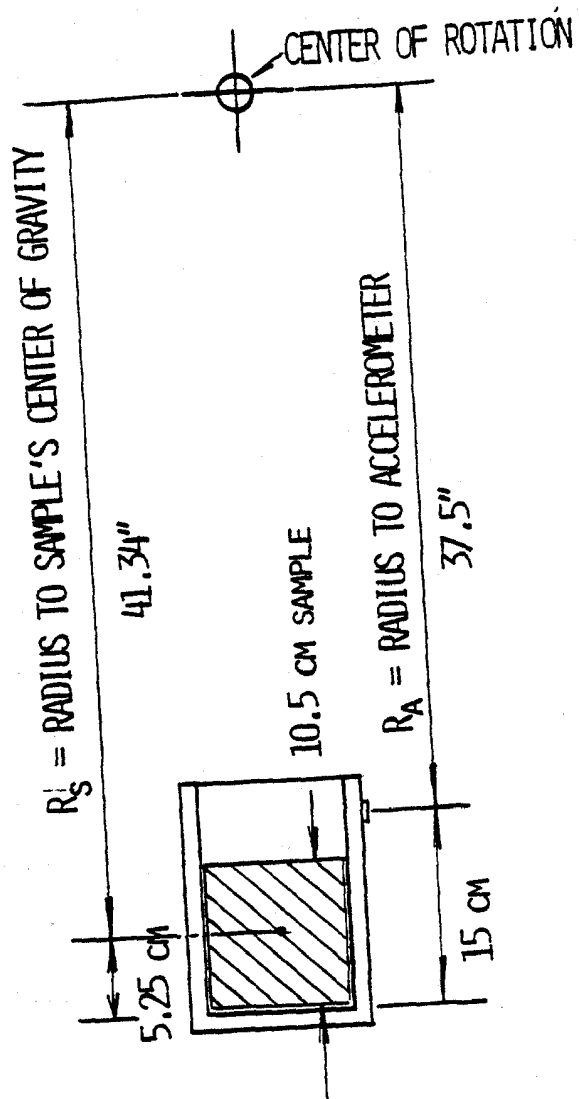
### INSTRUMENTATION

To determine accurately the acceleration levels of the centrifugal models a redundant system of a tachometer and miniature accelerometer is used. Since  $a = r \omega^2$ , a Power Instruments Model 1723 digital tachometer is used to measure the revolutions per minute (RPM) of the spindle. A photoelectric pick-off mounted on the spindle provides the input signal to the tachometer and permits reading the rotational speed to  $\pm 1$  RPM. By knowing the radius to the model centroid from the spindle axis, the test acceleration can be easily calculated as;  $a = (2.84 \times 10^{-5})(\text{RPM})^2 R$  where, R is in inches. For redundancy an Entran model EGA-125F-250D miniature damped accelerometer



is mounted on one of the aluminum buckets at a distance of 37.5 inches from the center of rotation. (Because the center of gravity of the sample is usually not at the same position of the accelerometer, an operational effect must be calculated as illustrated in Figure 10). The applied and output voltages to the accelerometer are conducted through a 32 track Superior Carbon Products, Inc. Model SK-2536-32 slip ring assembly. Coin silver rings are used in the rotor assembly, while silver graphite is used in the brush assembly. The excitation voltage and read-out from the accelerometer is provided by a Doric Series 420 digital voltmeter which reads directly in g units.

When operating the centrifuge at high g levels, the safety of the operator, other laboratory personnel, and the centrifuge becomes a major consideration. In previous testing programs, this meant that testing could be performed only while an operator was present which limited testing to only eight to twelve hours per working day. Accordingly, an electronic safety governor was designed and built to monitor the acceleration voltage of the accelerometer and sense any abnormal acceleration levels. The safety governor allows a predetermined acceleration to be selected; and an appropriate deviation "window" of operation set. In the event the g level rises or falls below the operation "window", power to the centrifuge is interrupted and also to a clock for noting the time of interruption. Typically an operation window of  $\pm 2$  g's is used and continuous centrifuge operation of 50<sup>+</sup> hours has been safely performed.



$$\text{OFFSET ACCELERATION} = N_A = \frac{R_A}{R_S} \times N = \frac{37.5}{41.3} \times 80 \text{ G} = 72.6 \text{ G}$$

WHERE  $N$  = TEST ACCELERATION LEVEL

Figure 10: Calculation of offset acceleration for a 10.5 cm sample

## **TESTING PROCEDURES**

The actual centrifugal model testing of the waste clays is a straightforward, albeit time consuming procedure. Figure 11 presents a flow chart of the procedures followed for these model tests, which shows 4 major events, e.g., (a) Waste Clay Preparation, (b) Centrifuge Operation (c) Post-Test Operations and (d) Data Reduction.

### **Waste Clay Preparation**

The Kingsford waste clay was received from IMC in 55-gal drums, where upon 5 gal subsamples were placed underwater in sealed containers prior to testing. The subsamples were thoroughly mixed with an 18 inch auger bit or wire whip powered by a 1/2 in. electric power drill for approximately 10 minutes prior to testing. An average solids content was obtained ( $S_o = 1/(1+w)$ ,  $w$  = water content) after 24 hours drying in an 110° C oven. The solids content was adjusted upward or downward by adding or siphoning off supernatant water, respectively. The material was then re-mixed and the test solids content verified by a 24 hr. water content determination.

In the cases of flocculant addition, sand/clay mixes, or capping models, additional preparation was required. Usually the untreated waste clay was placed inside the Plexiglas model container, mixed and weighed to determine the proper height of clay required for the model. Subsequently the prescribed flocculant dosage or amount of sand was added to the clay, thoroughly mixed for approximately 1 minute, or if required a cap was placed. A solids content sample was taken and the final model height recorded.

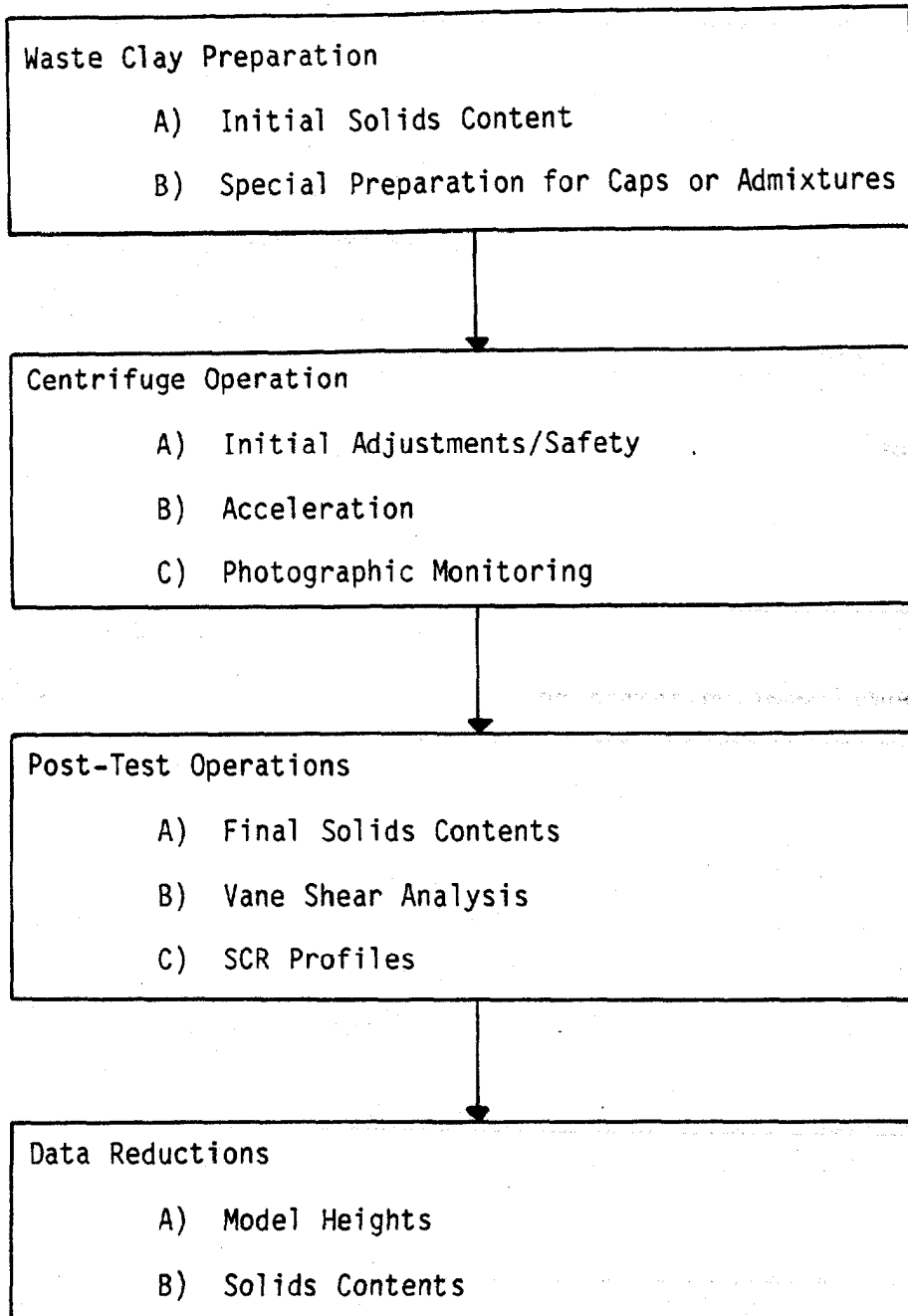


Figure 11 Flow Diagram of Testing Sequence

## Centrifuge Operation

Initial centrifuge preparation consisting of preventative maintenance of the gears, drive system and visual inspection for loose debris was performed. Calculation of the offset acceleration to the tachometer and accelerometer readings was determined, preflight balancing of the arms and adjustment of the over-rotation adjustment bolt performed. (See Parabolic Liquid Surface). The camera and close-up lens were prepared. Next, the safety governor was adjusted for the test acceleration. Subsequent to these pretest preparations, the Plexiglas containers of waste clay were placed in the aluminum buckets, and centrifugation initiated.

Photographic monitoring was initiated upon achieving the test acceleration and continued on a geometric time progression; (i.e., 1, 2, 4, 8 ... minutes). An example of a photographic record is illustrated in Figure 12, Photographic recording would continue until two sequential photos indicated no additional interface movements.

## Post-Test Operations

Upon completion of centrifugation, the Plexiglas containers would be removed and a final solids content determined by oven drying a small sample. In some cases miniaturized vane shear tests were performed to determine a shear strength profile. For some of the sand/clay mix and capped models, corings using a 1/4 inch syringe were made to determine solid content profiles, while sand/clay ratio (SCR) profiles were determined by washing the cored sections through a No. 200 sieve.

### Data Reduction

As the waste clay consolidates during a centrifugal model test, an interface develops between the consolidating clay and supernatant water. This interface is quite visible in the Polaroid® photographs as previously illustrated in Figure 12. Accordingly, the average solids content can be determined as presented in Appendix A;

$$S_i = \frac{S_0}{\frac{1 - (H_t - H_i)[1 - S_0(G_c^{-1})]}{H_t} \frac{G_c}{G_c}} \quad \text{Equation 3.1}$$

In the case of a sand/clay mix the average total solids content, which includes the sand can be determined as also presented in Appendix A:

$$S_i = \frac{1 + SCR}{1 + SCR + \frac{(1 - \epsilon H)(1 - S_0)}{S_0} - \epsilon H \left[ \frac{1}{G_c} + \frac{SCR}{G_s} \right]} \quad \text{Equation 3.2}$$

Equation 3.2 assumes that the clay solids content is the same for both the cap (if one exists) and the underlying clay or s/c mix. In the event that the cap and underlying material are different a more general solution is presented in Appendix B.

In cases of s/c mixes, the average effective clay solids content of the clay fraction only, can be determined as is also presented in Appendix B:

$$S_{ie} = \frac{1}{1 + \frac{1 - S_0}{S_0} (1 - \epsilon H) - \epsilon H \left[ \frac{1}{G_c} + \frac{SCR}{G_s} \right]} \quad \text{Equation 3.3}$$

For equation 3.1, 3.2 and 3.3,

$S_0$  = initial solids content of clays

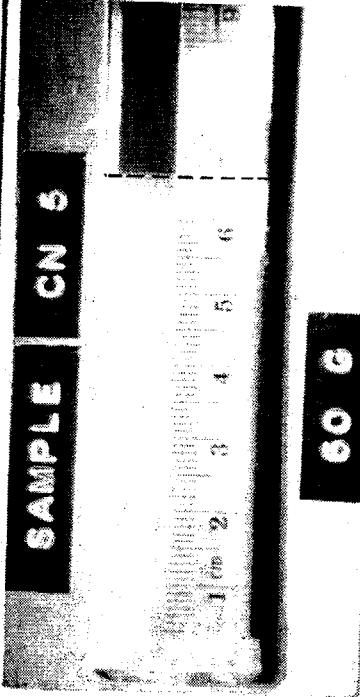
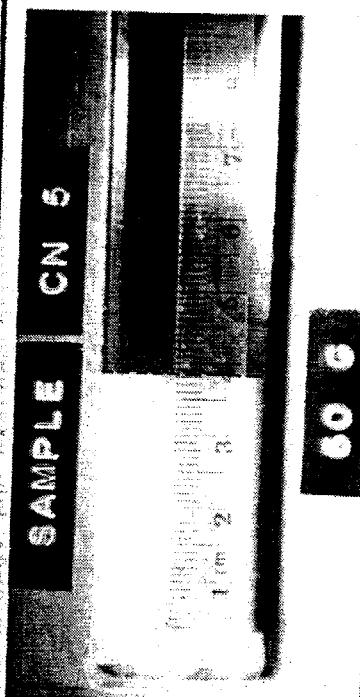
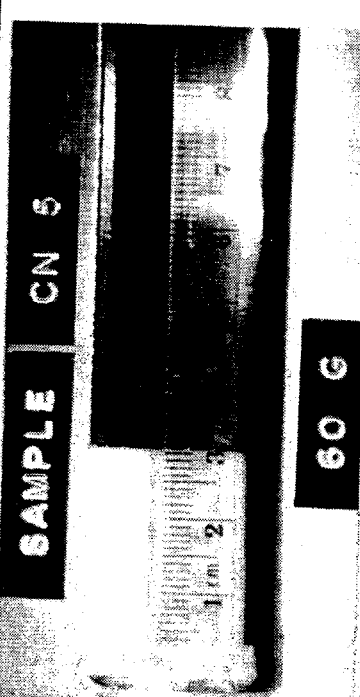
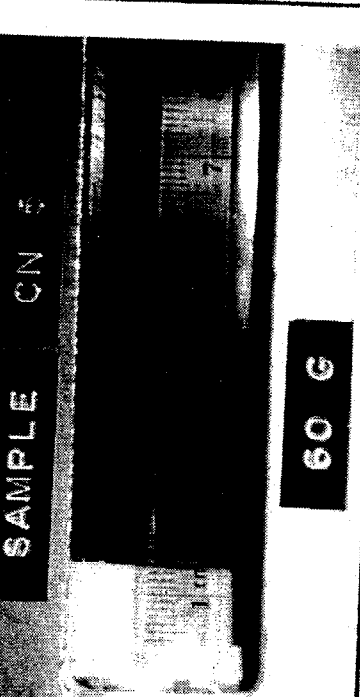
			
ELAPSED TIME : 30 min.	ELAPSED TIME : 17.5 min.	ELAPSED TIME : 28.0 min.	ELAPSED TIME : 611 min.
INTERFACE HEIGHT : 3.8 cm.	INTERFACE HEIGHT : 3.85 cm.	INTERFACE HEIGHT : 3.0 cm.	INTERFACE HEIGHT : 2.5 cm.

Figure 12: Example of Photographic Monitoring

SCR = initial sand/clay ratio of mixture

$G_c, G_s$  = specific gravities of clay and sand, respectively

$$\epsilon H = (H_0 - H_i)/H_0$$

$H_0$  = initial model height

$H_i$  = intermediate model height

## MATERIALS

**Two waste clays were used for different phases of the research reported herein. Specifically, the flocculation studies were performed using Noralyn clay (Bloomquist, 1982), while the sand/clay mix and capping studies (McClimans, 1984) were performed on Kingsford clay. Properties of these clays are shown in Table 3.**



Table 3

Properties of Noralyn and Kingsford Clays

Clay	LL	PI	Gs	pH	CEC	Clay Minerals					Source
						Mont	Interlayer (14A)	Kao	Qtz	Other	
Noralyn	213	181	2.82			Smectite & Palygorskite					Ardaman (1982)
Kingsford	230	156	2.71	7.2	81.9	90%	5%	2%	3%		McClimans (1984)
	231	168									Ardaman (1984)
	207	145				20-50%			5-20%		Lawver (1982)

## CHAPTER IV: PRESENTATION AND DISCUSSION OF RESULTS

### INTRODUCTION

The centrifugal model testing consisted of over 60 tests on Kingsford Clays (McClimans, 1984, Townsend & Bloomquist, 1983) with the objectives of evaluating; (a) the time scaling exponent, "modelling of models", (b) consolidation of sand/clay mixes, and (c) consolidation of capped and uncapped waste clays. In addition, over 15 test results on Noralyn clay (Bloomquist, 1982) evaluating the effects of flocculating agents are reported for completeness in evaluating disposal techniques.

### TIME SCALING RELATIONSHIP (MODELLING OF MODELS)

The objective of this model series was to confirm the modelling exponent for scaling times from consolidation centrifugal model tests. This is often referred to as modelling of models. The time relationship between prototype and model is expressed in equation form as

$$t_p = n^\alpha t_m$$

This equation not only relates prototype to model but may also be used to relate model to model. This is done by performing tests at two (or more) acceleration levels and comparing model times for equivalent solids contents or heights of interface and was the type of analysis performed during this series.

As previously presented in Chapter II, the time scaling relationship is a function of the solids content and varies from  $\alpha = 1$

for sedimentation to  $\alpha = 2$  for consolidation. Several researchers, including Mikasa and Takada (1973) and Croce (1982), have demonstrated the  $N^2$  factor for consolidation. However, their initial solids contents were substantially higher than those found in self weight settlement of phosphatic clays. Similarly, Davidson and Bloomquist (1980) performed a modelling of models on dilute (2-5%) Noralyn phosphatic clay slurry and obtained a time scaling exponent of  $\alpha=1$  for the initial stages of sedimentation. They also found that sedimentation ends when solids contents exceed six to ten percent.

Table 4 summarizes the "modelling of models" tests, while Figures 13 and 14 display the solids content vs time relationships for the waste clays. The series presented in Figure 13 consisted of accelerating three models, 12, 8, and 6 centimeters high to 40, 60, and 80 g's, respectively. The initial solids content for all three models was 14.6%. The duration of the tests varied with the longest (40 g's) requiring 4,200 minutes. All reached approximately 21.3% final average solids content. By selecting particular solids contents corresponding elapsed times of each test, the time scaling exponent,  $\alpha$ , was determined for the various solids contents using the equation (Note: this equation presumes that  $\alpha$  is independent of gravity)

$$t_A(N_A)^\alpha = t_B(N_B)^\alpha$$

The resulting exponents are shown in Figure 14. Similarly, Figure 15 presents the results of two models (KC60/6-0 and KC80-6/0) to confirm the scaling relationship in Figure 14. For these two models the initial solids content was 16.3 percent and initial model heights were 8, and 6

Table 4

## Summary of Time Scaling Relationship Centrifugal Model Tests of Kingsford Clay

Test (a)	Initial Model Conditions				Acceleration (g)	Test Duration (min)	Final Model Conditions		
	clay solids content %	SCR	Model Ht (cm)	Prototype Ht (ft) <sup>(b)</sup>			clay solids content %	Model Ht H <sub>f</sub> (cm)	Prototype Ht H <sub>f</sub> <sup>(b)</sup> (ft)
KC40-12	14.6		12.00	15.70	40	4,200	21.3	7.90	10.3
KC60-8	14.6		8.00	15.70	60	2,340	21.3	5.20	10.2
KC80-6	14.6		6.00	15.70	80	1,405	21.3	3.90	10.2
KC60-8/0	16.3		8.00	15.75	60	4,200	24.11	5.11	10.06
KC80-6/0	16.3		6.07	15.93	80	3,100	23.73	3.95	10.37
KC80-7.9	12.6		7.90	20.73	80	2,500	21.6	4.30	11.3
KC60-0/8	16.3	6:1	8.00	15.8	60	540	24.0	5.98	11.6
HC80-0/6	16.3	6:1	6.08	16.0	80	420	24.3	4.50	11.8
KC80-10	14.6		10.00	26.2	80	2,460	24.0	14.9	14.9
KC40-12	14.6		12.00	15.70	40	5,500	21.3	10.3	
KC60-10.55	12.6		10.55	20.80	60	580	21.8	11.2	
KC80-10.5/0	16.3		10.52	8.42	80	5,100	25.54	6.30	5.04
KC80-6/0	15.96		6.10	4.88	80	2,500	22.97	4.03	3.23

(a) Test Designation: KC80-6/0 means Kingsford Clay, 80 g acceleration level, 6 cm of waste clay, 0 cm cap

(b) Prototype Ht = Model Ht x Acceleration level

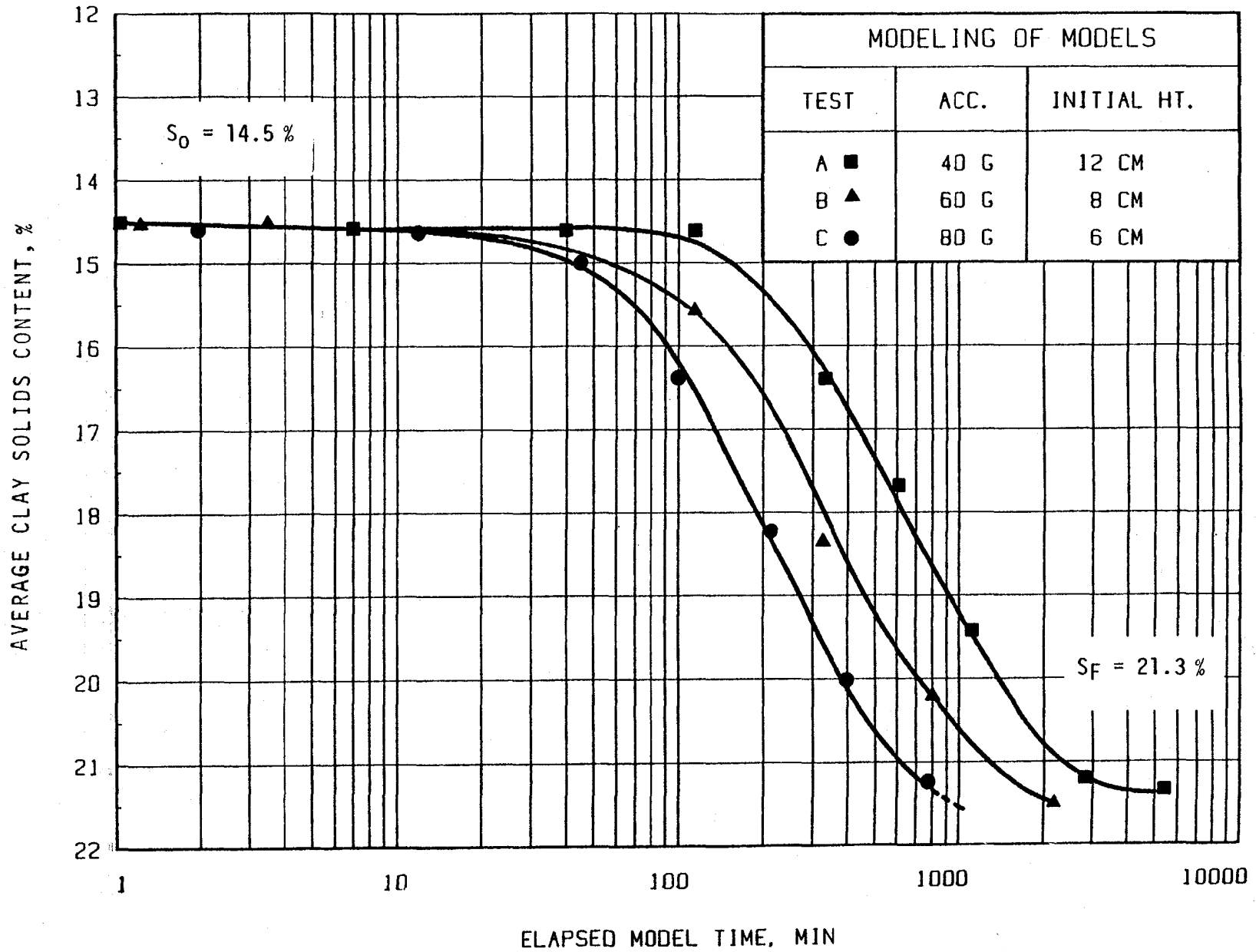


Figure 13: Modelling of Models Program Performed on Kingsford Clay

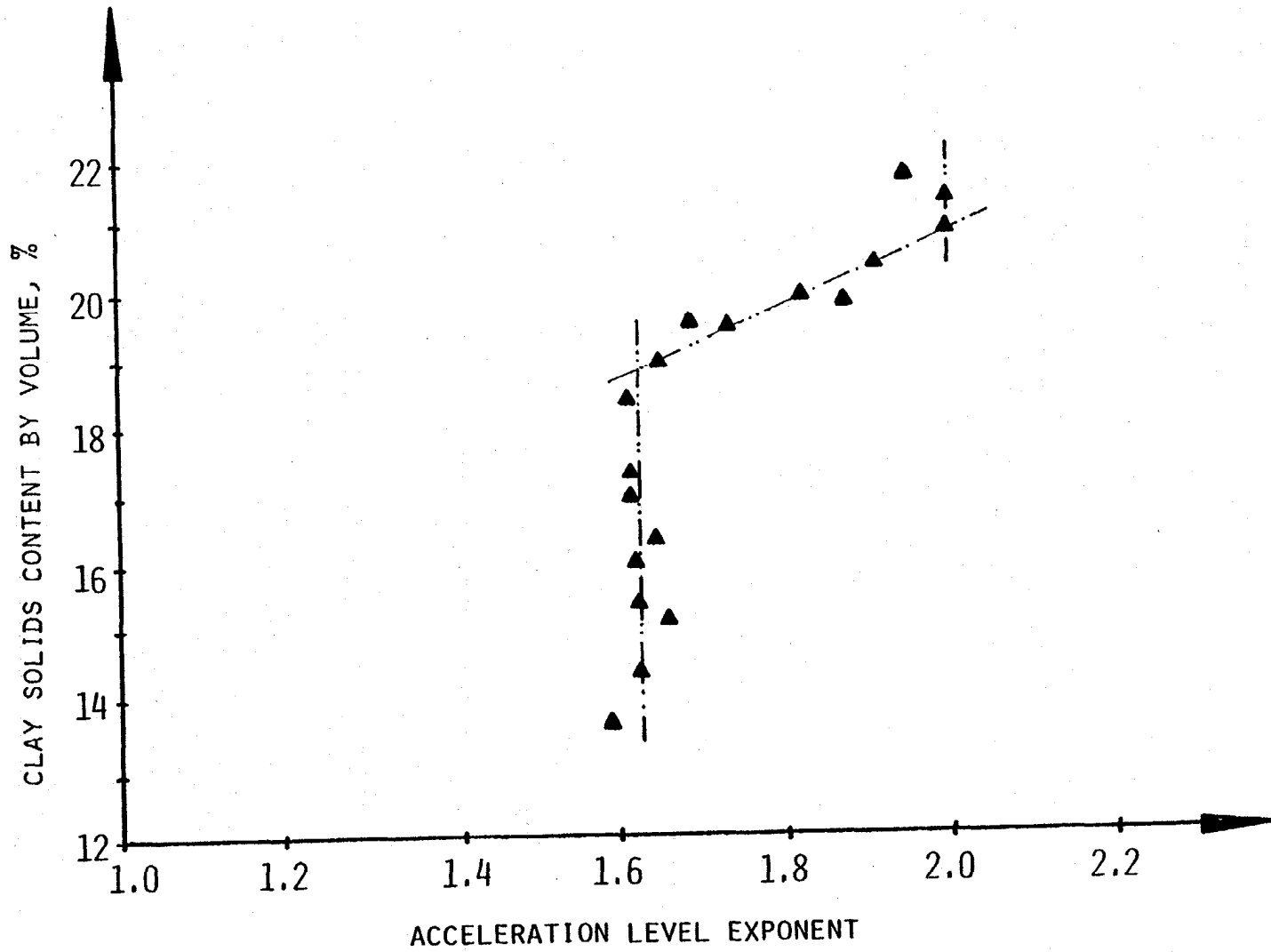


FIGURE 14: Time Scaling Acceleration Exponent, Computed from Modelling of Models Program Results

TEST DESIGNATION: MODELLING OF MODELS (60g AND 80g)

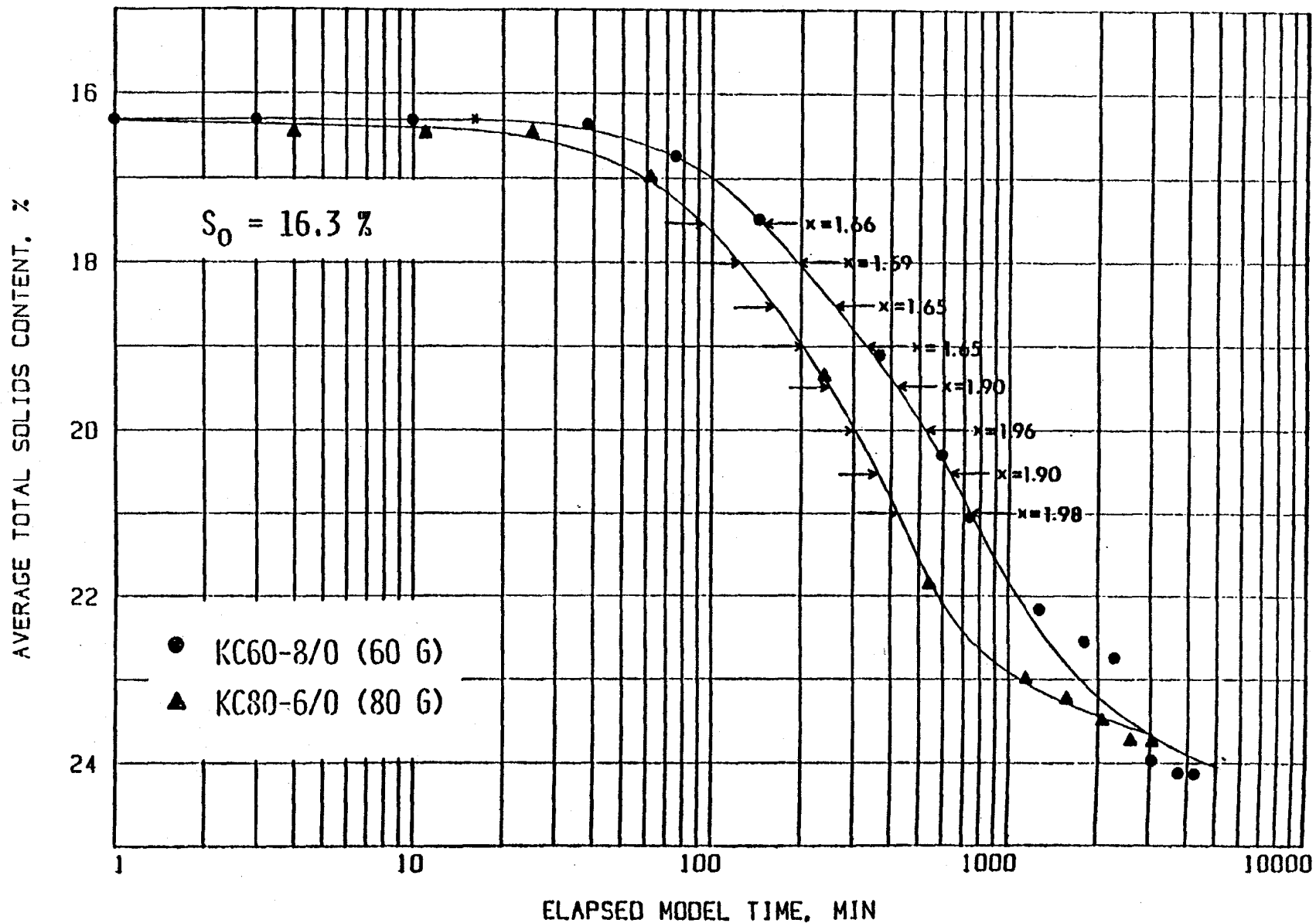


Figure 15: Modelling of Models Analysis Performed on Kingsford Waste Clay

cm respectively for 60 and 80 g acceleration levels. After 4,200 and 3,100 minutes respectively, both models achieved a final average solids content of approximately 24 percent.

The results of these model tests confirm that, while the scaling exponent is 1 for sedimentation and 2 for consolidation, there appears to be a third state (hindered settlement) in which the exponent assumes some intermediate value. For Kingsford clay, with solids contents ranging from 14 to 19 percent, this exponent is approximately 1.6. However, at approximately 19 percent the exponent rapidly increases to 2.0. By explanation, since only the waste clay interface is monitored during the centrifugal test, the time exponent represents a composite of "hindered settlement" plus "consolidation" zones within the model. As these two zones merge, consolidation predominates and the theoretical value of 2.0 is achieved. Since much of the consolidation has occurred prior to merging of these two zones, the value of 2.0 is only achieved at the final stages of the test. Thus from these considerations, it is apparent that scaling up the centrifugal models to prototype times is an incremental procedure and the appropriate time scaling exponent must be used.

#### Prototype Tank Test (Model KC80 - 7.9)

While it is extremely rare to encounter prototype events which can be used to compare centrifugal models, in July 1977, International Minerals and Chemicals filled a 9 x 14 x 22 foot deep metal container with Kingsford clay slurry. The initial solids content was 12.6% and the initial height 20.75 feet. This material was left to self weight settle for a period of 403 days, achieving a final solids content of



21.2 percent. The advantageous aspects of this test in addition to it being of prototype dimensions were: A) it was single drainage test, i.e., the water could only flow vertically upward, B) the tank walls were vertical, and C) the average percent solids was determined using the volume change of slurry. Obviously, these conditions can be exactly duplicated in a centrifugal model. Accordingly, model KC80-7.9 consisted of a 7.9 cm high model of Kingsford clay at 12.6% solids and was accelerated to 80 g's for 2,500 minutes. (Consolidation actually ceased after 1,470 minutes) Figure 16 presents a comparison between the IMC tank test and the centrifugal model using a time scaling exponent equal to 1.6. That is, 1 minute of model time is equivalent to  $(80)^{1.6}$  or 1,109 minutes of prototype time. The agreement is excellent, thereby validating the "modelling of models" technique of determining scaling exponents.

#### Self Weight Consolidation

An examination of all the centrifugal model tests summarized in Table 4 reveal that the final solids content achievable is slightly dependent upon the initial solids content and depth of the waste pond. Typically, for waste ponds between 15.7 and 26.2 ft. deep, a final solids content of approximately 21 to 24 percent will be achieved. Using a time scaling exponent of 1.6, approximately 2,000 days (5.3 yrs.) will be required for self-weight consolidation. Thus alternative reclamation methods become attractive.

#### SAND CLAY MIX EVALUATION

The objectives of this test series were to (a) evaluate the benefits of sand/clay mix for reclamation, (b) establish the time

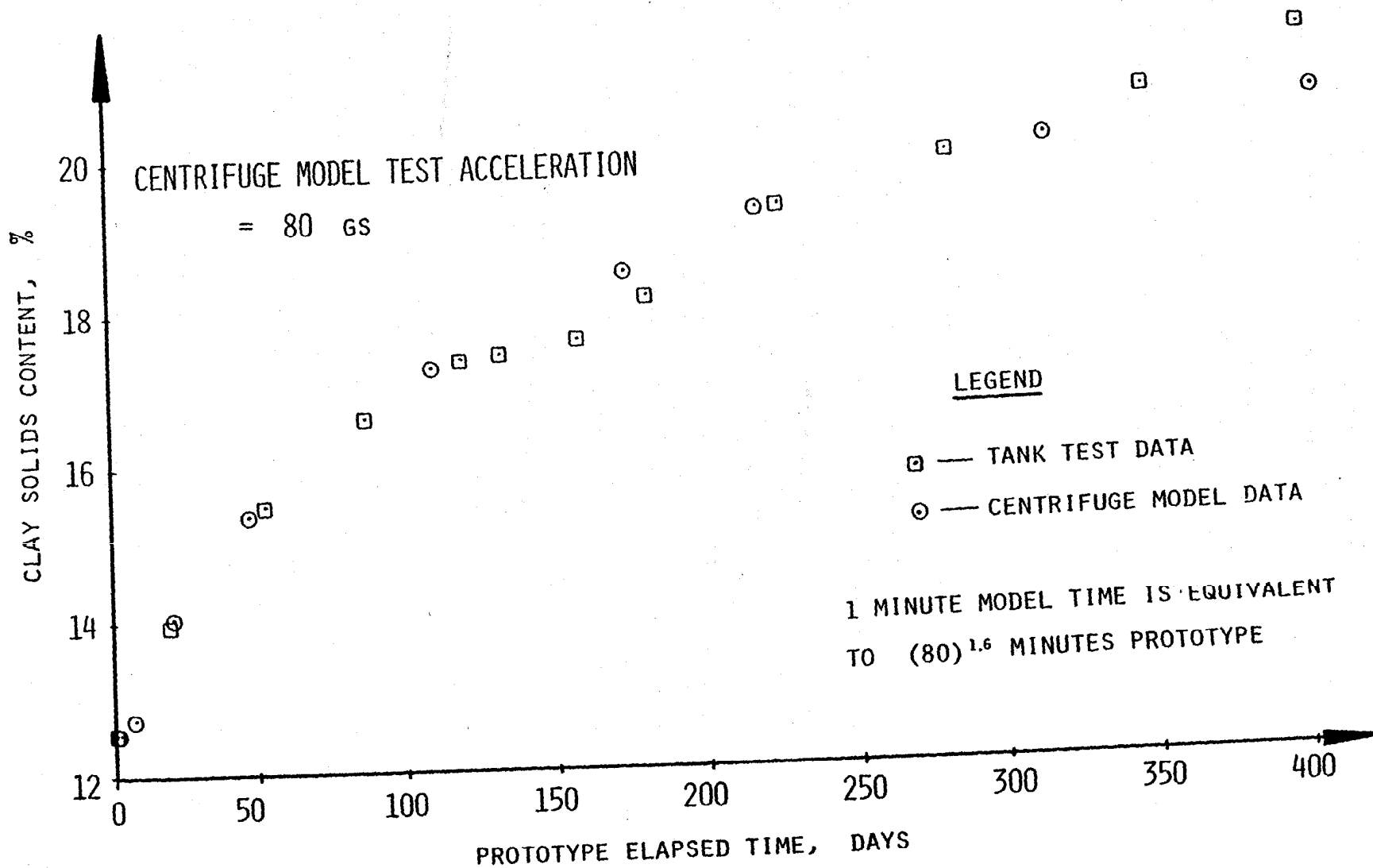


Figure 16: Comparison of Centrifuge Model and IMC Tank Test

scaling exponent for sand/clay mixes, (c) evaluate the effect of the sand:clay ratio (SCR), and (d) determine sand grain size effects (if any) on consolidation. Accordingly, three SCR (1:1, 3:1, and 6:1) were modelled centrifugally at 60 and 80 g's using various sand gradations as summarized in Table 5.

#### S/C Time Scaling Exponent

Having developed the time scaling exponent for Kingsford waste clay, two models (KC 60-0/8 and KC 80-0/6) were tested to determine this scaling exponent for s/c mixtures. Model KC60-0/8 of 8 cm with a 6:1 sand/clay ratio and initial clay solids of 16.3 percent was accelerated to 60 g's. (Figure 17 presents the grain size distribution curve for the material used in these tests.) The total duration of this test was about 500 minutes. The model had a final height of 6.0 cm and an effective clay solids content of 24.0 percent. Model KC 80-0/6 of 6 cm with a 6:1 sand/clay ratio and initial clay solids of 16.3 percent was accelerated to 80 g's. The total duration of this test was about 400 minutes. The model had a final height of 4.5 cm and an effective clay solids content of 24.3 percent. Figure 18 shows the relationship between effective clay solids content and elapsed model time.

A modelling of models analysis was performed. A particular solids content was chosen; the corresponding elapsed model time were noted. Using the equation

$$t_{60}(60)^x = t_{80}(80)^x$$

Table 5

## Summary of sand/clay mix centrifugal model tests

Test	Initial Model Conditions				Proto- type height $H_0$ (ft)	Proto- type height $H_0$ (ft)	Accele- ration (g)	Test duration (min)	Final Model Conditions				
	initial clay solids content, %	sand/ clay ratio	sand	total solids content, %					Model height $H_0$ (ft)	Effective clay solids content, %	Total solids content, %	Model height $H_f$ (cm)	Prototype height $H_f$ (ft)
KC80-0/6	16.0	1:1	20-40	27.7	6.00	15.8	80	1,420	23.9	39.0	3.95	10.4	34.2
KC80-0/6	16.0	1:1	40-100	27.7	6.00	15.8	80	1,420	25.3	40.8	3.72	9.8	38.0
KC80-0/6	16.0	1:1	100-200	27.7	6.05	15.9	80	1,420	24.9	40.6	3.78	9.9	37.5
KC80-0/6	16.0	1:1	200+	27.7	6.10	16.0	80	1,420	24.4	39.9	3.90	10.2	36.1
KC80-0/6	16.0	1:1	rock flour	27.7	6.05	15.9	80	2,070	24.8	40.4	3.80	10.0	37.2
KC80-0/2	16.0	3:1	40-100	43.2	2.10	5.5	80	1,120	22.7	54.1	1.52	4.0	27.6
KC80-0/3	16.0	3:1	40-100	43.2	2.90	7.6	80	1,120	24.0	55.8	2.00	5.3	31.0
KC80-0/4.5	16.0	3:1	40-100	43.2	4.60	12.1	80	2,490	24.6	56.7	3.10	8.1	32.6
KC80-0/10.5	16.0	3:1	40-100	43.2	10.50	27.6	80	3,110	27.4	60.1	6.45	16.9	38.6
KC60-0/4	16.3	6:1	Fig. 17	57.7	4.00	7.9	60	540	23.9	68.7	3.00	5.9	25.0
KC60-0.6	16.3	6:1	Fig. 17	57.7	5.85	11.5	60	540	23.8	68.6	4.40	8.7	24.8
KC60-0/8	16.3	6:1	Fig. 17	57.7	8.00	15.8	60	540	24.0	68.8	5.98	11.8	25.3
KC80-0/3	16.3	6:1	Fig. 17	57.7	2.90	7.6	80	925	22.1	66.5	2.30	6.0	20.7
KC80-0/4.5	16.3	6:1	Fig. 17	57.7	4.60	12.1	80	925	25.4	70.4	3.30	8.7	28.3
KC80-0/6	16.3	6:1	Fig. 17	57.7	6.08	16.0	80	420	24.3	69.2	4.50	11.8	26.0
KC80-0/5	16.0	6:1	20-40	57.1	6.00	15.8	80	1,325	25.4	69.8	4.30	11.3	28.3
KC80-0/6	16.0	6:1	40-100	57.1	6.00	15.8	80	1,325	24.4	68.6	44.3	11.6	26.2
KC80-0/6	16.0	6:1	100-200	57.1	6.00	15.8	80	1,325	22.6	66.5	4.68	12.3	22.0
KC80-0/10.5	16.0	6:1	40-100	57.1	10.50	27.6	80	1,330	25.8	70.2	7.45	19.6	29.1

KC80-0/6 means KC = Kingsford clay, 80 = acceleration level, 80 g's, - 0/6 = no untreated clay/6cm s/c mix

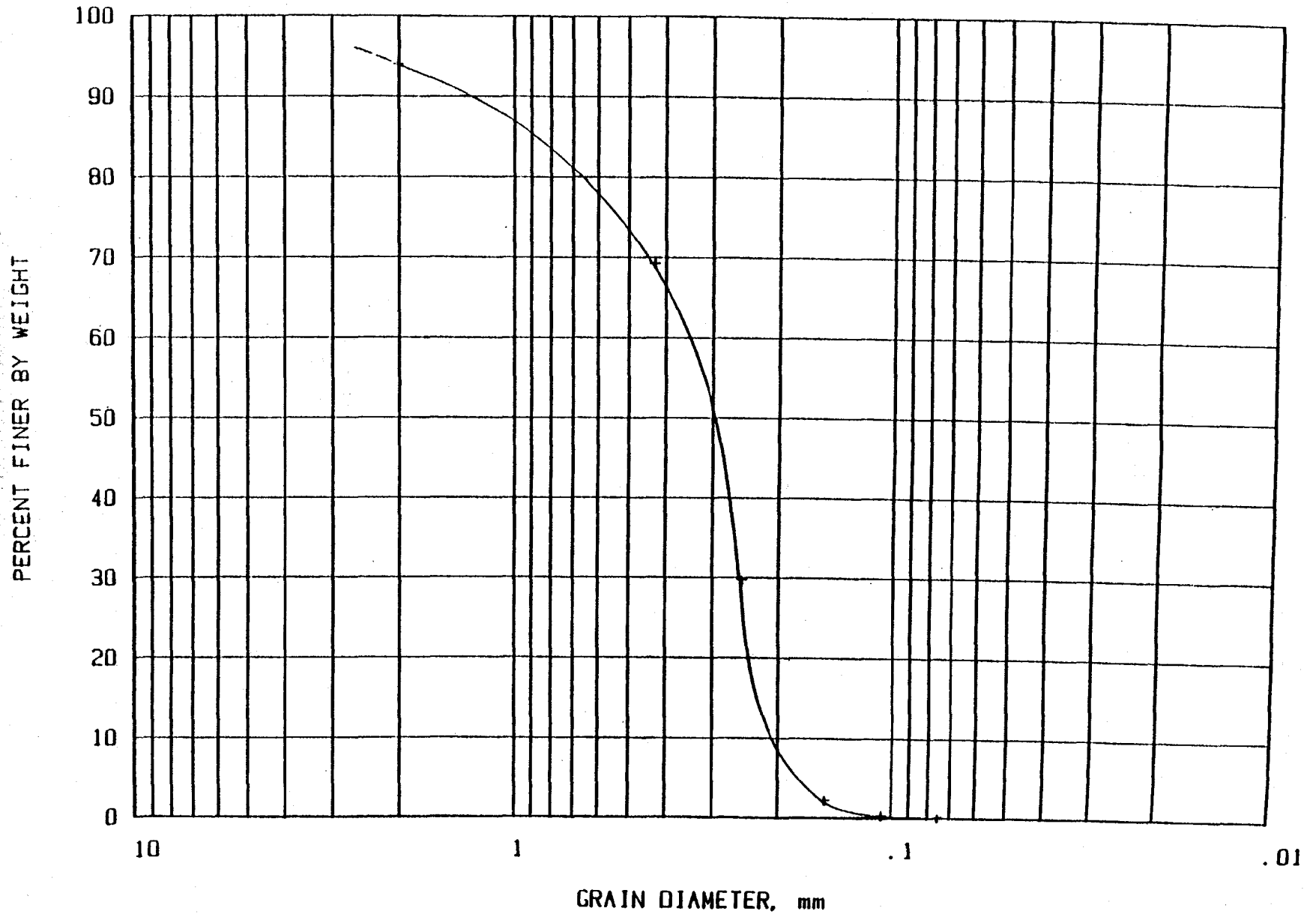


Figure 17. Grainsize distribution for sand used in sand/clay mix modelling of models and initial capping tests

TEST DESIGNATION: MODELLING OF MODELS (60g AND 80g (6:1 SCR))

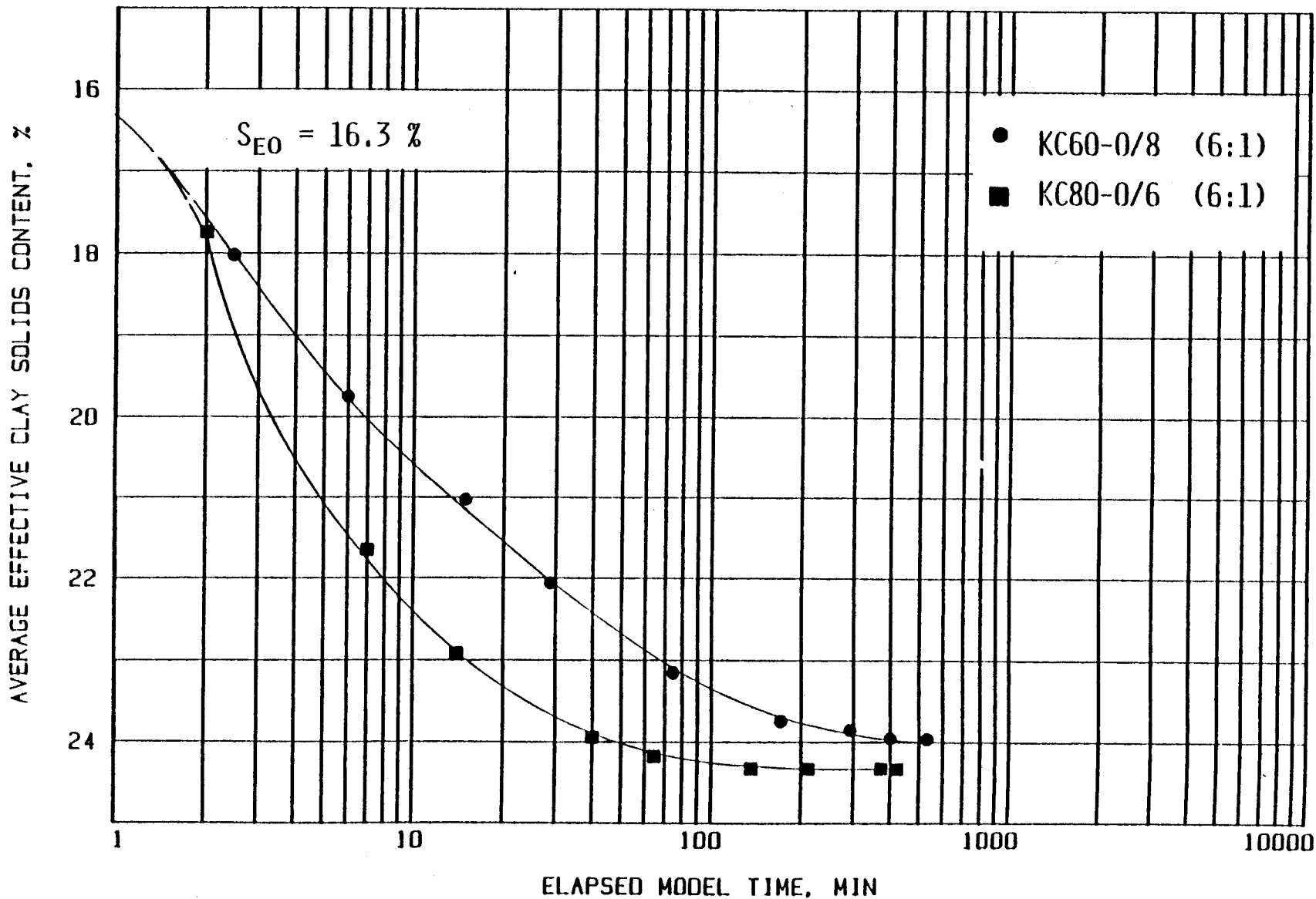


Figure 18: Modelling of models analysis performed on 6:1 sand/clay mix (effective clay solids content)

the exponent  $x$  was determined for a range of effective clay solids contents as presented in Figure 19.

As can be seen, it appears that no unique time relationship between model and prototype exists for high ratio (6:1) sand/clay mixes. At this time, we do not understand the phenomenon causing this discrepancy in scaling exponents, but suspect it is attributable to segregation of the sand and clay. While the lack of a time scaling exponent does not jeopardize centrifugal modelling of sand/clay mixes for comparing reclamation schemes, it does limit our abilities to estimate prototype times!

#### SCR Effect

The data presented in Figure 20 illustrates the effect of SCR on consolidation behavior. Models KC80-0/6 (1:1) and KC80-0/6 (6:1) were 6.0 cm high models of 1:1 and 6:1 SCR using a uniform sand size between the No. 40 to No. 100 sieves and clay solids content of 16.0%. For comparison, Model KC80-6/0 was a 6.07 cm high model of untreated waste clay at 16.30%. By accelerating these models to 80 g's, a prototype pond 15.8 ft. deep was simulated. As shown in Figure 20, the 6:1 mix settles most rapidly; however, the greatest reduction in height is obtained for a 1:1 mix. Thus a tradeoff exists between consolidation rate and final solids content. Obviously, as the SCR increases, the volume of sand in the mix increases correspondingly at the expense of a reduction in clay and water volume. If the SCR is high (6:1), the sand being incompressible quickly achieves its densest packing and interference between particles prevents further densification of the clay and less consolidation is achieved than for the untreated waste clay (SCR = 0).

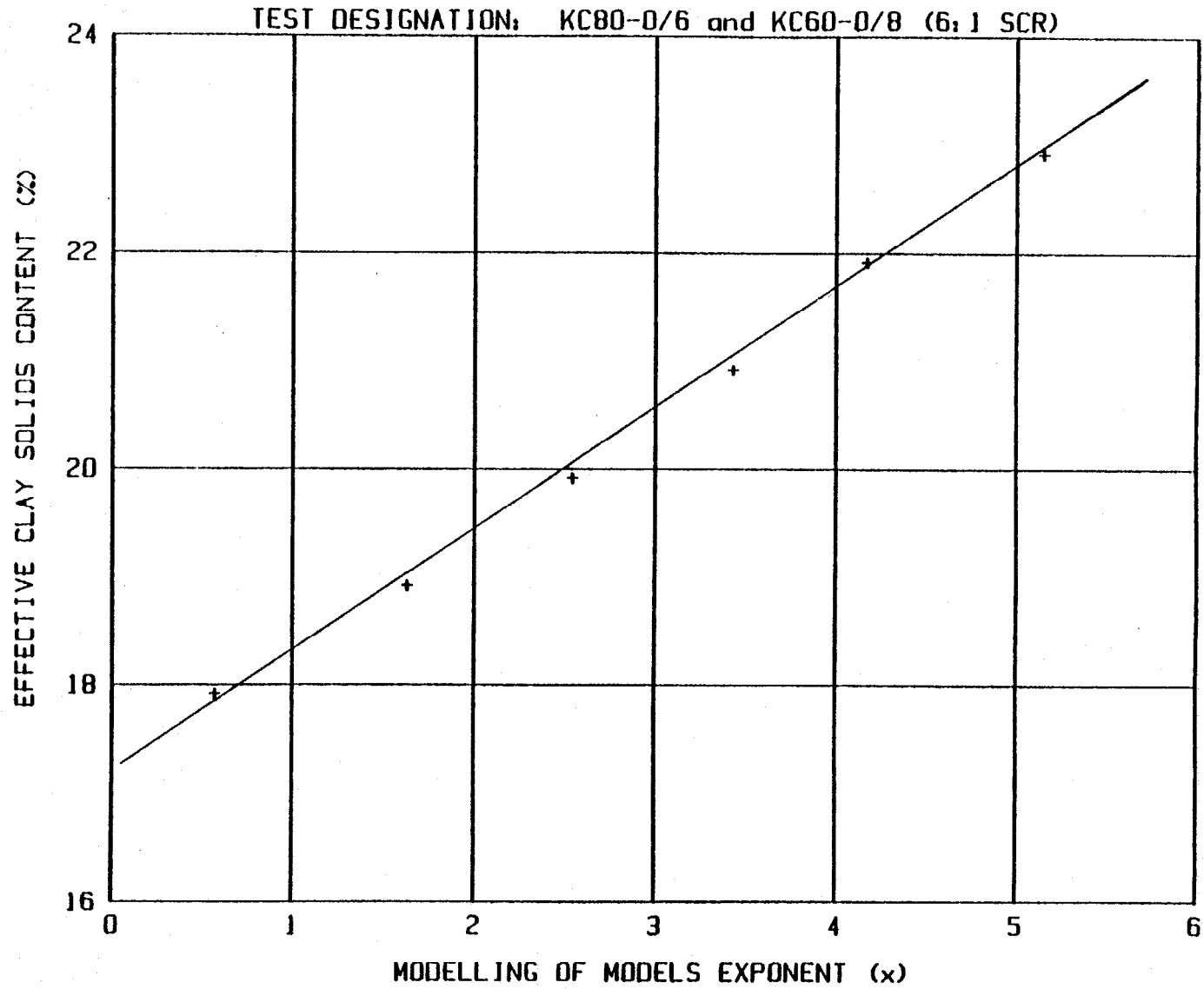


Figure 19: Time scaling exponent computed from modelling of models analysis, 6:1 sand/clay mix (effective clay solids content)



TEST DESIGNATION: KC80-0/6 (6:1 and 1:1 SCR)

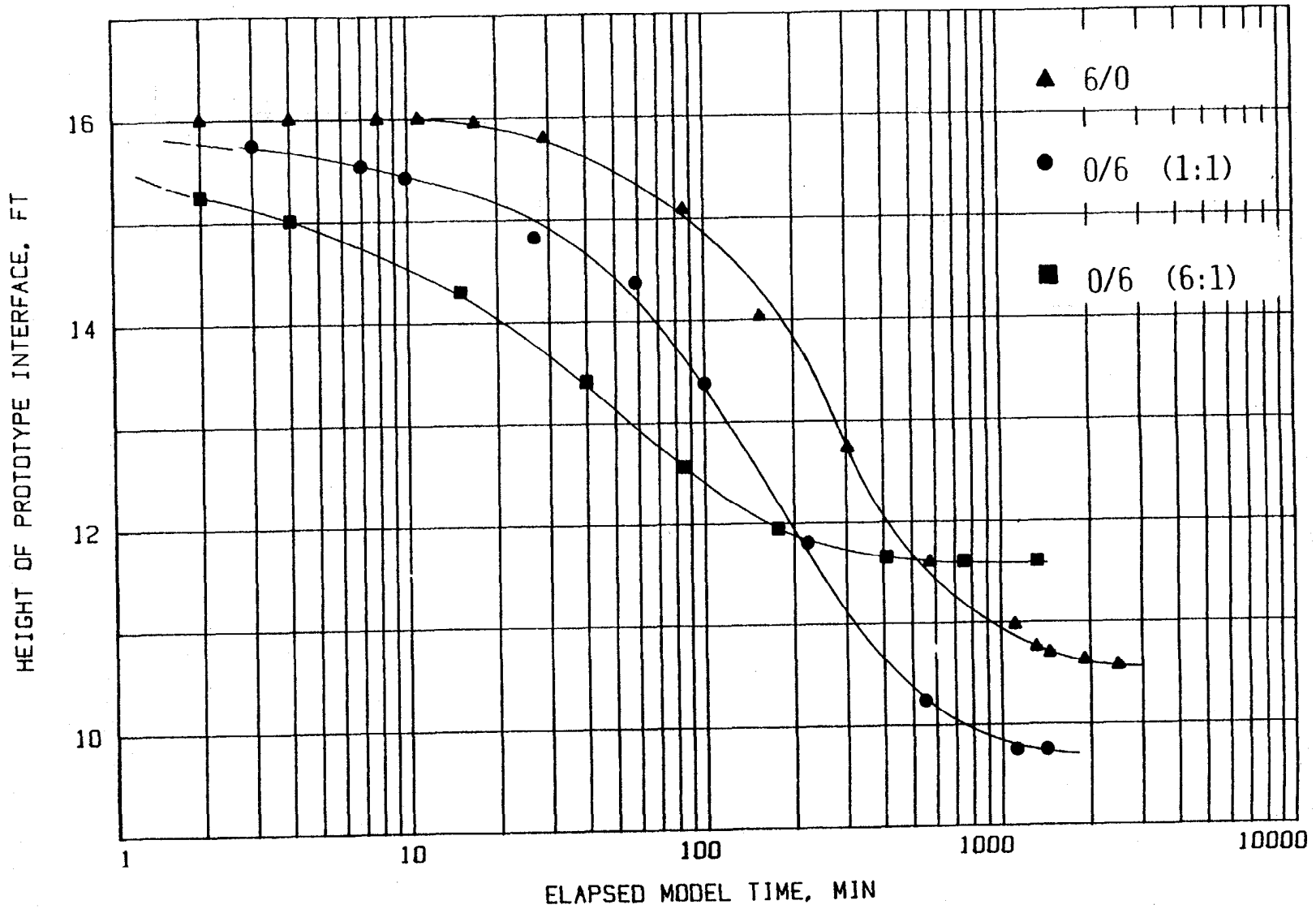


Figure 20: Prototype interface vs model time for test series KC80-0/6 (1:1 and 6:1 sand/clay mix, 40-100 sand) and KC80-6/0

Figure 21 presents the relationship between SCR and settlement, and suggests that the optimum SCR is 1:1 or 2:1 and that SCR's greater than 3:1 will produce less consolidation. Closer inspection of Figure 21 reveals that the advantage of using a 1:1 s/c mix compared to virgin clay results in a modest improvement in height reduction (37.5% vs 33.9%) or final clay solids content (24.9 vs 22.97). This result is consistent; in that the buoyant unit weight of the 1:1 SCR is 13.05 pcf (209.1 Kg/m<sup>3</sup>) compared with 6.96 pcf (111.50 Kg/m<sup>3</sup>) for the virgin clay. Accordingly, this higher unit weight produces a higher effective stress and consequently a high solids content.

#### Effect of Grain Size

During several of the capping tests (to be discussed later), entrained sand in the overlying cap tended to segregate and move through the underlying waste clay towards the bottom of the sample. (The gradation curve for the sand used during these initial tests can be found in Figure 17.) This segregation is a possible artifact of centrifugal modelling and warranted investigation.

The primary advantage of centrifugal modelling is that prototype stress levels can be modelled in a sample of reduced physical scale. While acceleration increases the stress levels within a sample, it does nothing to increase the shear strength of the clay slurry. A typical waste clay is more than 90 percent water (by volume). When a sand grain is introduced into the clay slurry and the sample is accelerated, the weight of the individual grain will increase proportionally. The shear strength will remain unchanged. While the shear strength of the slurry may be sufficient to support the sand grain under earth's gravity (1 g),

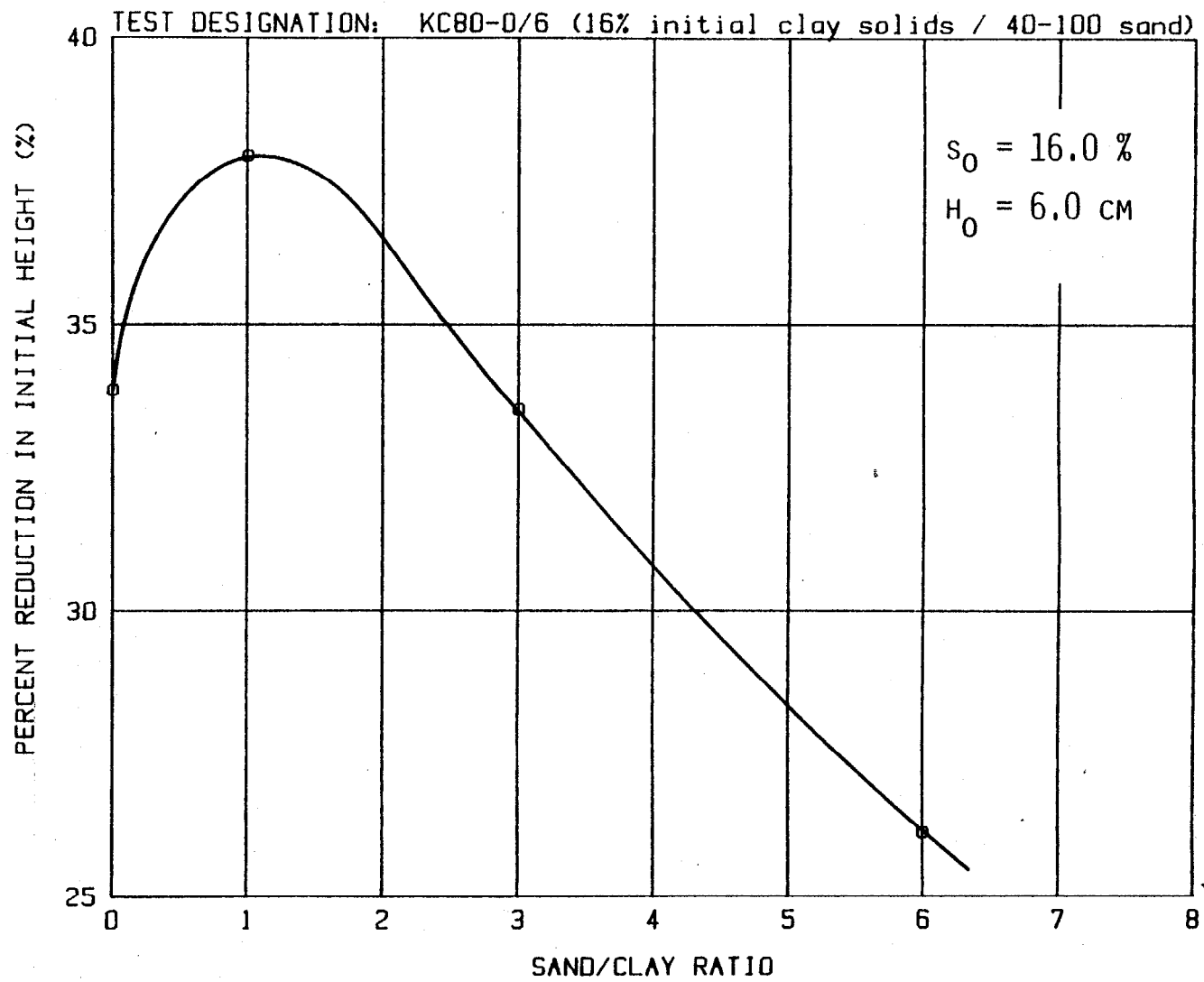


Figure 21: Percent reduction in height  $\left(\frac{H_0 - H_F}{H_0} \times 100\right)$  vs sand/clay ratio for test series KC80-6/0 and KC80-0/6.

it may or may not be able to support the grain under accelerated conditions. Thus segregation occurred when the weight of the entrained sand grains exceeded the clay slurry's small yield strength and the grains began movement toward the bottom of the sample. This phenomena needed to be studied more closely since it could have great bearing on the applicability of centrifugal modelling for sand/clay suspensions.

The segregation phenomena implies that a relationship exists between particle weight (hence size) and the ability of the slurry to keep such particles in suspension. Cardwell (1941) suggests the following relationship for mud suspensions.

$$D = \frac{6C_s}{(p - p_s) g}$$

where

- D is the particle diameter
- p is the density of the particle
- p<sub>s</sub> is the density of the slurry
- g is acceleration due to gravity
- C<sub>s</sub> is the shear strength of the slurry.

Weiss (1967) suggests a similar relationship.

$$D = \frac{3}{2} \frac{\tau_f}{\gamma - \gamma_f}$$

where

- D is the particle diameter
- $\gamma$  is the unit weight of the particle
- $\gamma_f$  is the unit weight of the fluid
- $\tau_f$  is the shear strength of the slurry.

As can be seen, both formulas are of similar form, they vary, however by a factor of 4. Since both equations require slurry strength as an input,

a series of viscosity tests using a co-axial viscometer were performed. Figure 22 presents these test results in terms of clay solids content and the Bingham Yield Point (shear strength). From these results (Figure 22) the relationships between maximum particle size, solids content, and acceleration level are presented in Figures 23, 24, and 25 for both the Weiss and Cardwell equations. These results indicate that the maximum particle size able to remain in suspension for a slurry with a clay solids of 16 percent accelerated to 80 g is 0.004 mm (Cardwell) or 0.001 mm (Weiss). This implies that it is not possible for particles larger than silt size (0.002 to 0.06 mm) to remain in suspension when such a slurry is accelerated to 80 g.

To evaluate this hypothesis, a series of seven tests KC80-0/6 (1:1) and KC80-0/6 (6:1) were performed; these tests also analyzed the effect of sand/clay ratios on consolidation characteristics (discussed earlier). Figures 26 and 27 present results for these 1:1 and 6:1 sand/clay mixes. Four different mix materials were tested: (1) sand passing the No. 20 sieve (0.84 mm) but retained on the No. 40 sieve (0.42 mm); (2) 40 to 100 (0.42 to 0.147 mm); (3) 100 to 200 (0.147 to 0.074 mm); (4) that material passing the No. 200 sieve (<0.074 mm).

Results for the 1:1 s/c mix tests indicate that grain size has a small, but measureable effect on the final height of interface. After analyzing the final results, however, it is difficult to say whether a distinct relationship exists between reduction in interface height and grain size. Interface height was reduced most by the 40 to 100 mix, followed by the 100 to 200, 200 minus, and 20 to 40 mixes. While grain size for each mix is different, the total weight of sand per unit volume

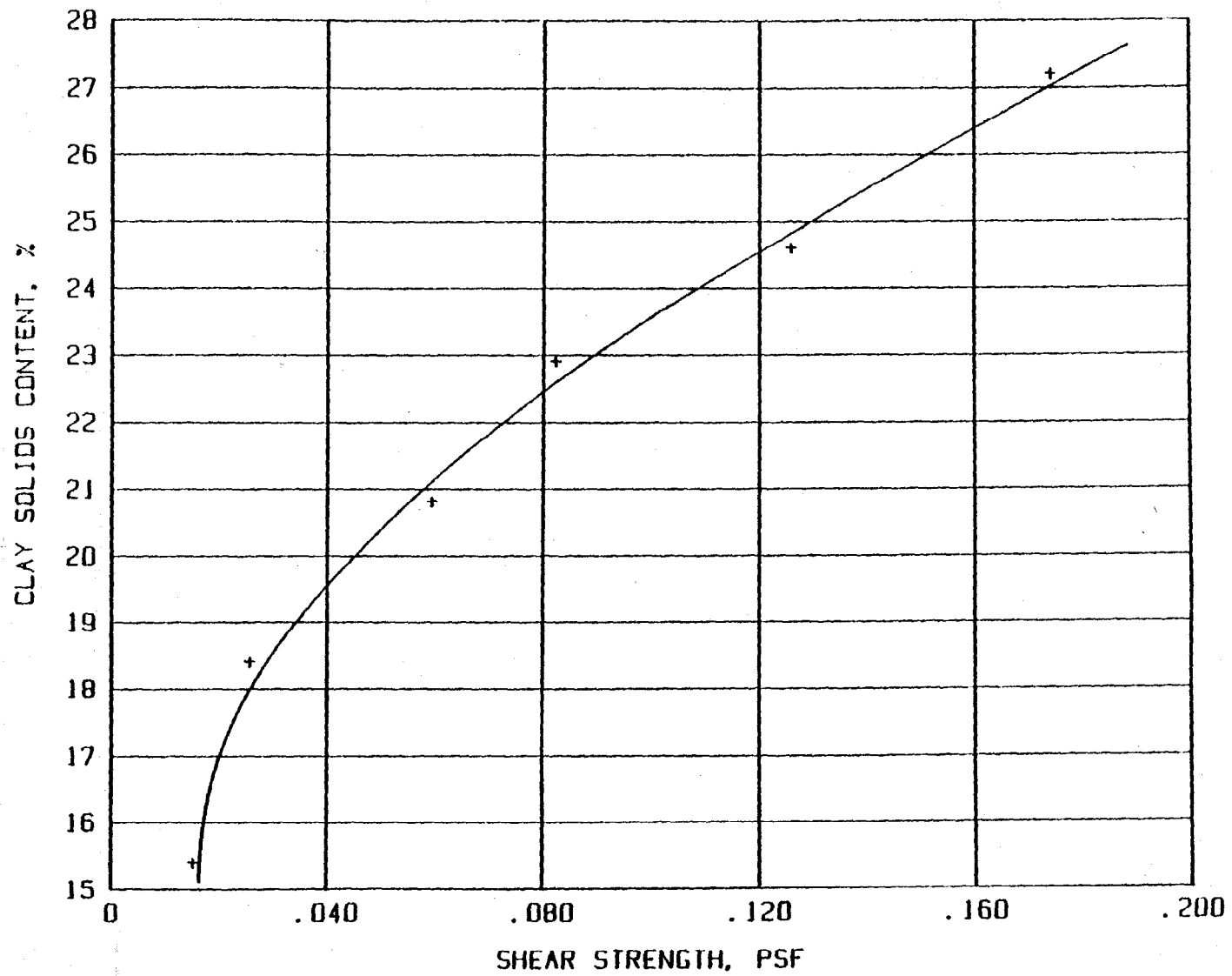


Figure 22: Clay solids content vs shear strength based on plastic viscosity

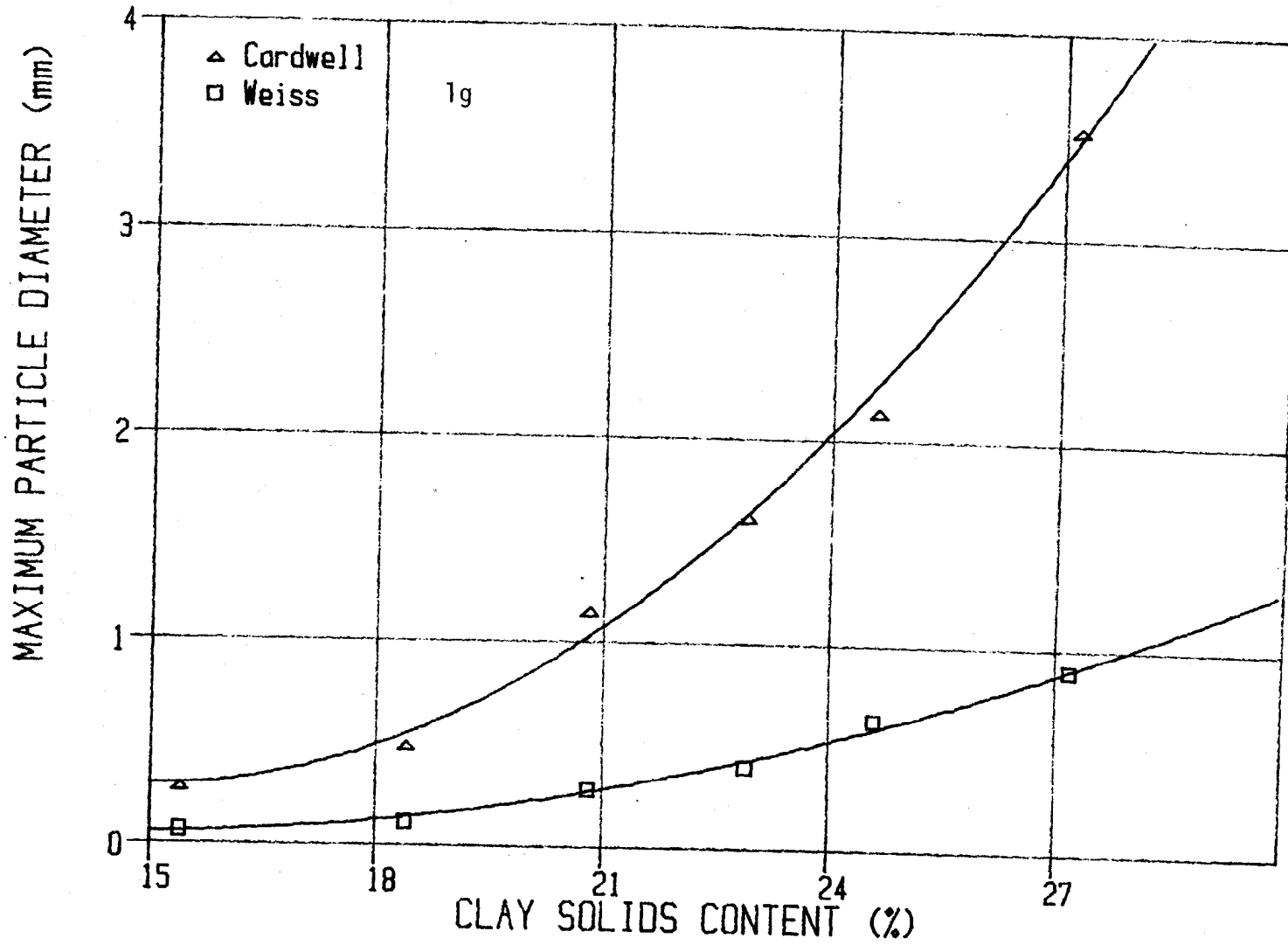


Figure 23: Maximum particle diameter vs clay solids content for both the Cardwell and Weiss equations (acceleration = 1g)

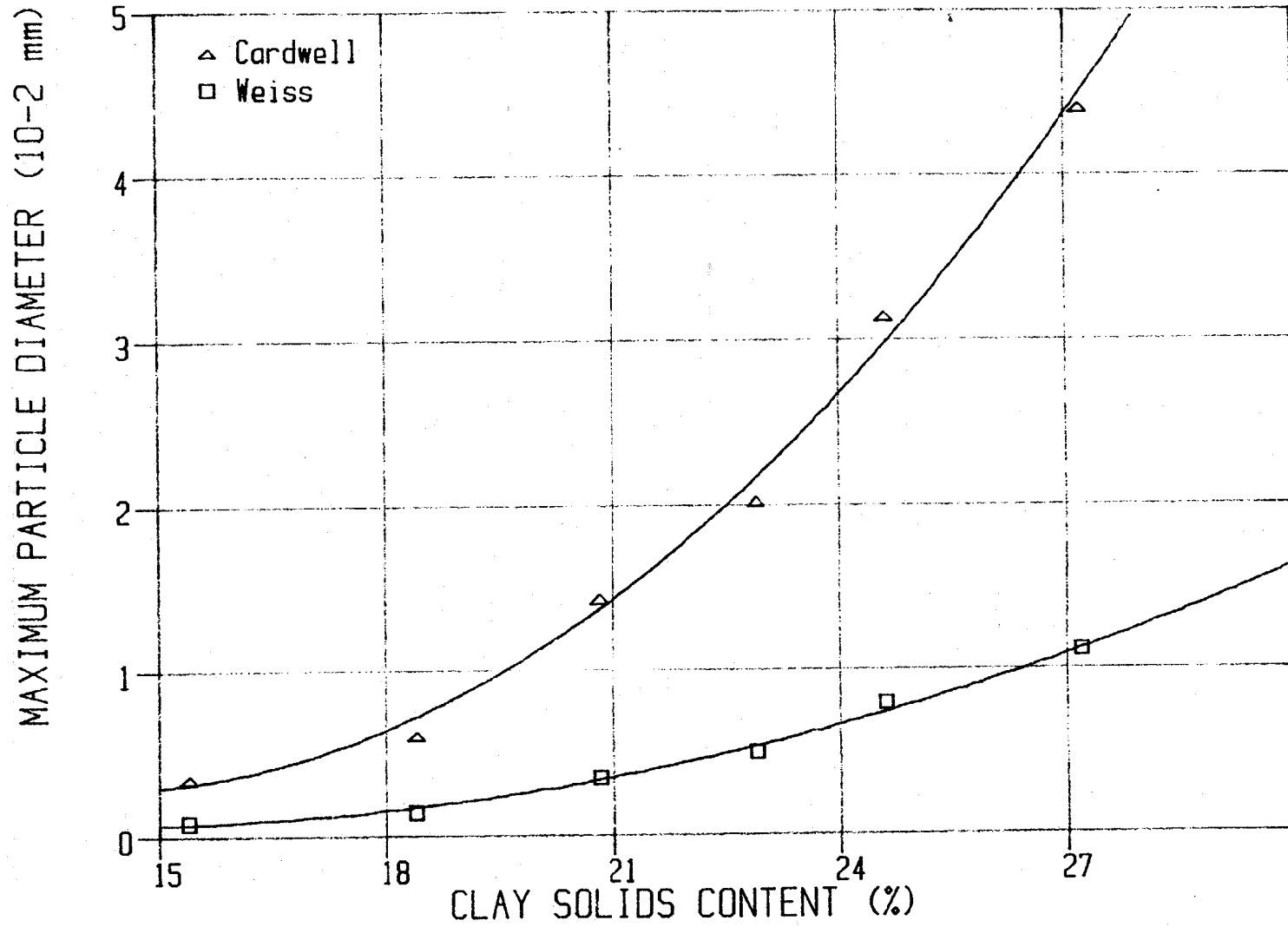


Figure 24: Maximum particle diameter vs clay solids content for both Cardwell and Weiss equations (acceleration = 80g)



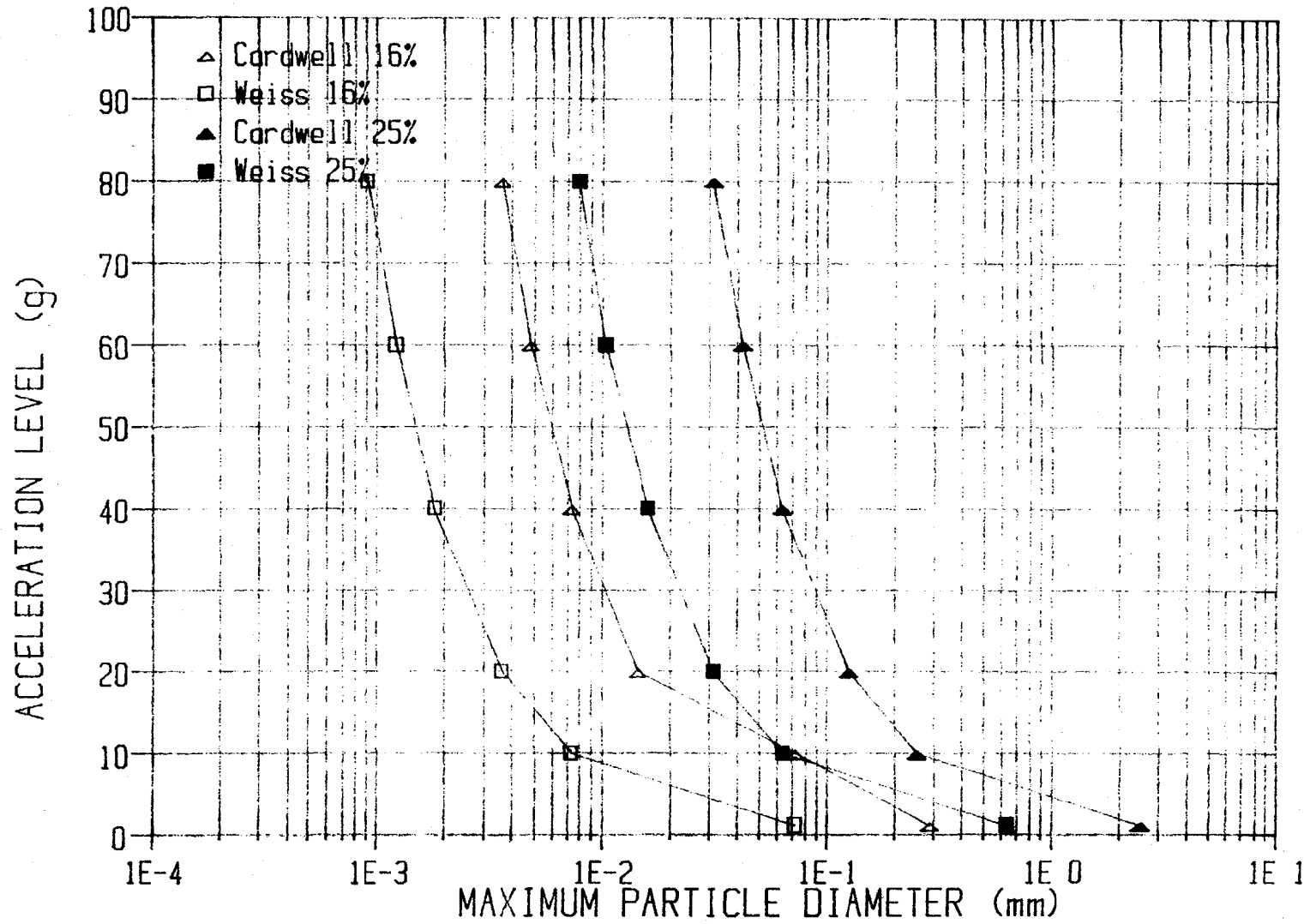


Figure 25: Acceleration level vs maximum particle diameter for both Cardwell and Weiss equations (16% and 25% clay solids)

TEST DESIGNATION: KC80-0/6 (1:1 SCR SERIES)

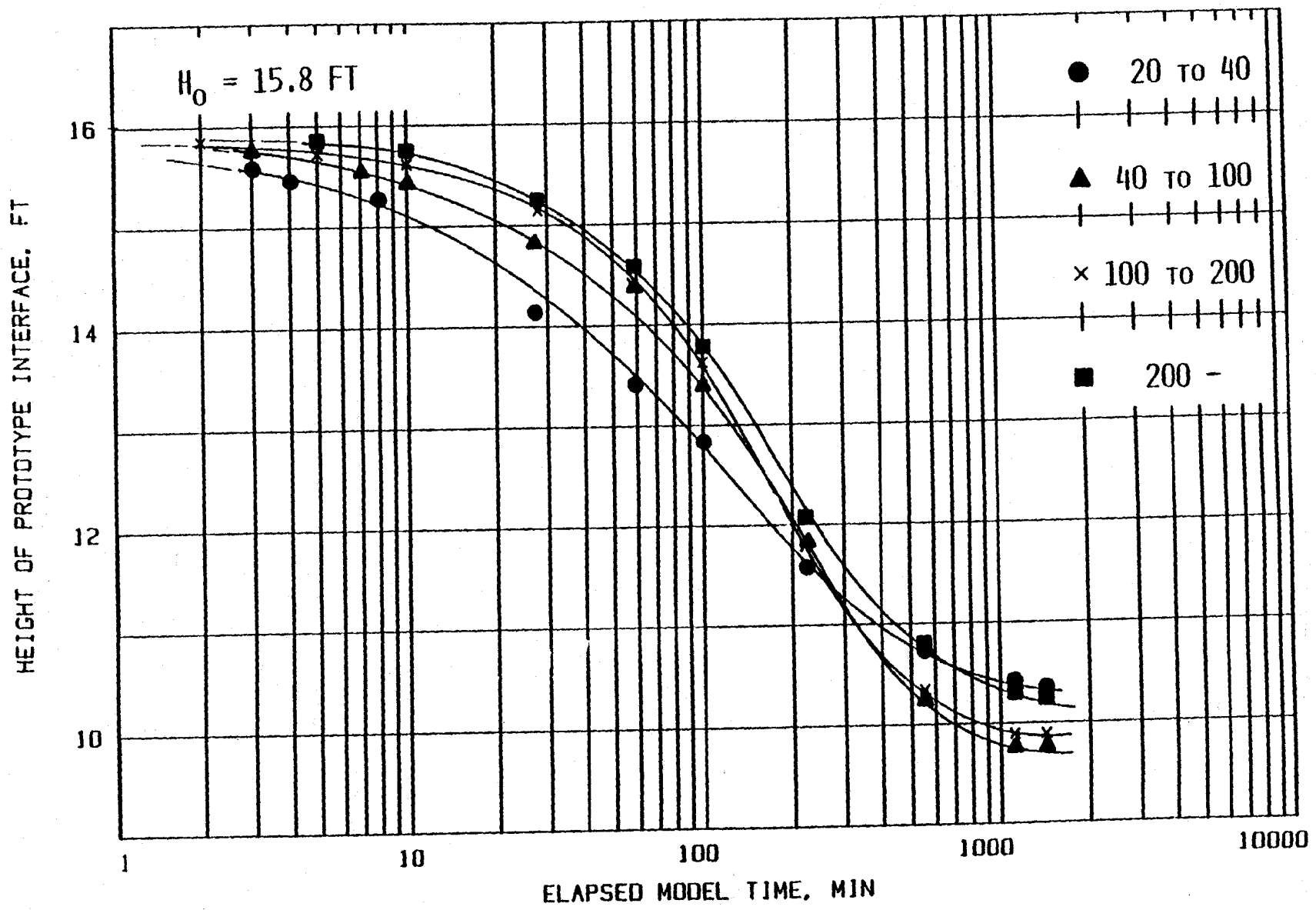


Figure 26: Prototype interface vs model time for the test series KC80-0/6 (1:1 sand/clay mix)

TEST DESIGNATION: KC80-0/6 (6:1 SCR SERIES)

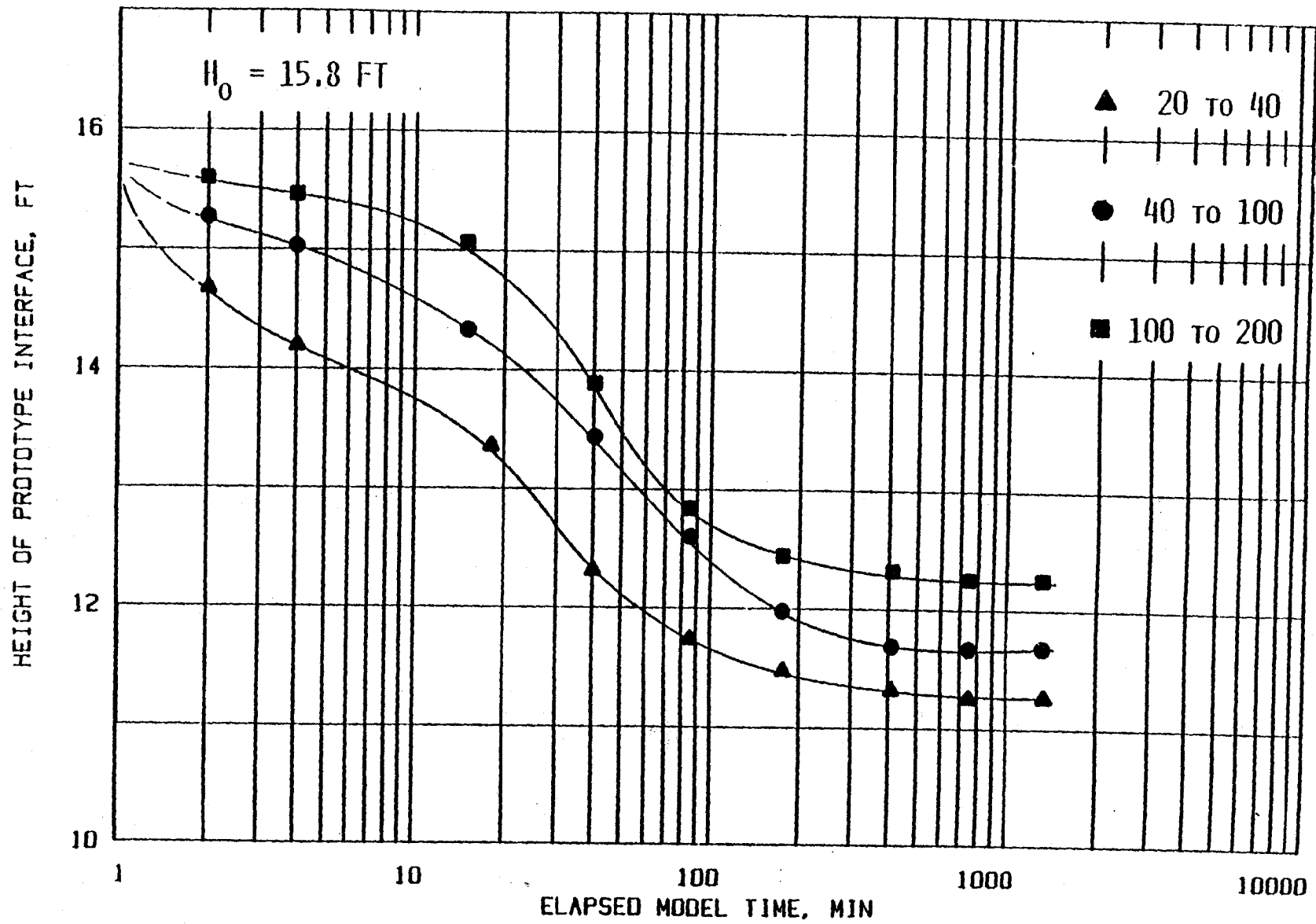


Figure 27: Prototype interface vs model time for the test series KC80-0/6 (6:1 sand/clay ratio mix)

is equal. Therefore, the number of grains per unit volume must also be different. The 20 to 40 mix would have the fewest grains per volume while the 200 minus mix would have the most. These test results may suggest that a variable relationship exists between grain size and reduction in interface height. If sand grains are too large, there are too few per unit volume to effect any major reduction in interface height. If grain size is too small, interstitial water forces may predominate; this, too, would prevent significant reductions in interface height. The 1:1 mix test results suggest that the optimum range of grain size falls between the No. 40 and No. 100 sieves.

Results of the 6:1 s/c mix tests suggest that grain size has a different effect at high/sand clay ratios. Interface height was reduced most by the 20 to 40 mix, followed by the 40 to 100 and 100 to 200 mixes. This implies that greater reductions in interface height may be achieved by increasing grain size. These results would appear to contradict the conclusions drawn from the 1:1 mix tests. It must be remembered, however, that the volume of sand (per unit volume) is now six times greater than the volume of clay. The volume of water has been reduced by almost 25 percent. The sand is now beginning to dominate the mix volume. With the 1:1 s/c mix, there were too few 20 to 40 sand grains to effect much height reduction. With a 6:1 s/c mix, however, there are now a sufficient number of grains in this size range to achieve large reductions in interface height.

Upon completion of the centrifugal testing, each test was cored and sectioned. After oven-drying and the calculation of total solids contents, each sectioned sample was washed and the retained sand dried

and weighed. A vertical profile of sand/clay ratios could now be developed. This information was necessary to test the applicability of the equations suggested by Cardwell and Weiss and the shear strength data provided in Figure 22. If earlier predictions were correct, sand/clay ratios should increase with depth. This would imply that shear strength was insufficient and that sand grains could no longer be held in suspension.

Figures 28 and 29 present final sand/clay ratios versus depth for both the 1:1 and 6:1 s/c mixes. For the finest sand fraction, some sand was obviously lost (e.g. SCR < 1:1 or 6:1) due to the difficulty of wet sieve analyses of fine sands. Nevertheless these results indicate that the sand/clay ratio remains relatively constant with depth, which tends to disprove the maximum grain size predictions made earlier. These results indicate that segregation under accelerated conditions is not a severe problem for homogeneous sand/clay mixes and confirm the applicability of centrifugal modelling techniques. However, they shed little light on the segregation problems associated with capped tests. These problems will be more fully discussed in the next section.

#### **CONSOLIDATION ENHANCEMENT BY CAPPING WITH SAND**

As an alternative to using a s/c mix to increase the unit weight and corresponding effective stresses to enhance consolidation, this test series examined the effects of placing sand as a cap instead of entrained as a mix. For perspective, a 1:1 s/c mix of a 10 ft. (3.05 m) deep pond of 16% clay solids will contain sufficient sand for a 1 ft. (0.32 m) cap of sand at 100 pcf (1602-kg/m<sup>3</sup>). Table 6 summarizes the results of these sand capped models.

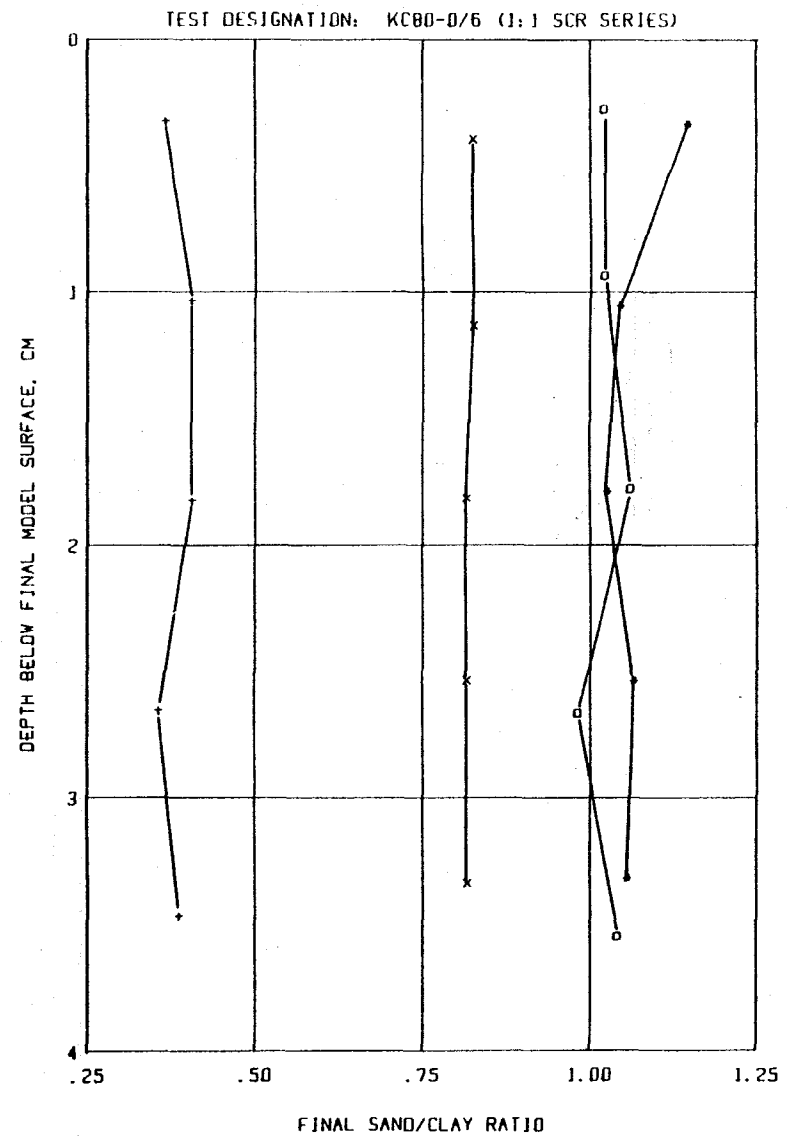
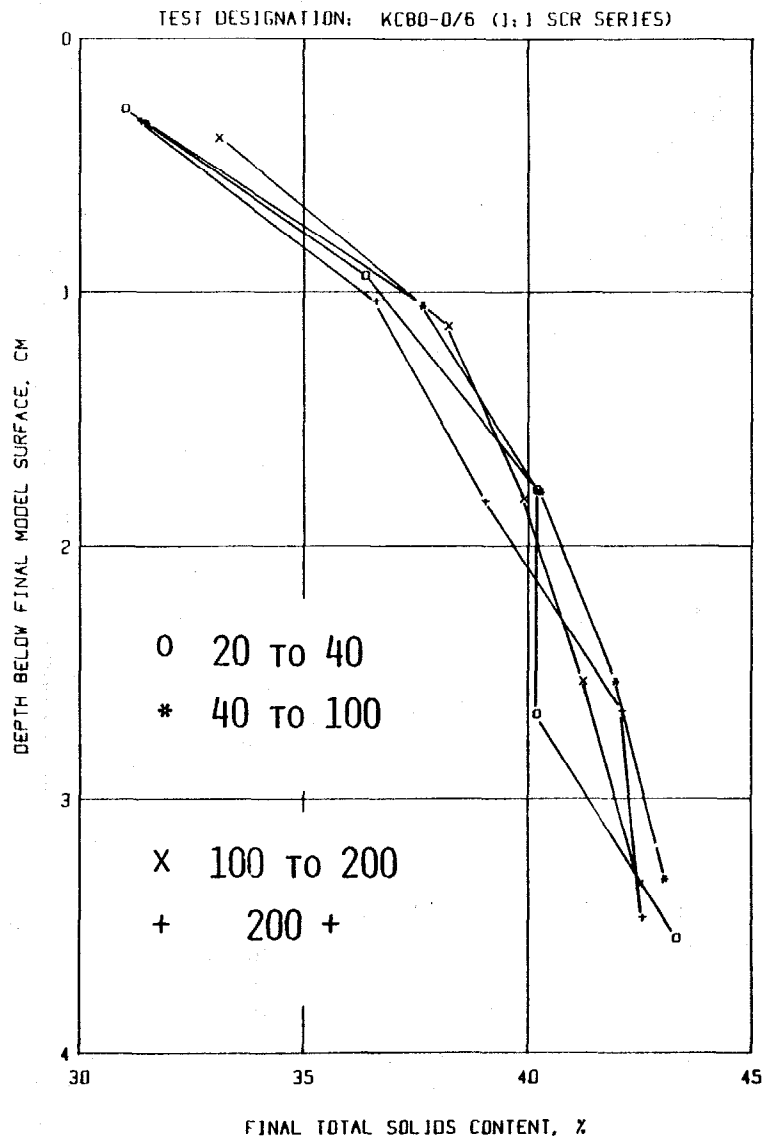


Figure 28: Profiles of total solids contents and sand/clay ratios with depth for the test series KC80-0/6 (1:1 sand/clay mix)

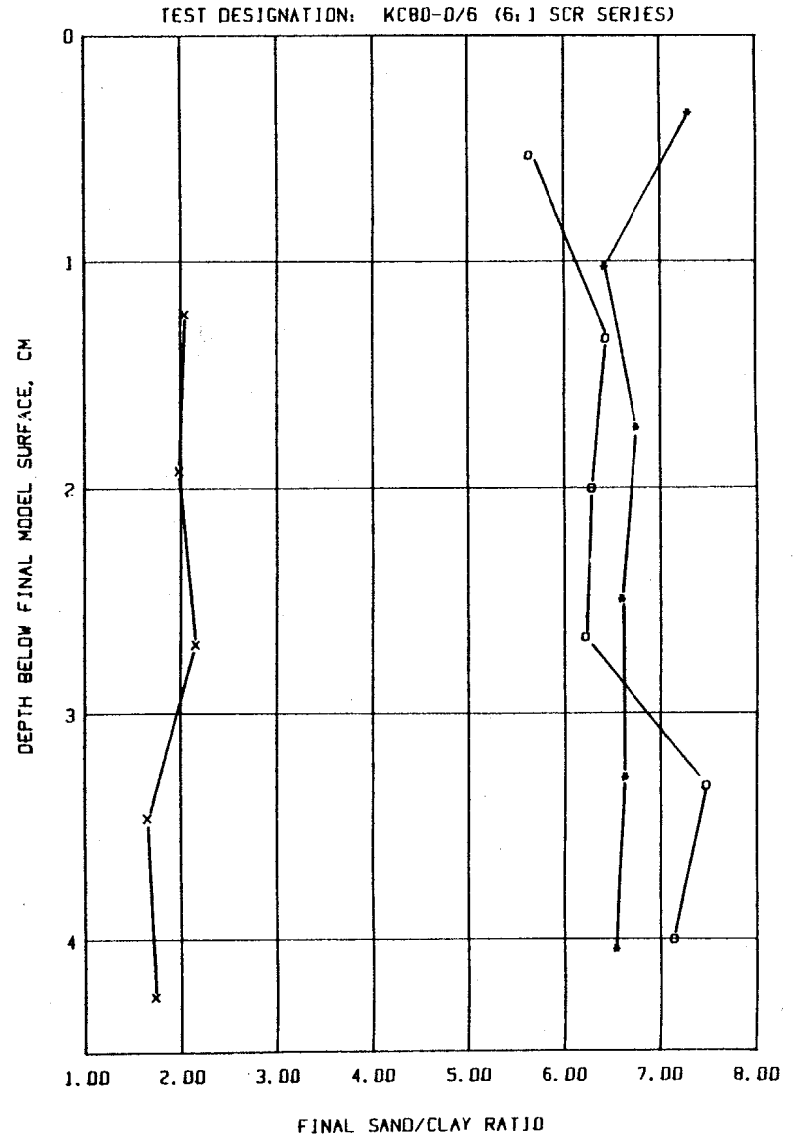
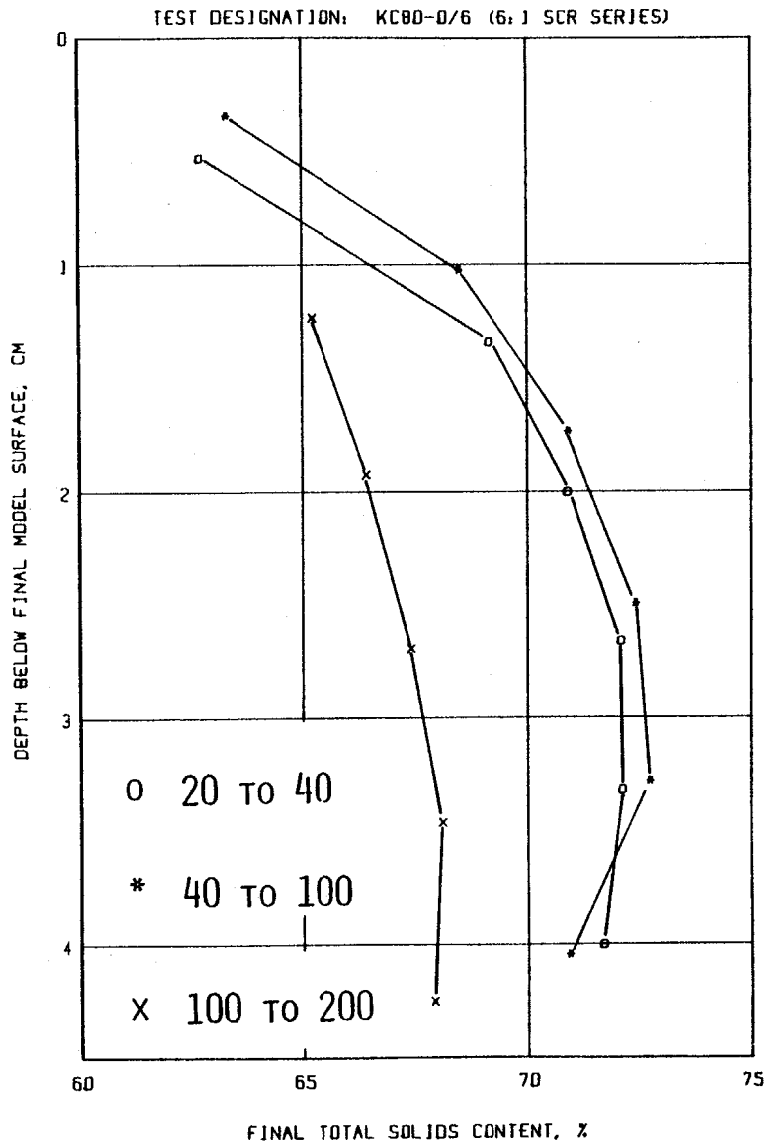


Figure 29: Profiles of total solids contents and sand/clay ratio with depth for the test series KC80-6/0 (6:1 sand/clay mix)

Table 6

## Summary of Sand Capped Centrifugal Model Tests on Kingsford Clay

Test (A)	Initial Model Conditions					Acceleration Level (g)	Test Duration (min)	Final Model Conditions				Remarks
	Initial clay solids content %	Clay Ht (cm)	Cap Ht (cm)	Model Ht (cm)	Prototype clay Ht (ft)			Final clay solids content (%)	Clay Ht (cm)	Model Ht (cm)	Prototype clay Ht (ft)	
KC40-12/0	14.6	12.00	0	12.00	15.70	40	4,200	21.3	7.90	7.90	10.3	Failed
KC60-8/2	14.6	8.00	2.00	10.00	15.70	60	45	-	-	-	-	
KC40-12/2	14.6	12.00	2.00	14.00	15.70	40	4,850	26.7	6.00	-	7.9	
KC40-12/3.2	14.6	12.00	3.20	15.20	15.70	40	5,200	28.6	5.50	-	7.2	
KC60-8/0	14.6	8.00	0	8.00	15.70	60	2,700	21.1	3.90	-	7.7	
-3.9/1.3	21.1	3.90	1.30	5.20	7.70	60	1,300	26.5	3.00	-	5.9	
KC60-3.1/2.1	21.1	3.10	2.10	5.20	6.10	60	1,310	28.6	2.22	-	4.4	
KC80-10/0	14.6	10.00	0	10.00	26.20	80	2,460	24.0	5.70	-	14.9	
-5.7/2	24.0	5.7	2.00	7.70	14.90	80	1,350+	30.4	4.27	-	11.2	
-4.3/4	30.4	4.30	+2=4.0	6.30	11.30	80	2,940+	40.0	3.00	-	7.9	
KC40-12/0	14.6	12.0	0	12.0	15.70	40	5,500	21.3	7.85	-	10.3	
-7.9/2	21.3	7.9	2.0	9.9	10.4	40	3,000	26.7	6.17	-	8.1	
KC60-7/6	23.8	7.0	6.0	13.0	18.40	60	2,350	37.0	4.1	-	8.1	
KC60-10.55/0	12.6	10.55	0	10.55	20.8	60	580	21.8	5.7	-	11.2	
-5.7/2	21.8	5.7	2.0	7.70	11.2	60	1,804	29.4	4.00	-	7.9	

(A) KC40-12/0 means KC = Kingsford Clay, 40 = 40 g's acceleration level, 12/0 = clay depth 12 cm/0 cm cap  
 Note: all caps became submerged shortly (approx. 1 to 2 minutes) after achieving prototype acceleration.



### Model Series Cap

A model series consisting of models KC60-8/2 and models KC40-12/0, -12/2, - 12/3.2 evaluated consolidation enhancement by placement of 2.0 or 3.2 cm caps over 14.6% solids clay. Model KC60-8/2 was a 60 g model simulating a 15.7 ft. deep pond with a 3.9 ft. submerged sand cap. The results presented in Figure 30 showed that the central portion had collapsed as a bearing capacity failure and the perimeter had heaved. Accordingly, a 40 g model series was performed in anticipation of avoiding a similar failure. Models KC40-12/0, - 12/2, - 12/3.2 simulated (1) a reference model, (2) a 2.6 ft. submerged sand cap, and (3) a submerged 4.2 ft. sand cap. The results presented in Figure 31 showed that surcharging with a 2.6 ft. or 4.2 ft. submerged cap resulted in final solids contents of 26.7% and 28.6%, respectively, as compared with a  $S_f = 21.3\%$  for uncapped clay. These solids contents were achieved after approximately 5,800 minutes, which using a scaling exponent of 1.6 for solids contents from 14.6% to 20%, and a scaling exponent of 2.0 for solids contents greater than 20%, results in 4,703 days and 5,263 days for the 2.6 and 4.2 ft. caps, respectively. Unfortunately, these caps showed minor distress suggesting that 14.6% solids content clay possesses only marginal strength to prevent a bearing capacity failure.

These tests also suggest a possible method of cap placement to minimize the possibility of a bearing capacity failure. The supernatant water level would be maintained such that cap placement would occur under water. In this fashion only the buoyant unit weight of the sand cap would be applied to the clay. Then, as consolidation occurred, the

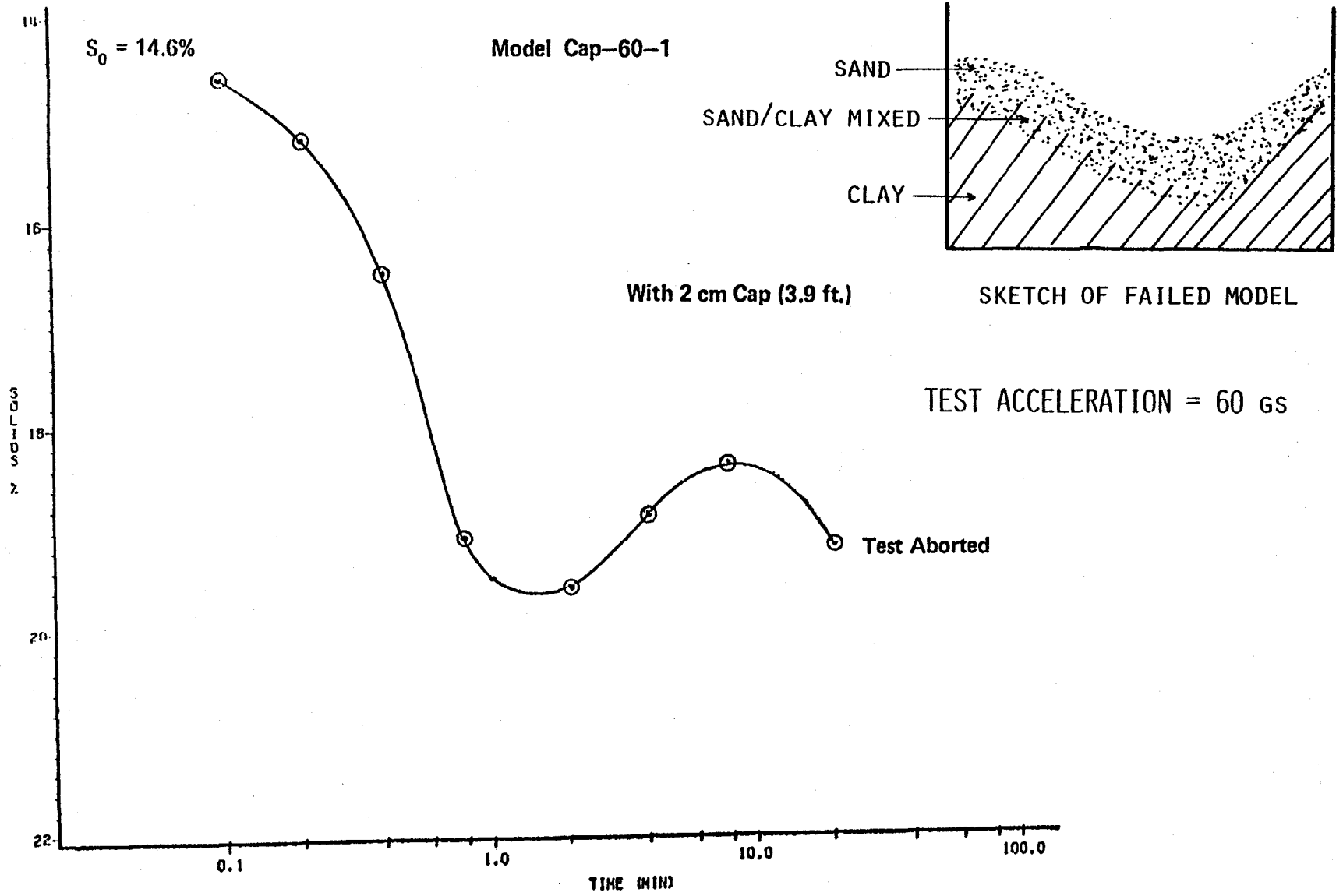


Figure 30: Plot of Solids Content Versus Elapsed Time of Centrifuge Capping Test

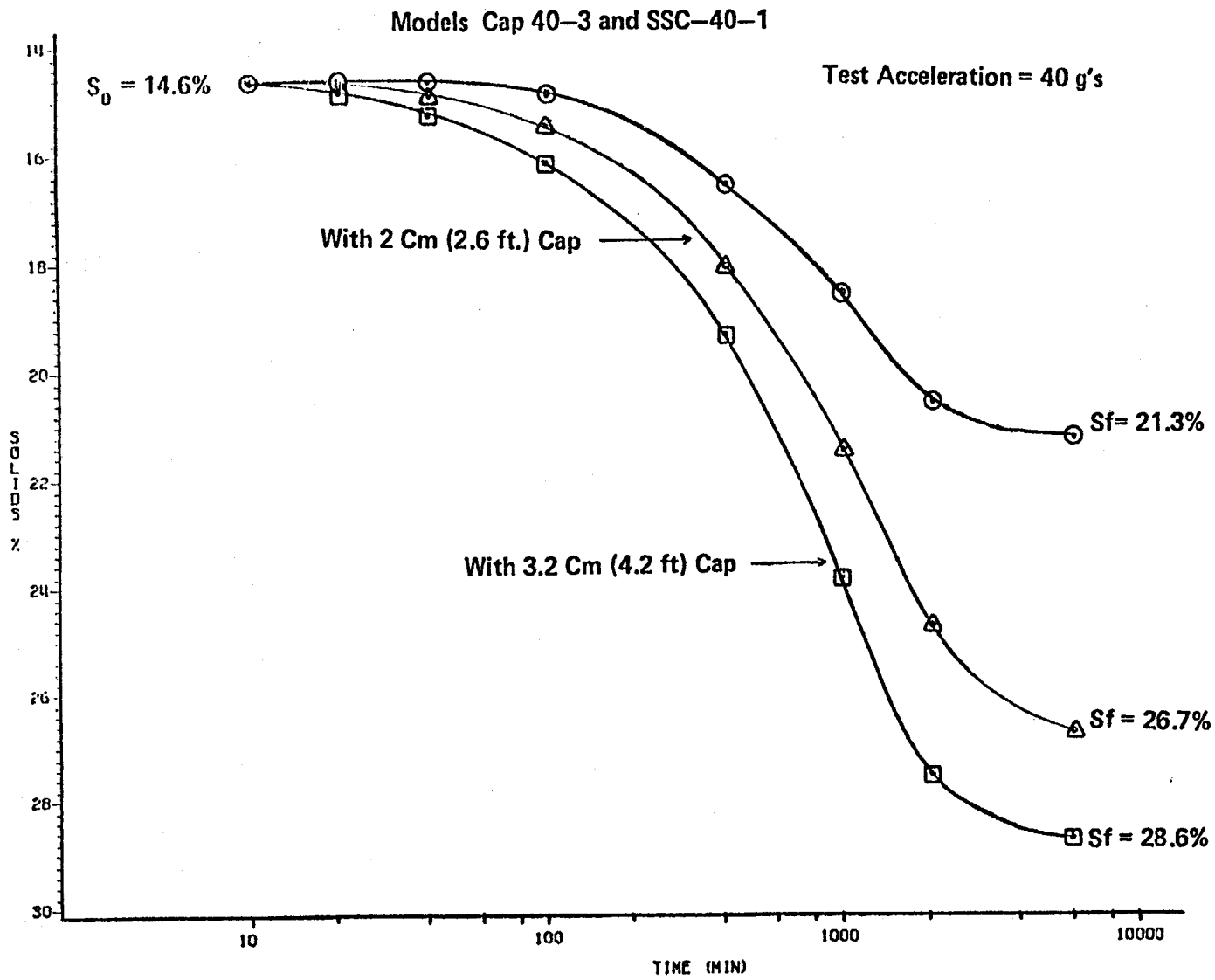


Figure 31: Comparison of Three Centrifuge Tests - Capped versus No cap.

water level could be slowly lowered, through a weir, progressively increasing the effective surcharge on the clay.

#### **Mdel Series Stage Sand Capping**

Because of the observed failure when caps were placed on 14.6% clays and success when caps were placed on approximately 20% clays, this model series, consisting of adding sand caps in stages as the clay achieved higher solids contents, was performed. This model series consisted of models KC60-8/0, KC60-3.1/2.1, KC80-10/0, KC40-12/0, and KC60-7/6.

Mdel KC60-8/0 consisted of accelerating at 60g's an 8 cm deep model of clay solids at 14.6% for 2,700 minutes until a final solids of 21.1% was achieved. This model simulates self-weight consolidation of a 15.7 ft. deep waste clay pond until equilibrium was achieved after 1,312 days. Subsequently, a 1.3 cm cap was placed over the 21.1% clay and reaccelerated to 60 g's for 1,300 minutes until a final solids content of 26.5% was obtained. The second phase of this model simulates placement of 2.6 ft. thick submerged sand cap over a 7.7 ft. deep waste clay pond for 3,250 days.

Mdel KC60-3.1/2.1 is practically identical to the second phase of model SSC-60-1, except that a 2.1 cm cap was placed over the 21.1% solids for 1,310 minutes until a final solids content of 28.5% was achieved under 60 g's. This model simulates placement of a 4.1 ft. thick sand cap over a 6.1 ft. deep waste pond of 21.1% solids for 3,275 days achieving a 28.6 final solids content. These results are presented in Figure 32.

Mdel KC80-10/0 consisted of accelerating at 80 g's a 10 cm deep clay model of 14.6% clay solids for 2,460 minutes until self weight

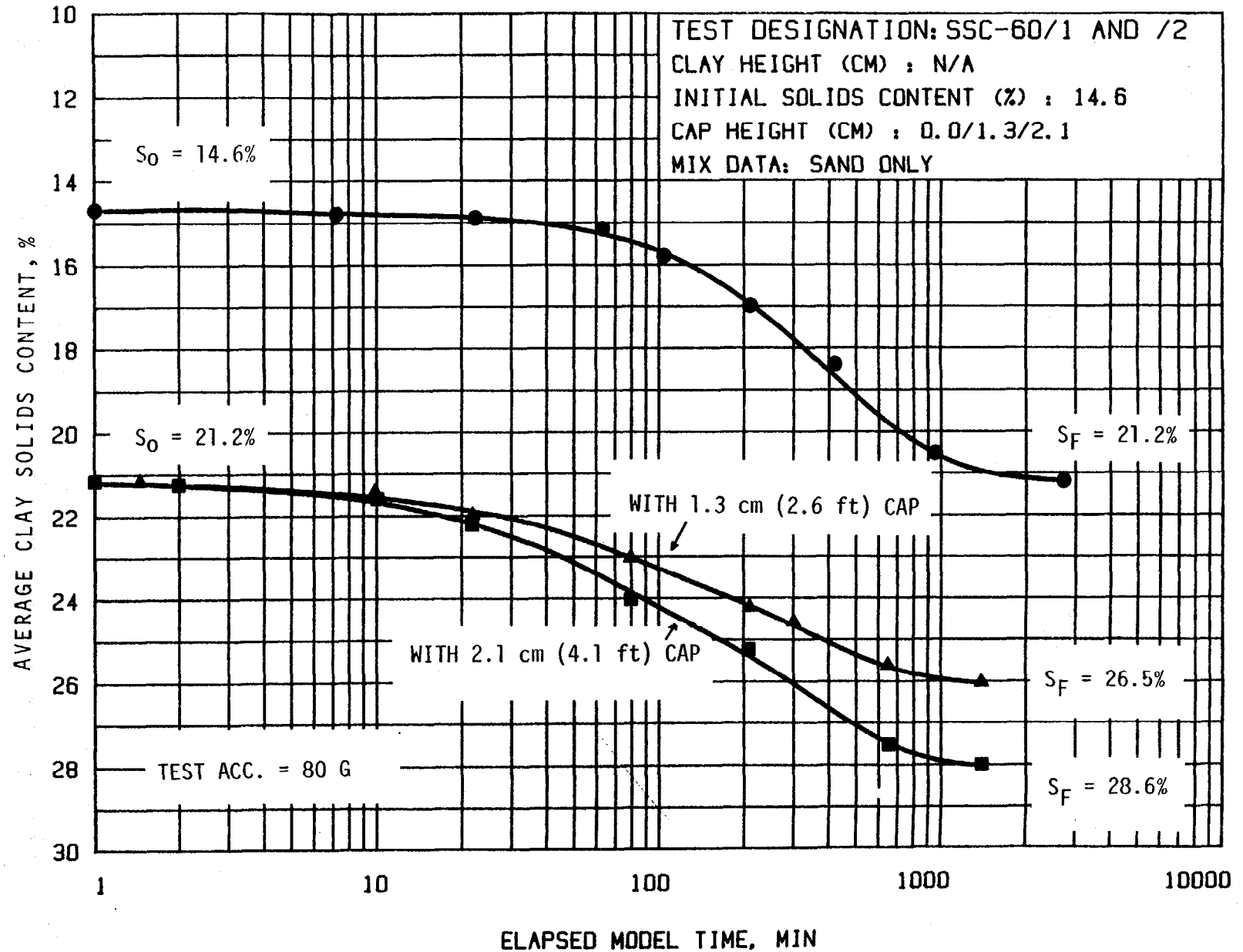


Figure 32: Effect of Capping on the Final Solids Content of Kingsford Waste Clays

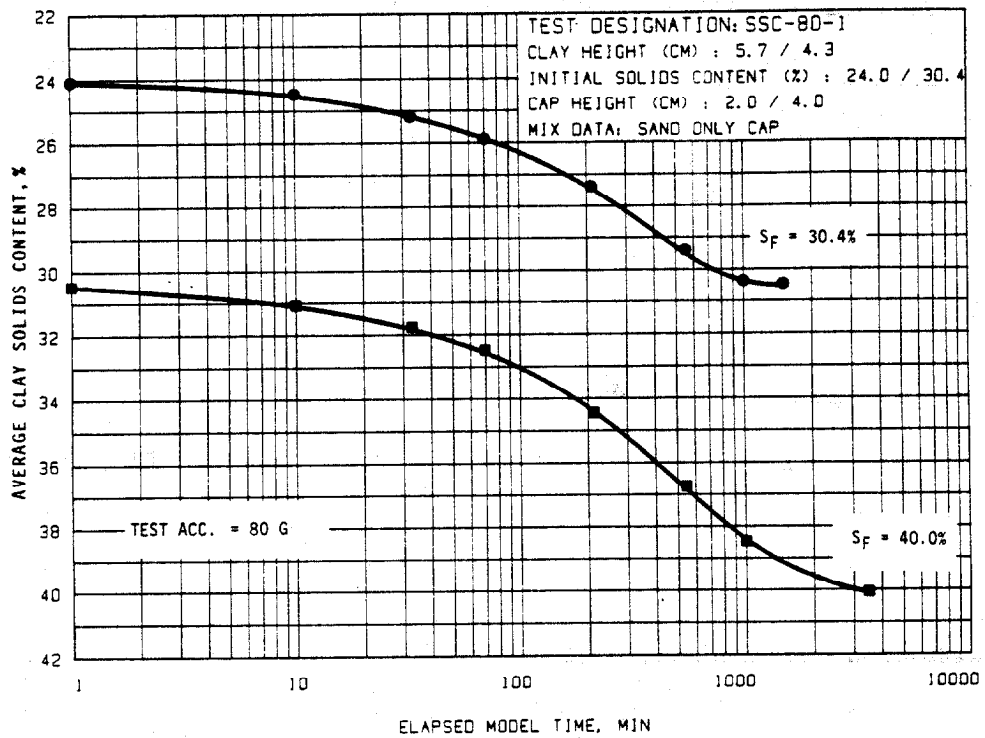
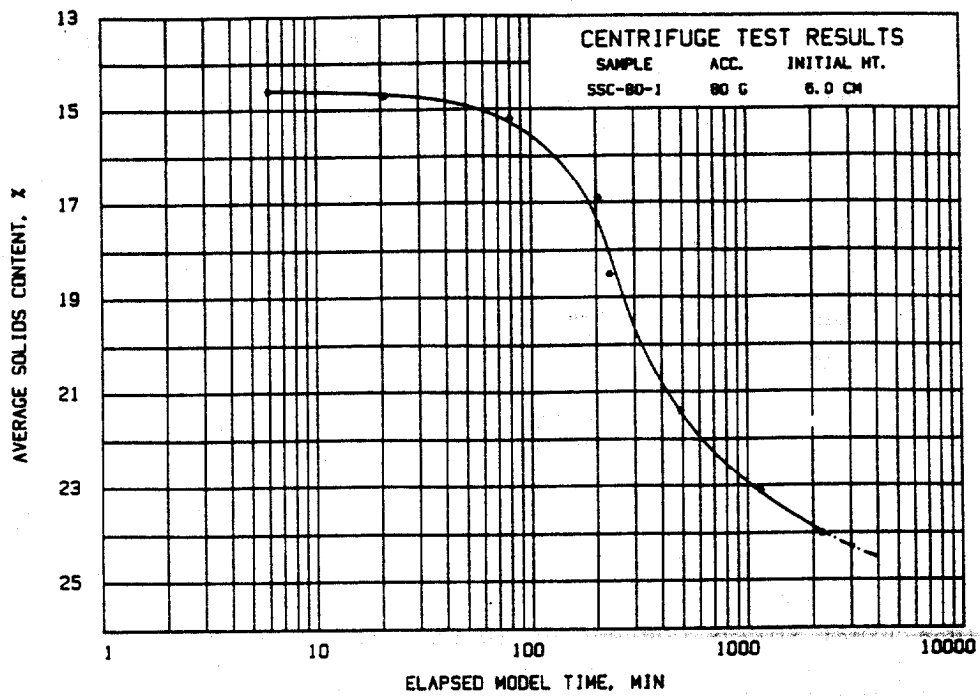


Figure 33: Effect of Stage Sand Capping on Final Clay Solids Content

equilibrium of 24% solids was achieved. This condition simulated a 26.2 ft. deep waste clay pond which after 1,895 days achieves a self weight solids content of 24%. At this time a 2 cm cap was placed on the clay and reaccelerated to 80 g's for an additional 1,350 minutes until a solids content of 30.4% was achieved. This condition simulated a 5.2 ft. cap placed on a 14.9 ft. deep pond of 24% solids for 6,000 days achieving a solids content of 30.4%. Lastly, an additional 2 cm sand cap creating a total of 4 cm cap was placed on the model and reaccelerated to 80 g's for an additional 2,940 minutes which resulted in a final solids content of 40.0%. This last phase simulates placement of an additional 5.2 ft. cap over a 11.2 ft deep waste pond of 30.4% waste clays. After 13,067 days a final solids content of 40% is achieved. The results are presented in Figures 33A and 33B.

Model KC40-12/0 consisted of accelerating a 12 cm deep clay slurry at 14.6% solids to 40 g's for 5,500 minutes achieving a final self-weight consolidation solids content of 21.3% solids. Subsequently a 2 cm sand cap was placed over the 21.3% solids and the test continued at 40 g's for additional 3,000 minutes achieving a 26.7% final solids content. This model replicates a 15.7 ft. deep waste pond which after 1,397 days consolidates to 21.3% solids. At this point a 2.6 ft. submerged cap is placed on the clay and consolidation continues for 3,333 days until 26.7% solids is achieved.

Model KC60-7/6 involved placing a 6 cm cap over 7 cm of 23.8% solids clay and accelerating to 60 g's for 2,350 minutes until a final solids content of 37.0% is achieved. This model replicated placement of an 11.8 ft. cap over an 18.4 ft. deep pond for 5,875 days until 37.0% solids is achieved.

### Sand Capping Summary

These results demonstrate that surcharging waste ponds by placement of a sand cap greatly enhances consolidation and the final achieved solids contents. Using the technique of stage capping; i.e., intermittently adding sand layers and thereby gradually increasing the cap thickness, solids contents up to about 40% were achieved (models KC80-10/0, KC60-7/6). Obviously, cap enhanced consolidation is a viable method for achieving high solids contents.

Fortunately, the fear that a sand cap would become immediately clogged and thus rendered useless by the waste clays forming an impermeable barrier at the cap-clay interface was alleviated by these model tests. In all cases, the water easily flowed from the clays through the cap. Generally the water level would rise to approximately 5 ft, (prototype) above the clay interface; thus the thinner caps became submerged, while the thicker caps were partially saturated. The submergence of the thin caps decreased the effective stress by passing from moist unit weights (107pcf) to a buoyant unit weight (44.6pcf). While this submergence decreases the stress causing consolidation of the underlying clay, it had the advantage of perhaps avoiding a bearing capacity failure until the clays consolidated sufficiently to reach supporting strengths. Thus a possible capping scenario would be to place the sand caps in a submerged condition and controlling the capping stress increase by draining the surface water, such that any bearing capacity failure of the cap could be avoided.

An estimation of the data unfortunately reveals that times achieve high solids contents by capping are rather lengthy; e.g., KC60-7/6 required 5,875 days (16 years) to consolidate from 23.8% solids to



**37.0% solids. Obviously as the solids content increases, the permeability of the soil must decrease, thereby increasing the consolidation times.**

#### **Maximum Cap Height vs Solid Content**

**An obvious drawback to capping is the careful consideration required to place the maximum cap height possible without creating a bearing capacity failure. Accordingly in addition to the sand capping tests listed in Table 7, a series of tests was performed in which a 1.5 cm cap was placed over Kingsford Clay at 17.7% solids content and accelerated in stages to 100 g's to observe at what acceleration level surface distress of the clay surface was observed. These, plus tests from Table 6 are presented in Table 7. Failure was usually observed as an irregular shaped surface resulting where the center of the cap migrated into the underlying soft clays. Because of the proximity of the container walls, full failures with heaved clays was not observed and the possibility exists that for thick caps, 3 cms<sup>+</sup>, the cap behaved as a plug and failure could not occur due to restraint by the container walls. Model test Spin-100 was designed to investigate specifically bearing failure and consisted of a 1.5 cm cap accelerated in stages to 100 g's. The cap did not become submerged and a center depression and irregular surface was observed. The calculated effective stress acting at the clay surface was based upon buoyant (44.6pcf) or moist (107pcf) unit weights. In some thicker models the phreatic surface was within the sand cap, usually about 4 ft, (prototype) above the interface.**

**Figure 34 presents estimated dividing boundry between safe and unfailed caps. Although the data is sparse and limited by container side effects, it is felt that the boundry is a pseudo representation of**

Table 7

## Summary of Bearing Capacity Failures of Capped Models

Model No.	Solids Content $S_o\%$	Prototype Cap Height ft	(a)	Status
			Effective Stress $\sigma'_o$ , psf	
KC60-8/2	14.6	3.9	174	Failed
KC40-12/2	14.6	2.6	116	Partial
KC40-12/3.2	14.6	4.2	187	Partial
KC60-3.9/1.3	21.1	2.6	116	Safe
KC60-3.1/2.1	21.1	4.1	183	Safe
KC80-5.7/2	24.0	5.2	232	Safe
-4.3/4	30.4	10.4	788	Safe
KC40-7.9/2	21.3	2.6	116	Safe
KC-60-7/6	23.8	11.8	1,013	Safe
Spin-60	17.7	2.9	306	Safe
Spin-80	17.7	3.9	408	Safe
Spin-100	17.7	4.9	450	Safe
Spin-100	17.7	8.2	816	Failed

a)  $\sigma'_o = \gamma z$ ,  $\gamma_m = 107\text{pcf}$   $\gamma' = 44.6\text{pcf}$

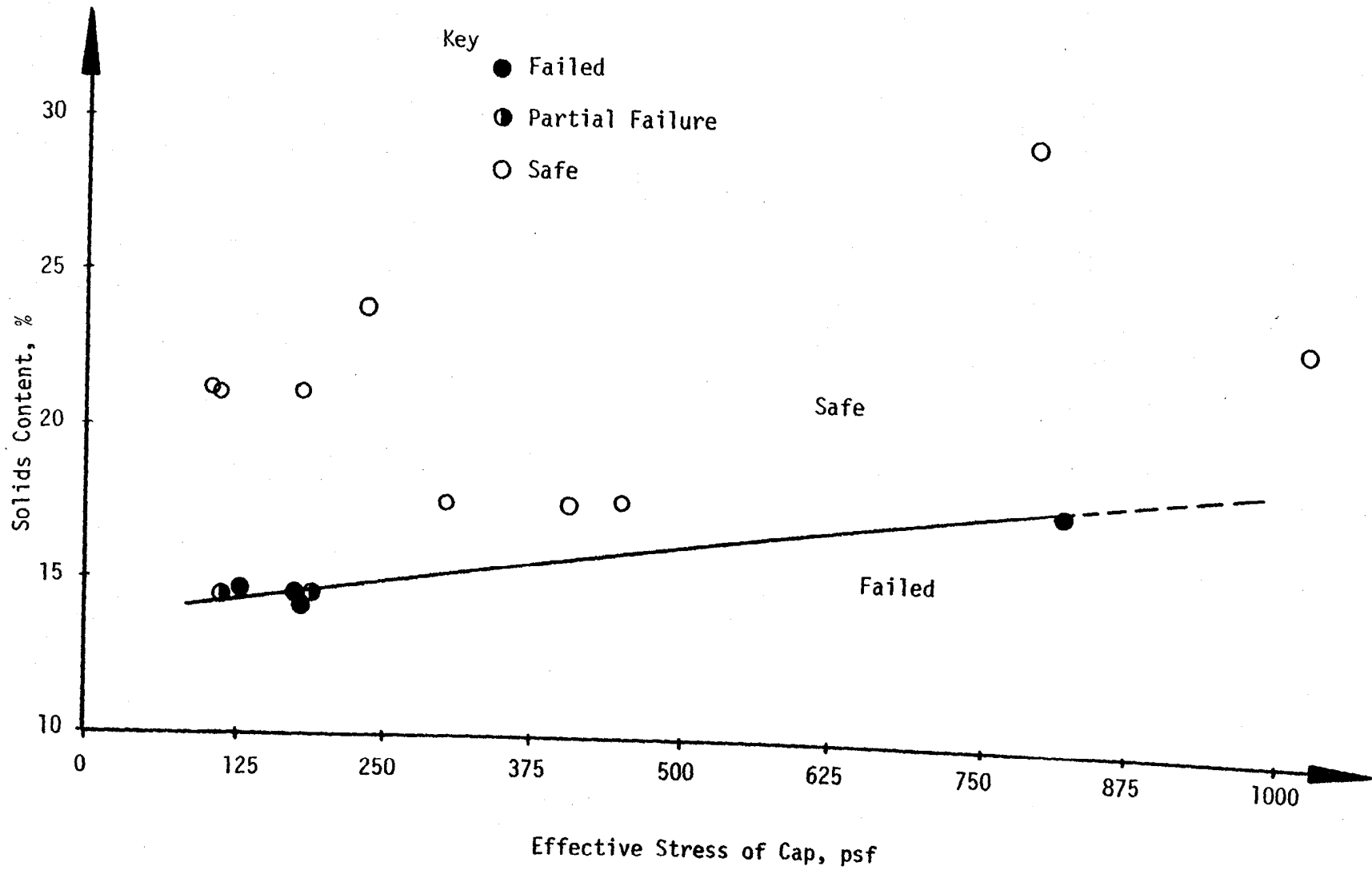


Figure 34: Summary of Bearing Capacity vs Solids Content/or Kingsfords Waste Clays.

anticipated field performance. Unfortunately application of this data suggests at 21% solids (the end of self weight consolidation) an 8 ft. sand cap unsubmerged could be placed without failure, which appears somewhat high. We would welcome additional research in this area.

#### **CONSOLIDATION ENHANCEMENT BY CAPPING WITH SAND/CLAY MIX**

While the results presented in Table 6 reveal that solids contents approaching 40% are possible by capping the pond with sand, sand/clay mixes which could be pumped directly onto the clay ponds offers an alternative capping material. This method of s/c mix caps not only reduces the possibility of a bearing capacity failure during cap placement, but also reduces the expense of cap placement. However foreseeable draw-backs of this technique include: (a) to achieve the same effective stress as a sand cap, a larger volume of s/c mix must be placed, and (b) the permeability of the s/c mix is less than that for a sand cap thus impeding drainage and lengthening consolidation times. Accordingly this test series of s/c mix caps was undertaken, with results summarized in Table 8.

Figure 35 provides a comparison between three tests with initial model heights of 10.5 cm and solids contents of 16.3 percent, which were accelerated to 80 g's. Two cap tests, KC80-6/4.5 (3:1) and -6/4.5 (6:1) consisted of 4.5 cm caps of 3:1 and 6:1 s/c mix using 40-100 sand and 16.3% clay placed over 6.0 cm of waste clay. These are compared to a 10.5 cm homogeneous clay model KC80-10.5/0 (Table 4). Final results indicate that capping provides no benefit in the reduction of interface height. Indeed, as the unit weight of the cap increases, total settlement decreases!

Table 8  
Summary of sand/clay cap centrifugal model tests

Test	Initial Model Conditions							Final Model Conditions							Remarks	
	Clay height H (cm)	Cap height H <sub>c</sub> (cm)	Model height H <sub>o</sub> (cm)	Proto-type height H <sub>o</sub> (ft)	clay solids content S <sub>o</sub> (%)	clay solids content S <sub>c</sub> (%)	Sand/clay ratio	Acceleration level	test duration (min)	Model height H <sub>f</sub> (cm)	Model height H <sub>f</sub> (ft)	Segregation	Avg. Solids content underlying clay S <sub>f</sub> (%)	εHX100 (%)		
KC60-8/2	8.0	1.92	9.92	19.5	16.3	16.3	6:1	Fig. 17	60	3,740	6.75	13.3	yes	N/A	31.8	remixed
KC60-8/6	8.0	5.68	13.68	27.0	16.3	16.3	6:1	Fig. 17	60	4,200	9.17	18.1	yes	N/A	33.0	before
KC80-6/4.5	6.0	4.50	10.50	27.6	16.0	16.0	3:1	40-100	80	3,110	6.75	17.7	yes	N/A	35.7	capping
KC80-6/4.5	6.0	4.40	10.40	27.3	16.0	16.0	6:1	40-100	80	1,870	7.40	19.4	yes	N/A	28.9	+
KC80-6/4.5	6.0	4.33	10.33	27.1	16.3	16.3	6:1	Fig. 17	80	5,050	7.00	18.4	yes	N/A	32.2	+
KC80-6/4.5	6.0	4.50	10.50	27.6	25.1	16.0	6:1	Fig. 17	80	2,070	8.10	21.3	yes	N/A	22.9	+
KC80-6.6/4.0	6.6	4.00	10.60	27.8	24.0	16.0	6:1	Fig. 17	80	1,870	7.60	20.0	no	31.4	28.3	capped
K80-7.5/4.0	7.5	3.90	11.40	29.9	26.6	12.7	1:1	40-100	80	1,770	8.85	23.2	no	unk	22.4	after
+2.0	unk	2.05	10.90	28.6	unk	12.7	1:1	Fig. 41	80	930	9.65	25.3	no	31.5	11.5	self-
KC80-7.5/4.0	7.6	4.00	11.60	30.5	26.6	12.7	3:1	Fig. 41	80	1,770	9.05	23.8	no	unk	22.10	weight
+2.0	unk	2.10	11.15	29.3	unk	12.7	3:1	Fig.	80	930	9.80	25.7	no	32.2	12.1	consoli-
KC80-7.5/4.0	7.4	3.85	11.25	29.5	26.6	12.7	6:1	Fig.	80	1,770	8.80	23.1	no	unk	21.8	dation
+2.0	unk	2.00	10.80	28.4	unk	12.7	6:1	Fig.	80	930	9.55	25.1	no	35.2	11.6	+
KC80-7.5/2.0	7.4	2.10	9.50	24.9	26.6	12.7	3:1	Fig.	80	1,890	7.80	20.5	no	unk	17.9	+
+2.0	unk	2.00	9.80	25.7	unk	12.7	3:1	Fig.	80	930	8.80	23.1	no	32.3	10.2	+

100

TEST DESIGNATION: KC80 -10.5/0 -6/4.5 (3:1) -6/4.5 (6:1)

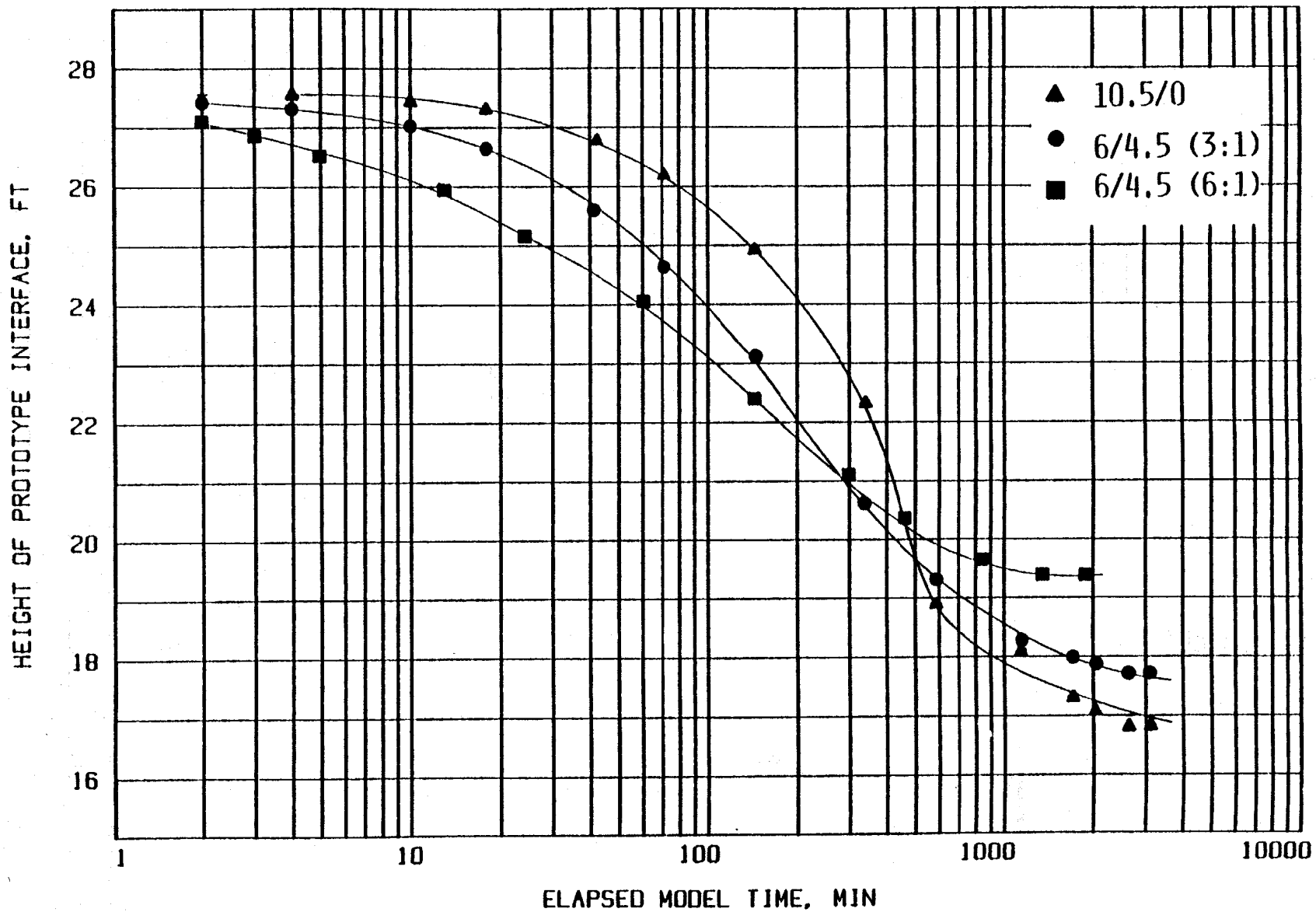


Figure 35: Prototype interface vs model time for the test series KC80-6/4.5 (3:1 and 6:1 sand/clay cap) and KC80-10.5/0

After completion of the centrifugal testing, the sand/clay samples were cored and the final sand/clay ratio profiles are shown in Figure 36. As can be seen, the sand/clay ratios increase rapidly at about mid-depth, which is indicative of the segregation phenomena. The entrained sand has migrated through the capping layer and underlying waste clay towards the bottom of the sample.

This information helps explain the results presented in Figure 36. Intuitively, one would expect a sample with a 6:1 sand/clay cap to settle more than one with a 3:1 sand/clay cap or a homogeneous clay sample. However, as the sand migrates through the sample, the initial sample profile is in effect inverted. The sand is now at the bottom while the clay has been displaced to the top of the sample. The following section examines this segregation behavior.

#### S/C Mix vs S/C Cap Segregation Behavior

Figure 37 presents the results of centrifugal tests [KC80-0/10.5(3:1 & 6:1) {Table -5}, and KC80-10.5/0{Table 4}] performed on 3:1 and 6:1 (10.5 cm) sand/clay mixes (40-100). Figure 38 presents the final sand/clay ratios versus depth for both samples. As can be seen in Figure 38 no appreciable segregation was observed in these homogeneous s/c mix models as the s/c ratios remained 3:1 and 6:1. Conversely, the profiles presented in Figure 36 showed appreciable segregation occurred for the s/c caps.

When a homogeneous sand/clay mix is accelerated, it is theorized that individual sand grains are supported by underlying grains which, in turn, are supported by the container bottom. The grains, in effect, "stand" on lower grains. This action prevents appreciable migration. Conversely, if a sand/clay cap at an equivalent sand/clay ratio is

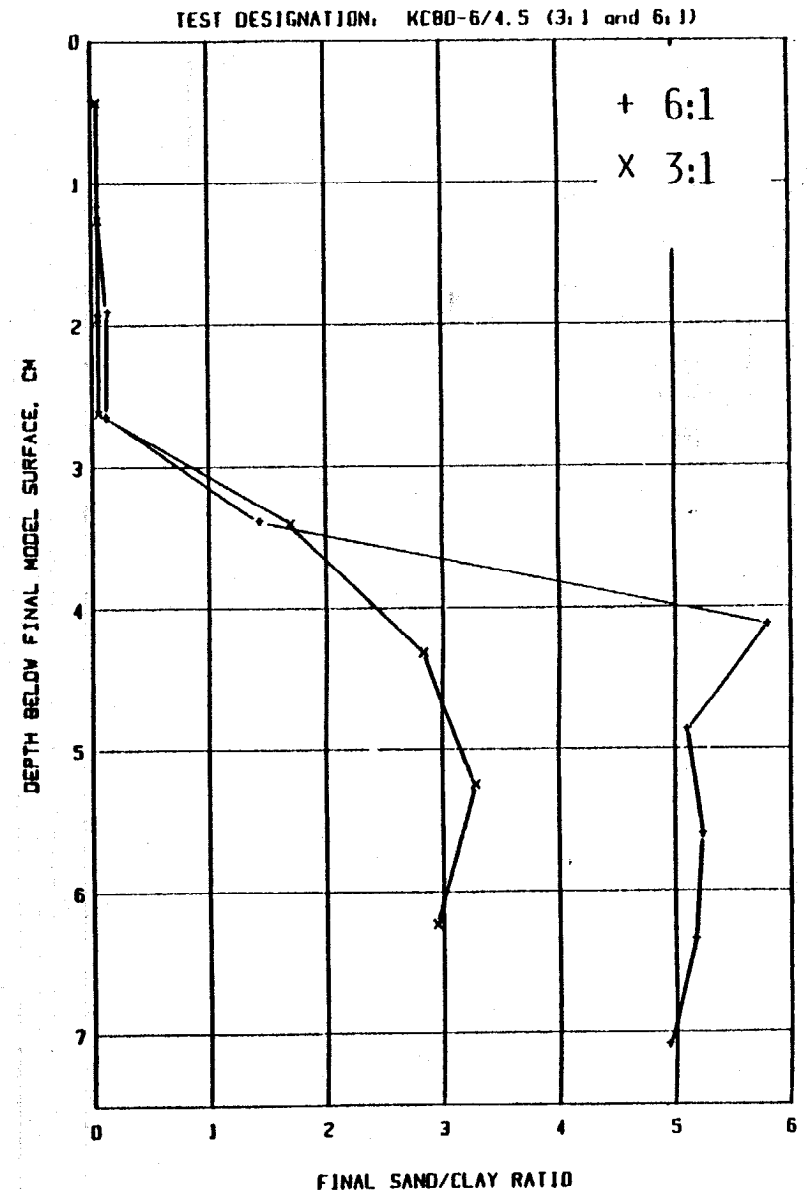
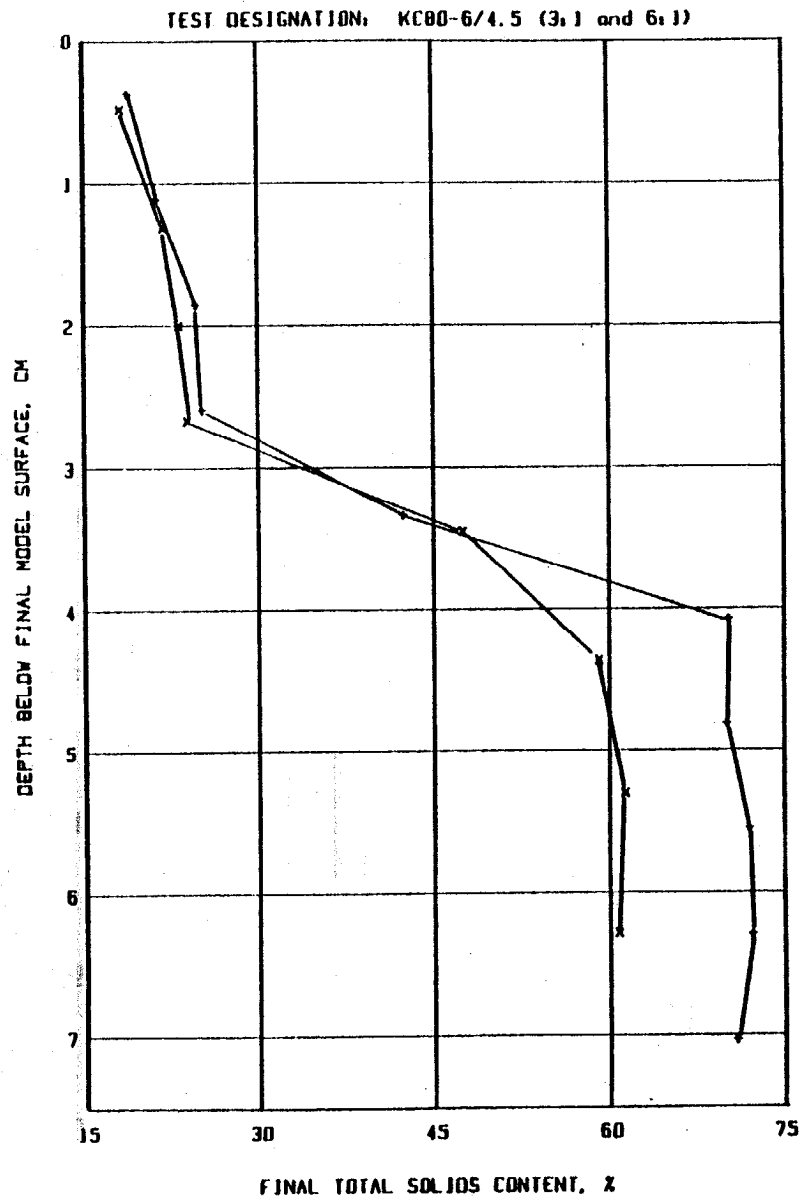


Figure 36: Profiles of total solids contents and sand/clay ratios with depth, test series KC80-6/4.5 (3:1 and 6:1 sand/clay caps)



TEST DESIGNATION: KC80 -10.5/0 -0/10.5 (3:1) -0/10.5 (6:1)

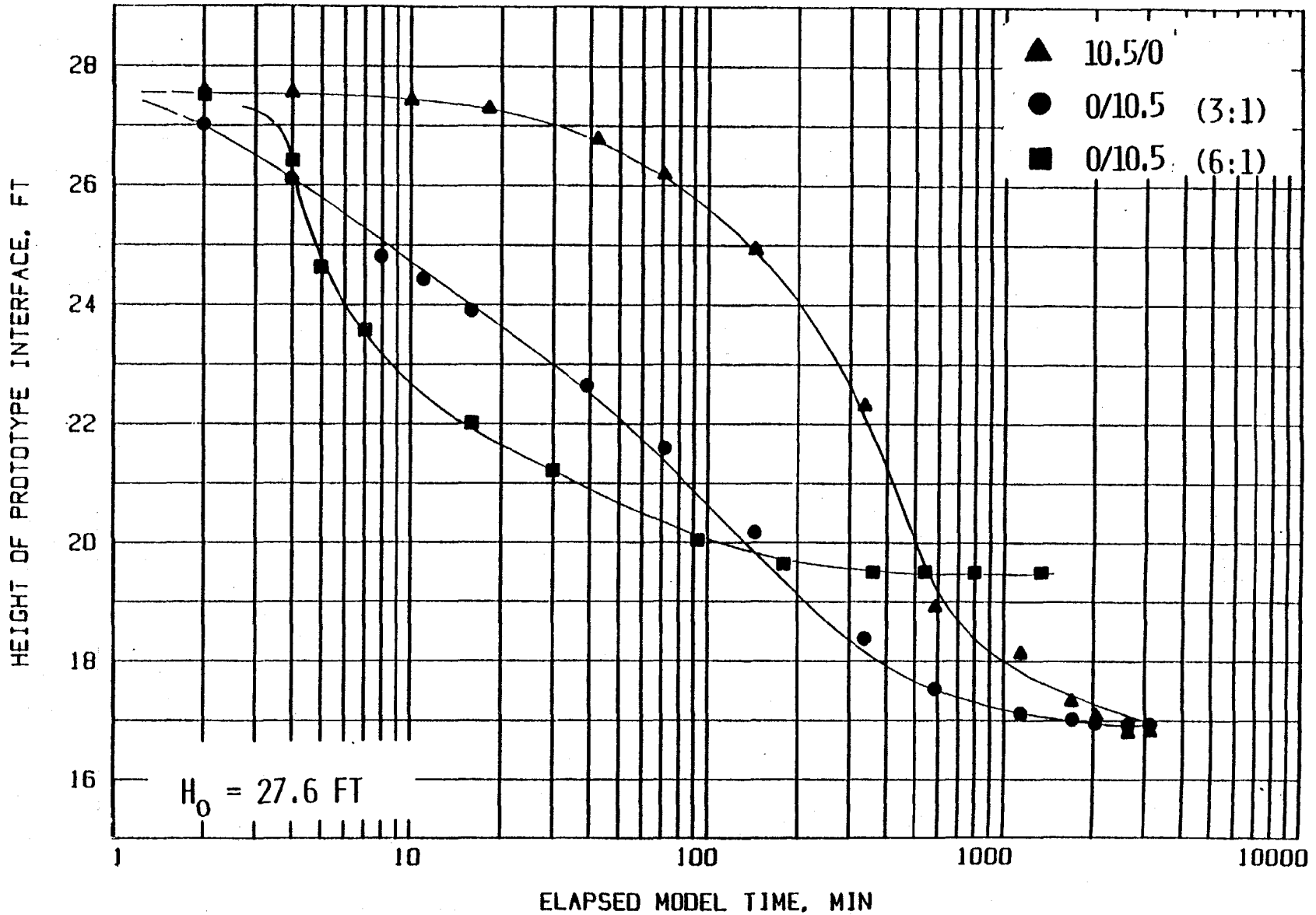


Figure 37: Prototype interface vs model time for the test series KC80-0/10.5 (3:1 and 6:1 sand/clay mix) and KC80-10.5/0

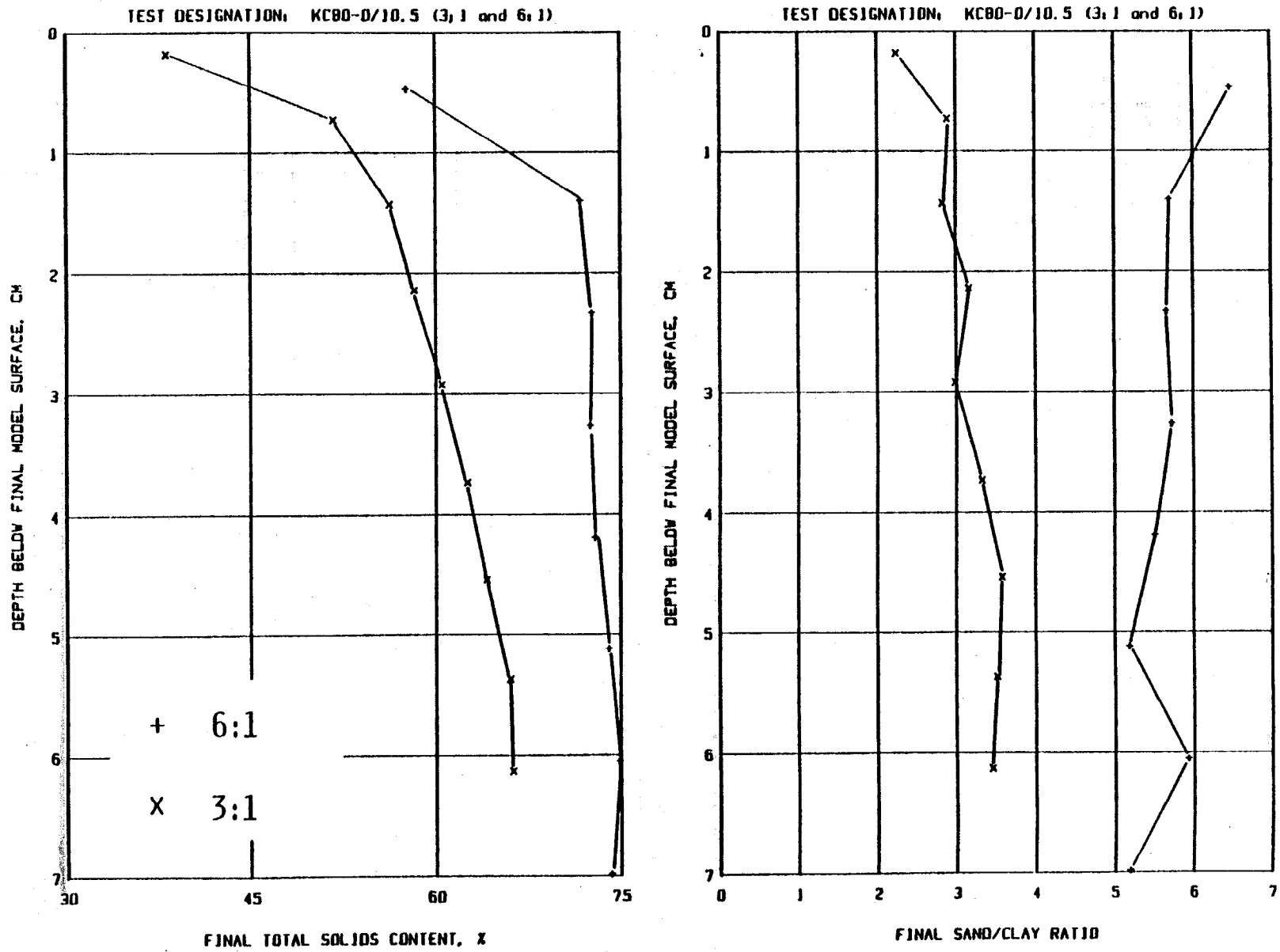


Figure 38: Profiles of total solids content and sand/clay ratio with depth for the test series KC80-0/10.5 (3:1 and 6:1 sand/clay mixes)

TEST DESIGNATION: KC80-6.6/4.0 (23.96%) - 6/4.5 (25.12%)

106

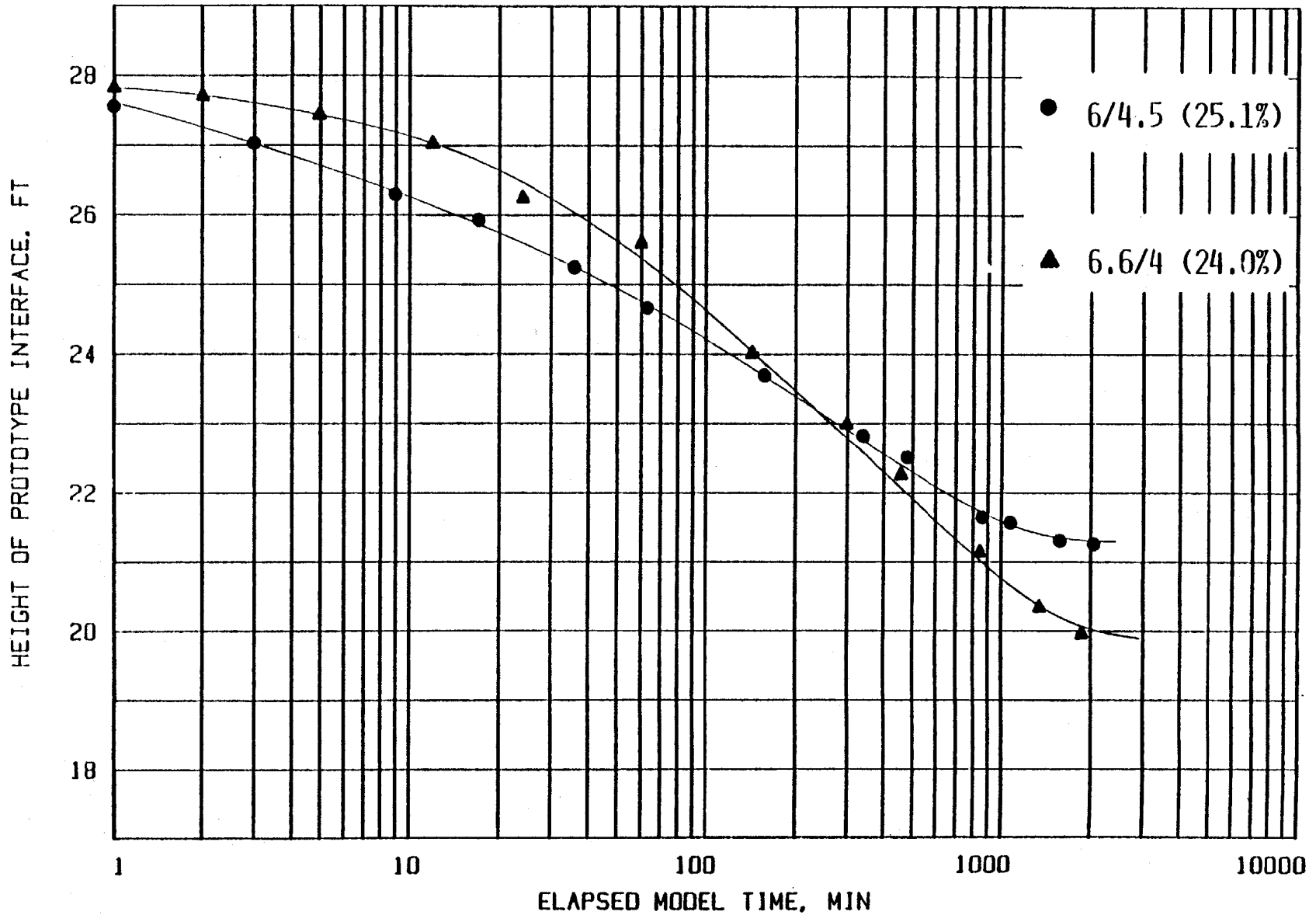


Figure 39: Prototype interface vs model time for the test series KC80-6/4.5 (6:1 sand/clay cap over remixed clay at 25.1% solids) and KC80-6.6/4.0 (6:1 sand/clay cap over undisturbed clay at 24.0% solids)

tested in a similar manner, the behavior is quite different. The grains in the sand/clay cap are ultimately supported by the underlying soft clay. If the shear strength of the clay is unable to support the combined weight of the grains, the sand begins to move toward the bottom of the sample and segregation occurs.

### Segregation Phenomena

In an attempt to minimize segregation of the sand from the s/c mix cap passing through the underlying clay, a capping test [KC80-6/4.5 (6:1)] was performed on 6.0 cm of clay of 25.1 percent solids. A 4.5 cm 6:1 sand/clay (16.3 percent initial clay solids) was used (see Figure 17 for the grain size distribution of the sand used). Results are presented in Figure 39. Upon completion of the centrifugal testing, the sample was cored and the sand/clay ratio profile was plotted, and the results presented in Figure 40. Again, the sand/clay ratio begins to increase rapidly at about mid-depth. The higher clay solids content did not prevent segregation.

A second test [KC80-6.6/4 (6:1)] was performed in another attempt to examine segregation. A 10.5 cm 16.0 percent clay solids sample was accelerated until self-weight consolidation was completed. A 6.6 cm 24.0 percent clay solids sample resulted. This sample was capped with a 4.0 cm 6:1 sand/clay cap (16.0% initial clay solids, 40-100 sand). The sample was then reaccelerated to 80 g's and these results are also presented in Figure 39.

Upon completion of the centrifugal testing, the sample was cored and the sand/clay ratio profile was plotted in Figure 40. Unlike the previous test, this profile indicates high sand/clay ratios until

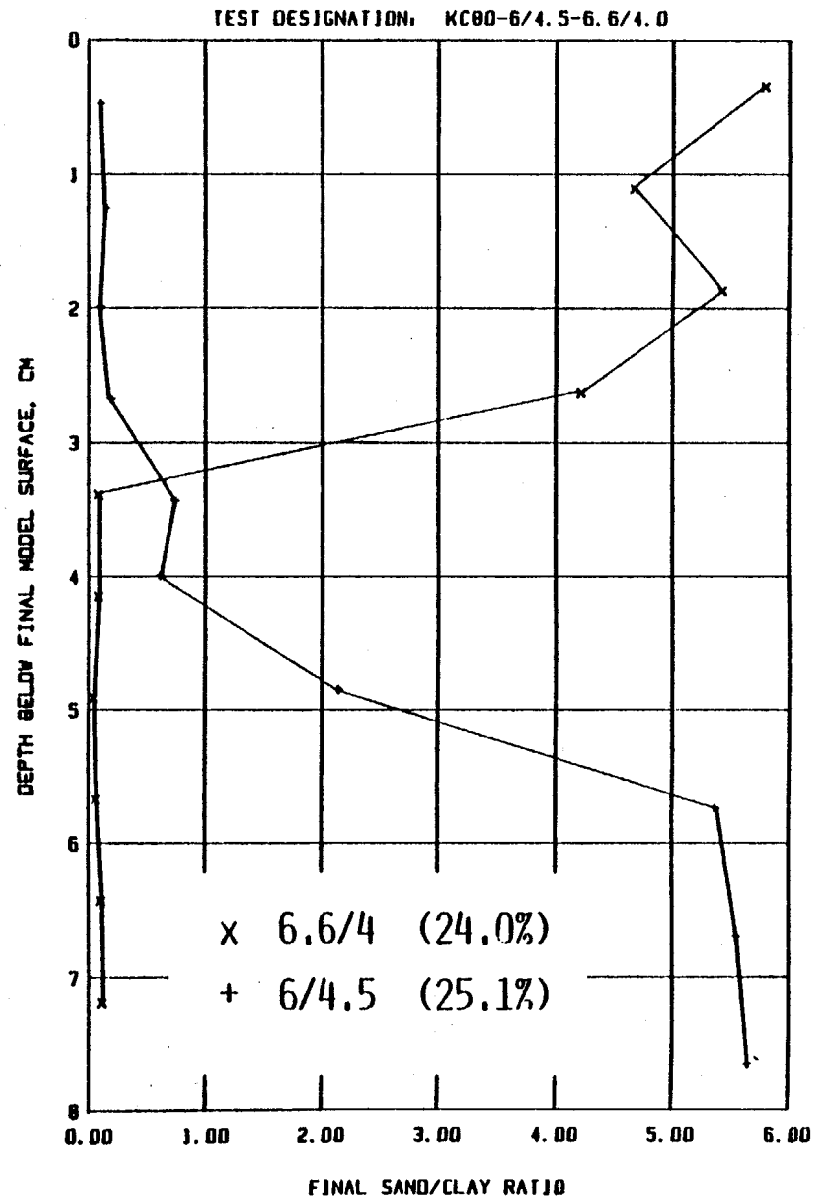
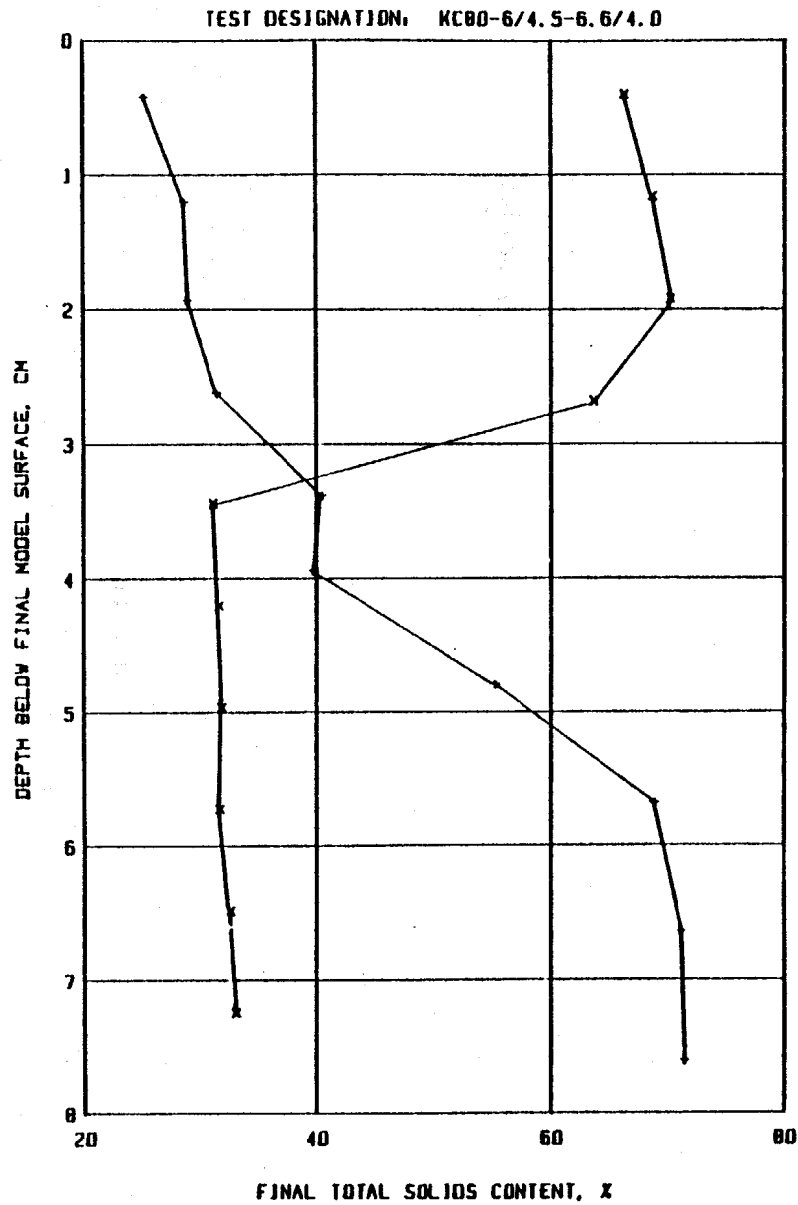


Figure 40: Profiles of total solids content and sand/clay ratio with depth for test series KC80-6/4.5 and KC80-6.6/4.0

approximately mid-depth. These values then rapidly decrease.

Segregation had not occurred!

Upon analyzing the initial conditions of these two tests, both appear very similar; however, there is one important difference. In the first test, the underlying clay (25.0% solids) was thoroughly mixed before being placed in the container and capped. In the second test, the underlying clay was capped after achieving self-weight consolidation (24.0% solids); it was never remixed. Although the initial average solids contents are very similar, only the undisturbed clay has sufficient strength to support a cap. Remixing or remolding the clay reduces this strength to the point where it is unable to support a cap and segregation then results as was observed during the first test.

#### Capping with Limited Segregation

Once the relationship between clay shear strength and segregation was better understood, a series of sand/clay capping tests were performed in which the segregation of sand was limited or controlled. These tests were performed in a similar manner to test KC80-6.6/4.0 where no mixing of the clay was performed prior to capping and in which the segregation of sand was limited.

Three models of approximately 10.2 cm in height and 20.5 percent clay solids were accelerated at 80 g until self-weight consolidation was completed. This resulted in samples with an approximate final height of 7.5 cm and 26.6 percent clay solids [KC80-7.5/4 (1:1), (8:1), & (6:1)]. Each model was then capped with a 4.0 cm sand/clay cap of either 1:1, 3:1, or 6:1 sand/clay ratio. Actual phosphate sand tailings were used (see Figure 41 for grain size distribution). The initial clay solids

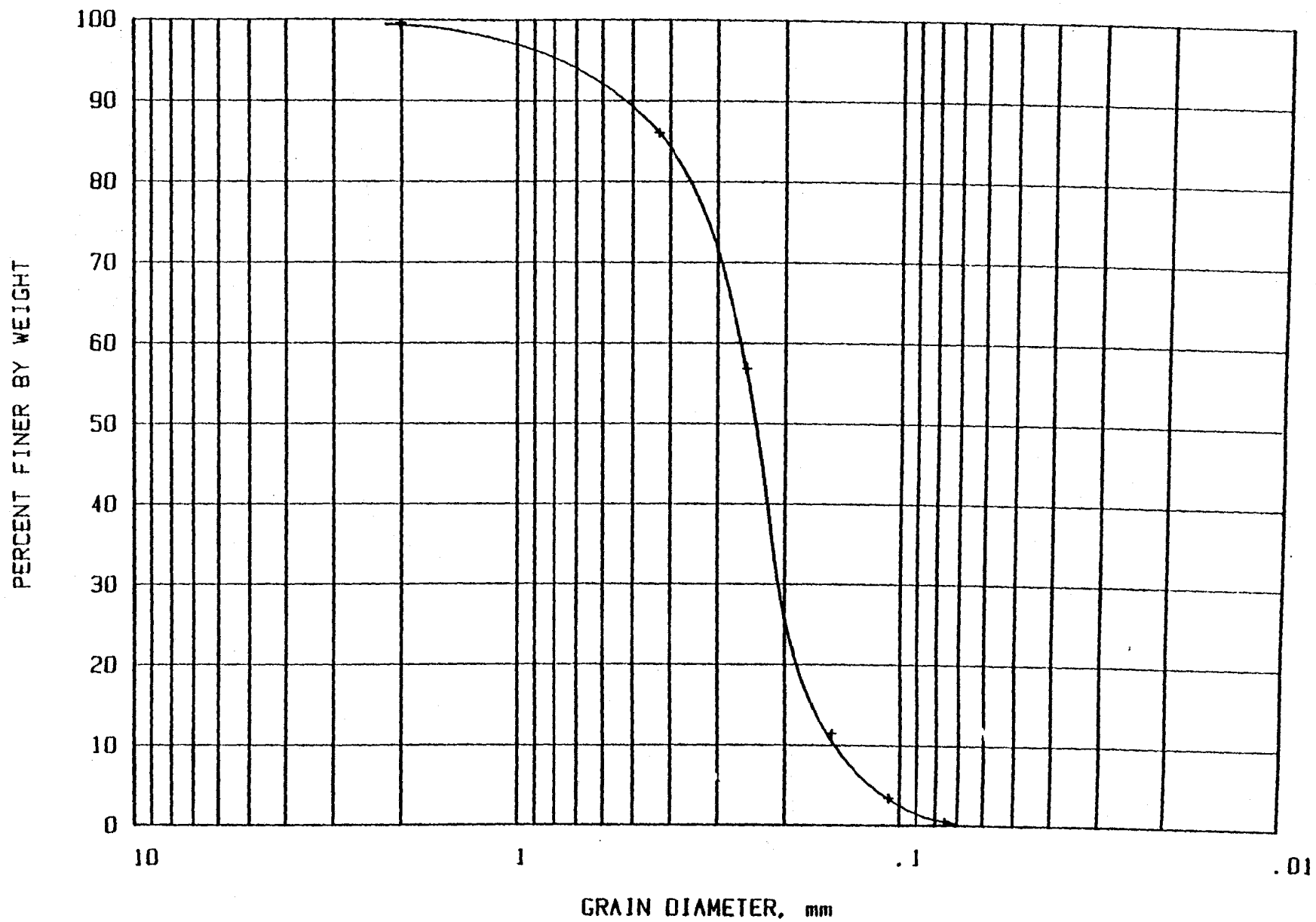


Figure 41: Grain size distribution for phosphate sand tailings

content for these caps was 12.7 percent. Each model was then accelerated at 80 g's until interface movement had stabilized. The models were then staged capped by placing an additional 2.0 cm sand/clay cap of the same sand/clay ratio as the initial cap. The models were then accelerated at 80 g's until interface movement had again stabilized. Figure 42 presents the results of the 4.0 cm capping test and Figure 43 presents the results of the additional staged 2.0 capping tests.

Although the initial model height of the KC80-7.5/4.0 tests were slightly different, the prototype interface/model time curves generally parallel one another. Considering the small differences in initial height, there is little difference in the final heights of the models. The results of the KC80-7.5/4.0 + 2.0 capping tests indicate similar results. The curves generally parallel one another and the differences in final height can largely be attributed to differences in initial height.

These test results summarized in Table 9 indicate that reduction in interface height is relatively independent of the sand/clay ratio of the overlying cap. As the sand/clay ratio increases, the unit weight of the capping material increases and the surcharge on the underlying clay also increases. This increase aids in the compression of the underlying cap and therefore serves to increase its solids content. For example in Table 9, a 18.4% increase in solids content occurred for the 1:1 s/c mix, while a 32.3% increase occurred for the 6:1 s/c mix. This increase in solids content, however, does not translate into a considerable reduction in interface height when compared to Tower sand/clay ratio



TEST DESIGNATION: KC80-7.5/4.0

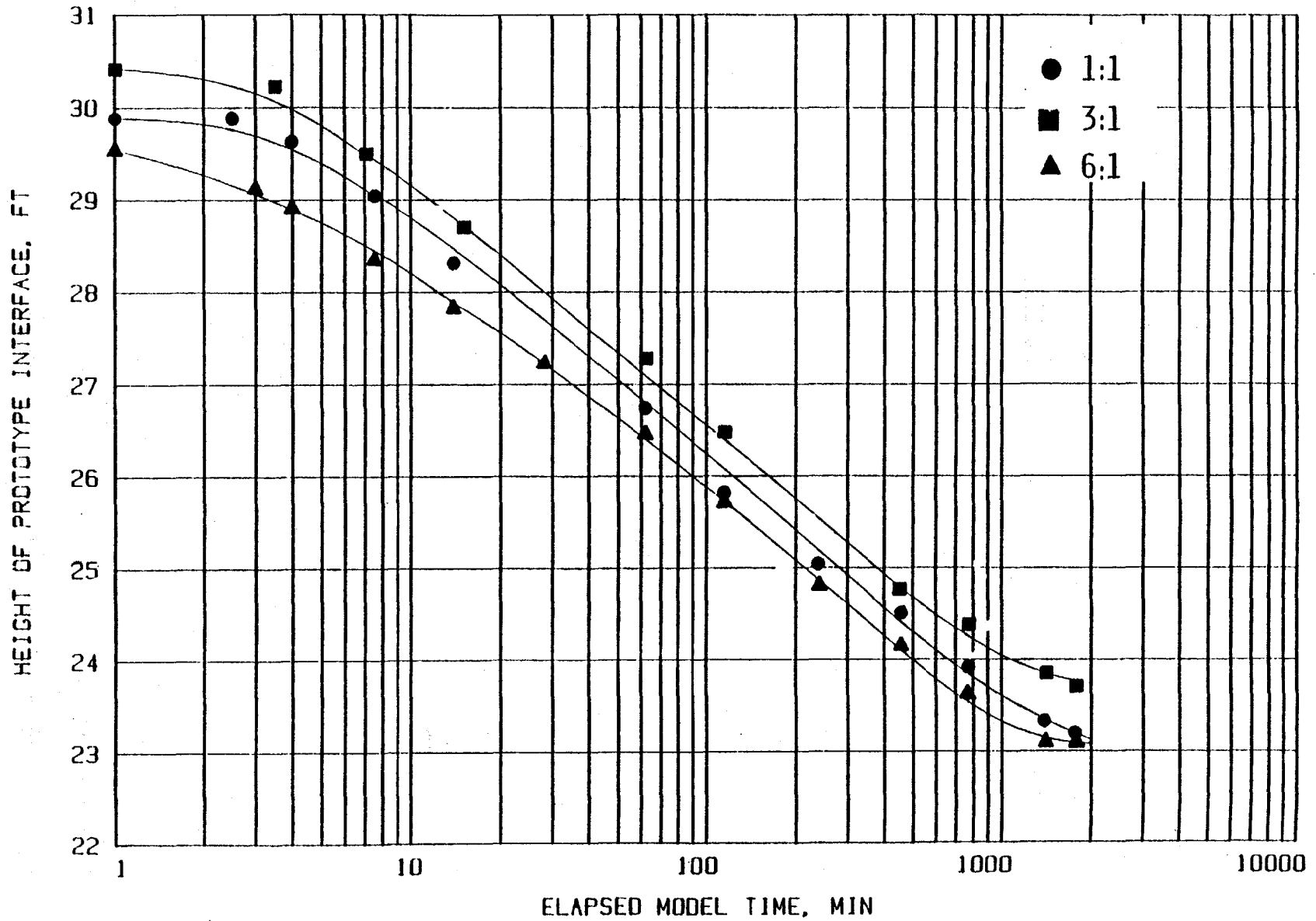


Figure 42: Prototype interface vs model time for 4 cm cap, test series KC80-7.5/4.0

TEST DESIGNATION: KC80-7.5/4.0+2.0

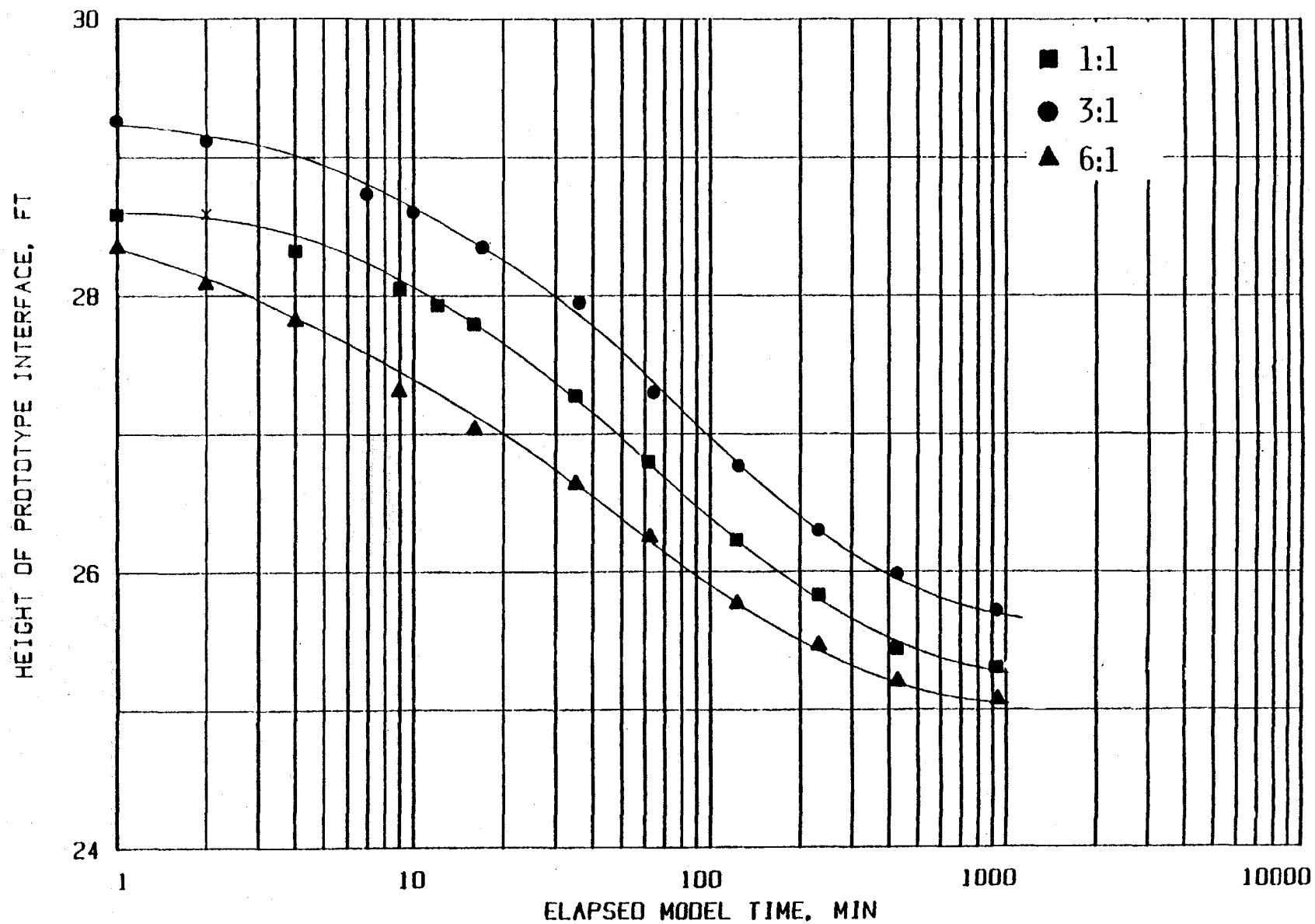


Figure 43: Prototype interface vs model time for 2 cm cap, test series KC7.5/4.0 + 2.0

Table 9  
Comparisons of SCR Effects in S/C Caps

Test	Initial Conditions		Final Conditions		Percent (a) Consolidation %	Percent Increase (b) in Solids Content %
	Prototype	Solids	Prototype	Solids		
	H <sub>t</sub> , H <sub>0</sub> (ft)	Content S <sub>0</sub> %	H <sub>t</sub> , H <sub>f</sub> (ft)	Content, S <sub>f</sub> %		
KC80-7.5/4 (1:1)	29.9	26.6	23.2		22.4	
KC80-7.5/4 (3:1)	30.5	26.6	23.8		22.0	
KC80-7.5/4 (6:1)	29.5	26.6	23.1		21.7	
KC80-7.5/4+2(1:1)	28.6	unk	25.3	31.5	11.5	18.4
KC80-7.5/4+2(3:1)	29.3	unk	25.7	32.2	12.3	21.0
KC80-7.5/4+2(6:1)	28.4	unk	25.1	35.2	11.6	32.3

$$(a) \text{ \% Consolidation} = \frac{(H_0 - H_f)}{H_0}$$

$$(b) \text{ \% Increase in Solids} = \frac{S_0 - S_f}{S_0}$$

**capping tests. As the sand/clay ratio increases, the volume of relatively incompressible sand also increases, which tends to negate any reduction in interface height due to compression of the underlying clay.**

**After completion of the centrifugal tests, each sample was cored. The profiles of effective clay and total solids content are presented in Figure 44. The final sand/clay ratio profile is presented in Figure 45. While higher sand/clay ratio caps may not provide any real reduction in interface height, they do increase the average solids content of the underlying clay. The 6:1, 3:1, and 1:1 sand/clay caps produced average clay solids contents in the underlying layer of 35.2, 32.2, and 31.5 percent, respectively. For reference, the initial clay solids content of this layer (due to self-weight consolidation) prior to capping was 26.6 percent.**

**Migration of the sand into the underlying clay was not a severe problem. The initial clay solids content of the sand/clay caps (12.7%) was insufficient to keep the sand in suspension, however. This is indicated by fluctuating sand/clay ratios down to approximately mid-depth. A sand/clay ratio in excess of 19 was observed approximately 4 cm below the surface of the 6:1 sand/clay capping test. This is a striking example of the segregation problems associated with low clay solids sand/clay mixes under accelerated conditions.**

#### **Staged Capping with S/C Mix Caps**

**A comparison was made between the 4 cm 3:1 sand/clay capping test [KC80-7.5/4 (3:1)] and a staged 2 cm plus 2 cm 3:1 capping test [KC80-7.5/2+2 (3:1)]. A 7.5 cm, 26.6 percent clay solids sample was capped with a 2.0 cm 3:1 sand/clay cap (12.7% initial clay solids) and**

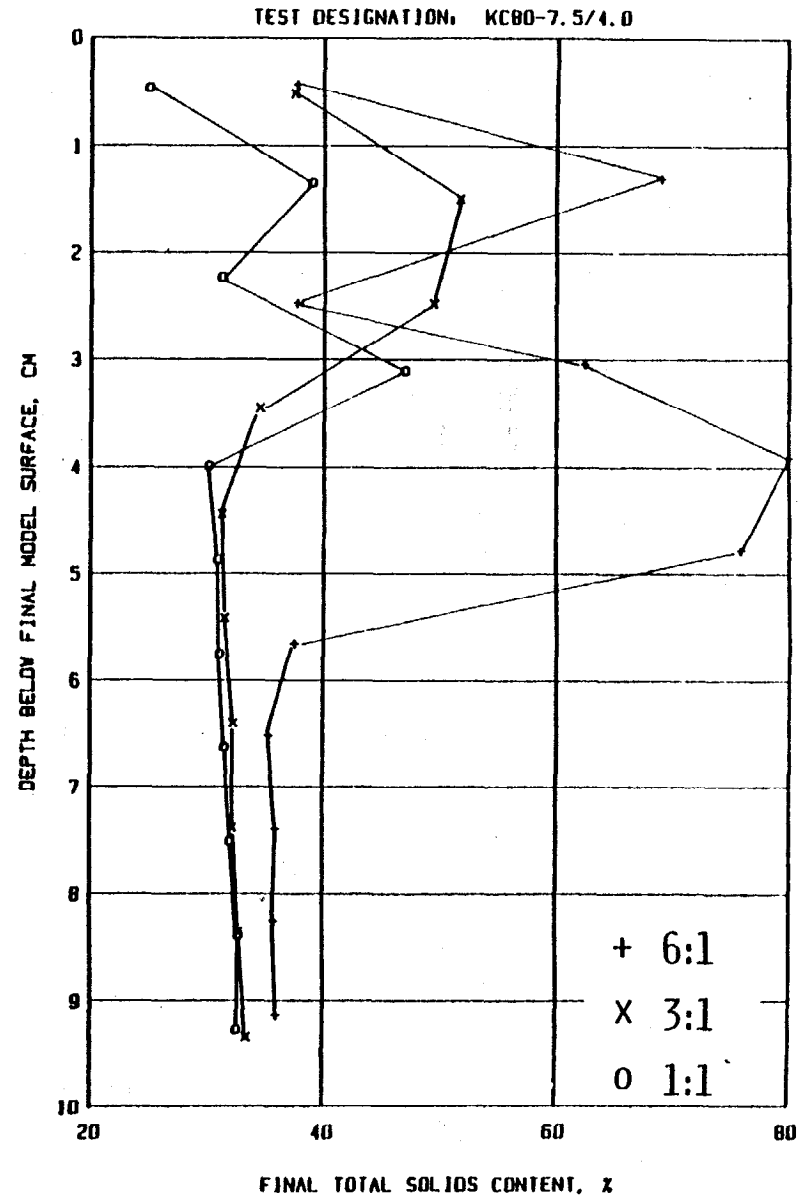
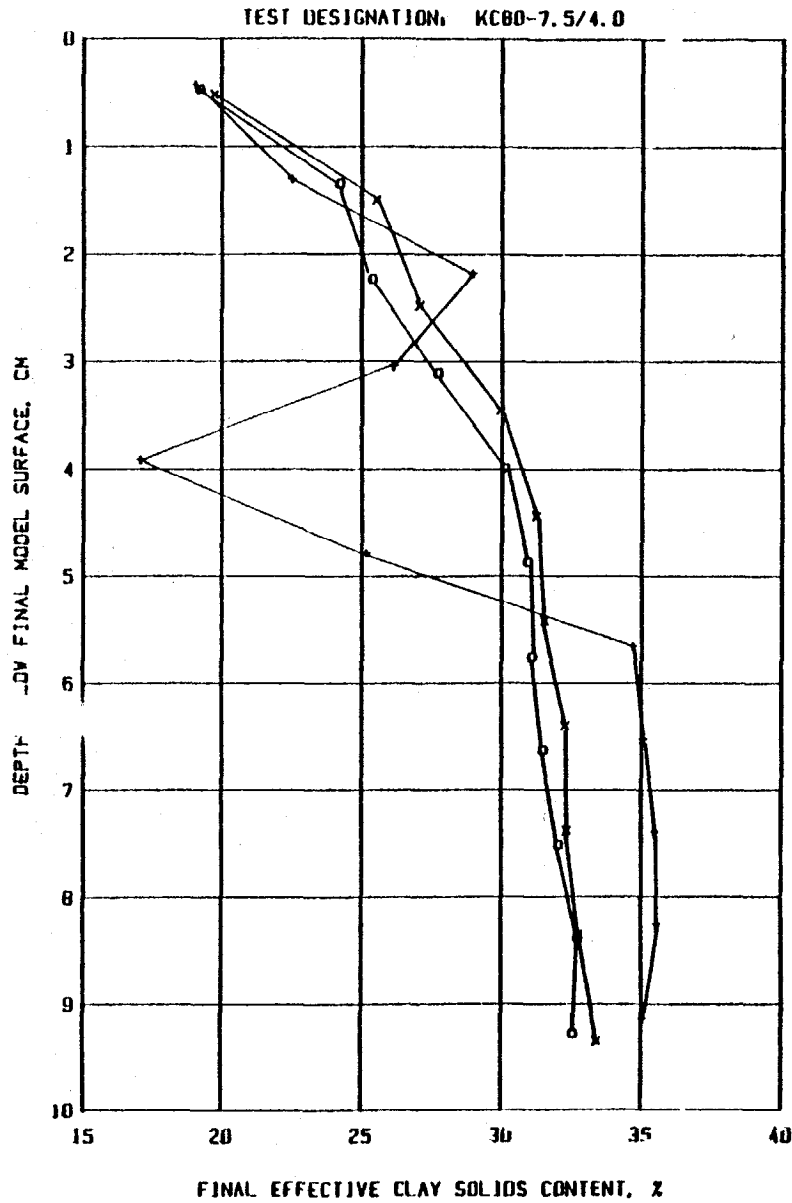


Figure 44: Profiles of effective clay and total solids contents with depth, test series KC80-7.5/4.0+2.0

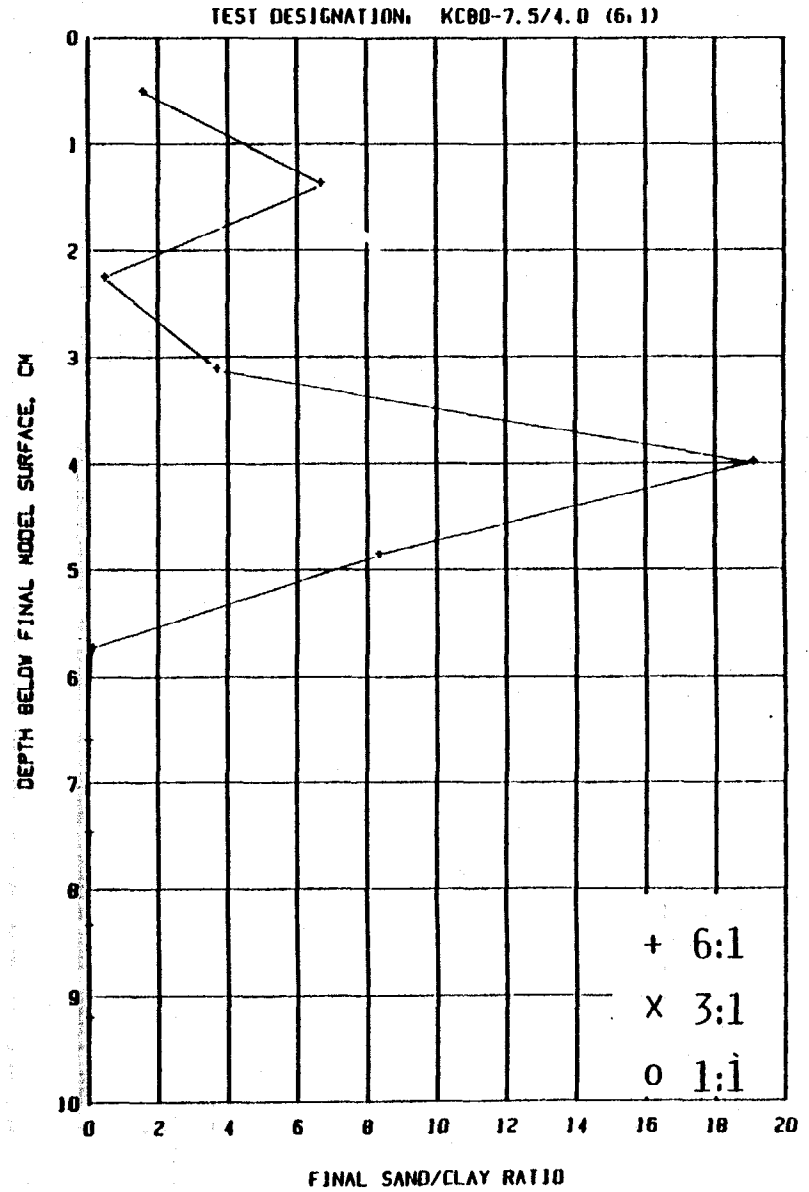
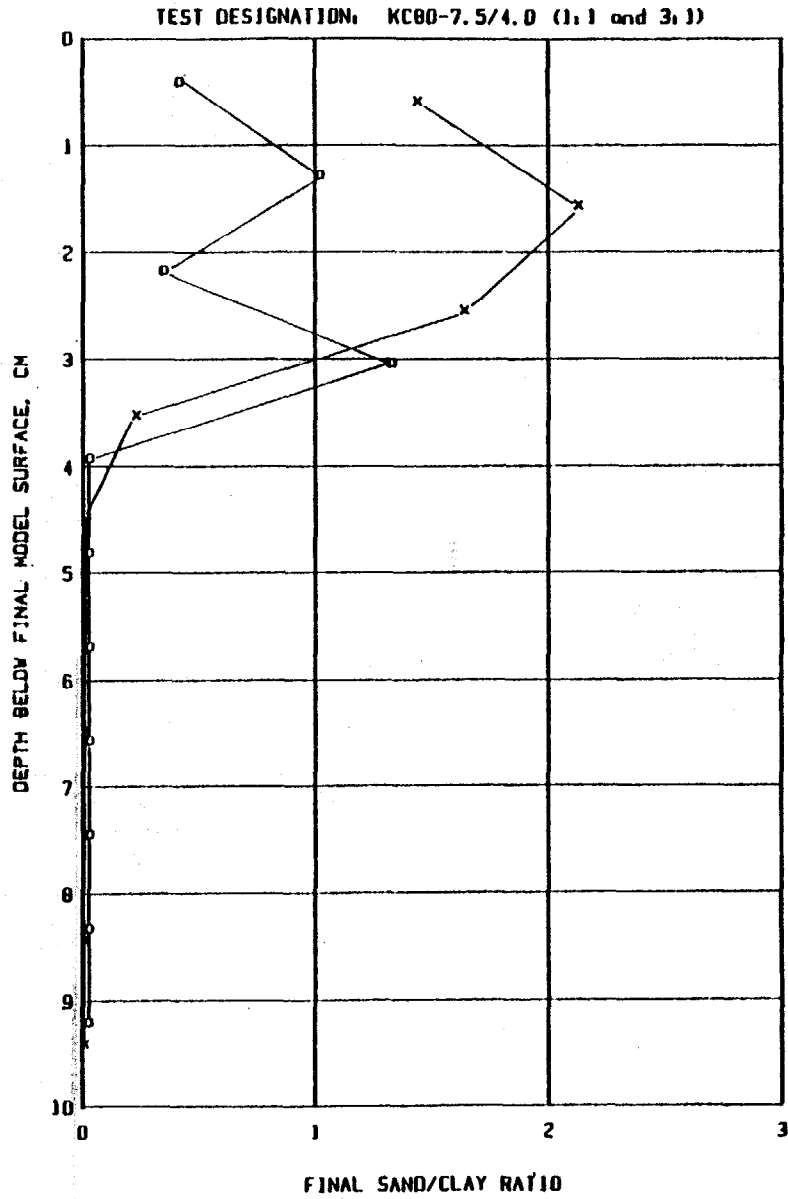


Figure 45: Profiles of sand/clay ratios with depth for KC80-7.5/4.0 series (1:1, 3:1, and 6:1 sand/clay caps)

accelerated at 80 g's until interface movement had stabilized. It was then capped with another 2.0 cm 3:1 sand/clay cap and again accelerated at 80 g's until interface movement had stabilized. Figure 46 presents the results of both the 4 cm and 2 cm plus 2 cm capping tests. For the 4 cm cap model, the height reduction was 22.1%, while for the staged 2 cm plus 2 cm cap had a height reduction of 28.1%[17.9 + 10.2]. Thus, greater reductions in interface height can be achieved when a staged capping procedure is used. The total volume of capping material used during each test was equal. However, the staged application of the 3:1 mix resulted in a final interface height approximately one foot lower than that obtained with a single application. The obvious disadvantage of the staged application is that it took approximately twice as long as a single application of equivalent capping material.

**Comparison of S/C Mix vs Capping**

An examination of the centrifugal model data for s/c mix and capped ponds presented in Tables 4, 5, 6 and 8 and summarized below, reveal the hierarchy of consolidation magnitude as: (a) sand caps (staged), (b) s/c mix cap (staged), (c) homogeneous s/c mix (1:1), and lastly (d) treated waste clays.

**Summary of Treatment Effects**

Treatment	Hts of Pond H <sub>0</sub> (ft)	Initial Solids Content, S <sub>0</sub> (%)	Final Solids Content, S <sub>f</sub> (%)
Untreated	15.9 - 26.2	14.6 - 16.3	23.7 - 24.0
S/C Mix (1:1)	15.8	16.0	25.3
S/C Mix Cap (Staged)	29.9	26.6	31.5
Sand Cap (staged)	26.2	14.6	40.0

TEST DESIGNATION: KC80-7.5/4.0 and 7.5/2.0+2.0

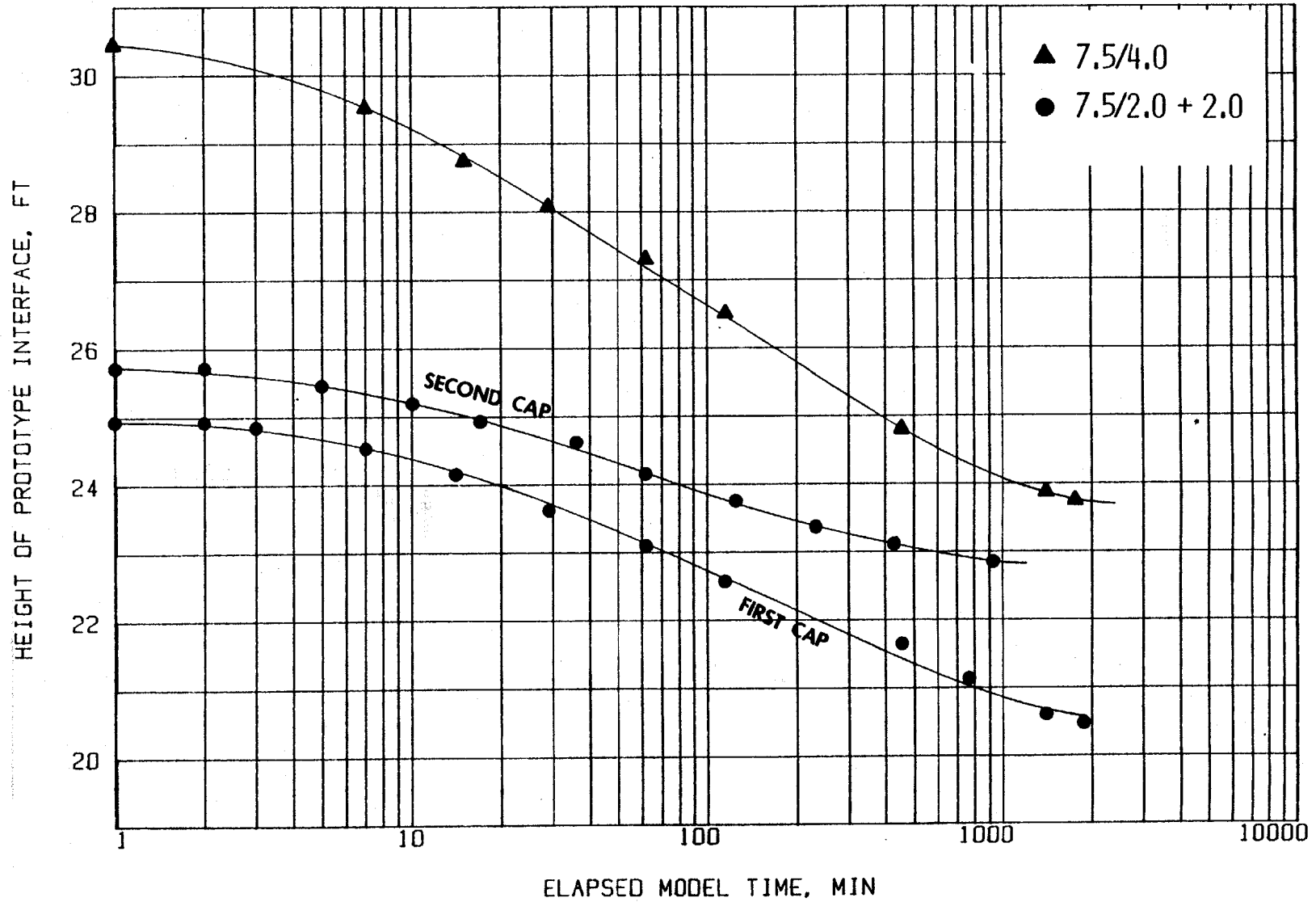


Figure 46: Prototype interface vs model time for KC80-7.5/4.0 and KC80-7.5/2.0 + 2.0



Considering that consolidation magnitudes are governed by the magnitude of effective stress change, the purpose of a s/c mix is to increase the unit weight and thereby the effective stress. Similarly, a cap increases the effective stress by placing a surcharge on the underlying clays. Accordingly, this section examines and compares the effective stresses and consolidation enhancement induced by s/c mix or capping.

For these comparisons an illustrative example is posed.

Specifically, consider a waste pond 10 ft. deep for which the following options for disposal are available

Case A: Fill the pond with untreated clay,  $S_o = 16\%$

Case B: Fill the pond with 2:1 s/c mix,  $S_c = 16\%$

Case C: Instead of mixing sand to form a s/c mix as in Case B, use the sand to form a cap with  $\gamma_s = 100$  pcf. The amount of sand in both Case B and C is equal.

Case D: Same as Case C, but the sand cap becomes submerged causing the effective stress to be reduced due to buoyancy effects on the cap, i. e.,  $\gamma'_s = (100 - 62.4) = 37.6$  pcf.

Case E: Using the same amount of sand, create a 3:1 s/c mix as a cap over the underlying clay, as an alternative method for capping with sand only.

These cases assume an unlimited supply of waste clays for filling the pond; however, the sand used in the s/c mixes and caps is equal for all appropriate cases. Appendix C provides the supporting calculations for these comparisons.

Effective Stress Profile. Since the effective stress,  $\sigma'_0 = \sigma'_z$  (where  $\gamma'$  = buoyant unit weight, and  $z$  = depth), the Equations C-1 and

C-2 are the buoyant unit weights respectively for untreated clay and s/c mix

$$\text{untreated clay} \quad \gamma' = \frac{S \gamma_w (G-1)}{S(1-G) + G} \quad (\text{Eqn. C-1})$$

and s/c mix where  $G$  (clay) =  $G$  (sand)

$$\gamma' = \frac{S \gamma_w (SCR)(G-1)}{G(1-S) + (1+SCR)} \quad (\text{Eqn. C-2})$$

For example, considering a SCR = 2:1,  $G = 2.65$ , and  $S = 16\%$ , the  $\gamma'$  values for untreated clay and s/c mix are:

$$\begin{aligned} \text{untreated clay} \quad \gamma' &= \frac{(0.16)(62.4)(2.65-1)}{(0.16)(1-2.65) + 2.65} = 6.90 \text{ pcf} \\ \text{s/c mix} \quad \gamma' &= \frac{(0.16)(62.4)(2+1)(2.65-1)}{2.65(1-.16) + 0.16(1+2)} = 18.3 \text{ pcf} \end{aligned}$$

Thus 265% increase in  $\gamma'$  is achieved by a 2:1 s/c mix.

Having determined the buoyant unit weights for untreated clay and s/c mix, we now need to calculate cap height for cases C, D, and E. If we now consider that the height of a sand cap that can be achieved by using an equal amount of sand as a s/c mix is equal to the weight of sand ( $W_s$ )  $\div$   $\gamma_s$ ; then per unit depth of pond

$$\frac{W}{s} (\text{Sand in s/c mix}) = \frac{S \gamma_w G (SCR)}{G(1-S) + S(1+SCR)} \quad (\text{Eqn. C-3})$$

$$\text{and } H_c (\text{Ht of cap}) = \frac{W_s}{\gamma_s} \quad \text{where } \gamma_s = \text{unit wt. of cap} \quad (\text{Eqn. C-4})$$

For example, placing the sand present in a 10 ft. deep pond filled with a 2:1 s/c mix as a cap with a  $\gamma_s = 100$  pcf results in a 1.95 ft. cap creating a surcharge (8) of 195 psf as shown below:

$$W_s = \frac{(0.16)(62.4)(2.65)(2)}{(2.65)(1-0.16) + 0.16(1+2)} \times 10 \text{ ft.} = 195.54 \text{ lbs.}$$

$$H_c = W_s / \gamma_s = 195.54 / 100 = 1.96 \text{ ft.}$$

$$q = \gamma_s H_c = (100)(1.96) = 196 \text{ psf}$$

**For a cap composed of a s/c mix (Case E) the  $W_s$  of sand available in for the cap was given by Equation C-3, and the height/unit depth of pond for the s/c mix cap ( $H_{SC}$ ) is given as Equation C-4**

$$H_{SC} = W_c [G(1-S) + S(1+SCRC)] / SG\gamma_w$$

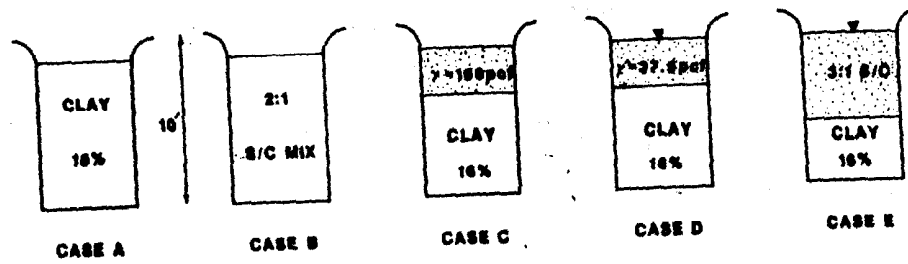
$$W_c = W_s / SCRC$$

**where SCRC = sand/clay ratio of the cap**

**From these equations the effective stress profile as presented in Table 10 can be calculated for Cases A through E. Likewise Figure 47 presents these profiles. An examination of the effective stress profiles presented in Figure 47 reveals that sand capping (Case C) provides the greatest effective stress and hence the greatest consolidation. However, the effective stress profiles of the s/c mix (Case B) compared with those of submerged sand caps (Case D) or s/c mix caps (Case E) are mixed and no clear distinction of which provides the greatest effective stress can be made.**

**Consolidation Magnitude. Since the magnitude of consolidation is the desired result, by assuming the constitutive relationship for effective stress-void ratio can be expressed as  $e = A\bar{\sigma}^{-B}$  (Somogyi, 1979), then result in the consolidation magnitude (McVay, 1984) as shown below: (also Appendix C).**

Table 10  
 Effective Stress Profiles for S/C Mix vs Capped 10 Ft. Waste Pond



Effective Stress,  $\sigma'$  (psf) @ Depths, z (Ft)

Case	$\gamma'$ clay pcf	$\gamma'$ cap pcf	$D_{clay}$ (ft)	$H_{cap}$ ft	0	$H_c$	5'	10'
A	6.90	-	10.0	0	0	0	34.5	69.0
B	18.26	-	10.0	0	0	0	91.3	182.6
C	6.90	100	8.04	1.96	0	196	21.7	251.5
D	6.90	37.6	8.04	1.96	0	73.7	94.7	129.2
E	6.90	22.99	2.94	7.06	0	162.3	114.9	182.6

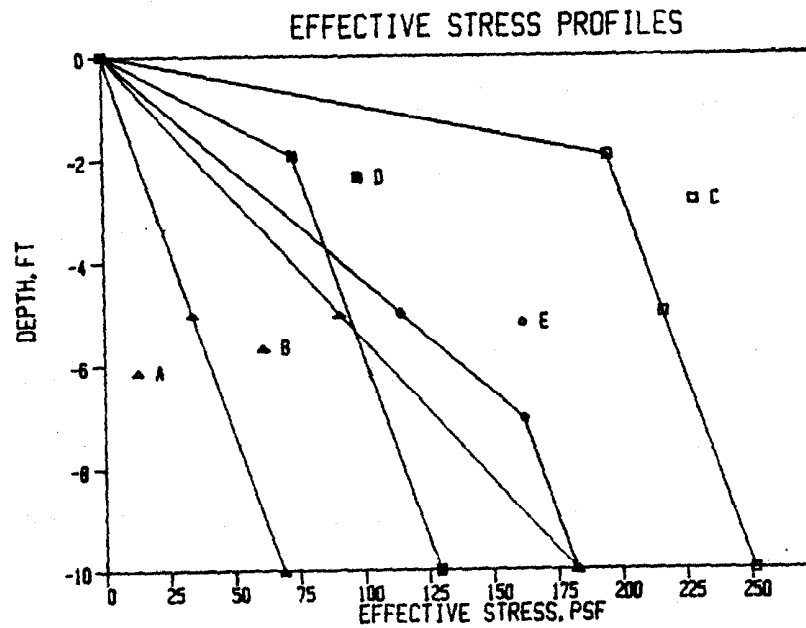


Figure 47 Comparison of Effective Stress Profiles for S/C Mix vs Capped 10 Ft Deep Waste Pond

In the case of homogeneous clays or s/c mix

$$\frac{\Delta e}{1+e_0} = \frac{\Delta H}{H_0} \rightarrow \Delta H = \frac{H_0 \Delta e}{1+e_0} \quad \text{or} \quad \Delta H = \int_{H_i}^{H_f} \frac{\Delta e}{H e_0} dz$$

If  $\Delta e = e_0 - e_f$  and  $e_f = A\bar{\sigma}^{-\beta}$ , the  $\Delta e = e_0 - A\bar{\gamma}^{-\beta}$

Since  $\bar{\sigma} = \gamma'z$ , then  $\Delta e = e_0 - A(\gamma'z)^{-\beta}$

$$\text{Finally, } \Delta H = \int_{H_i}^{H_f} \frac{e_0 - A(\gamma'z)^{-\beta}}{1+e_0} dz = \frac{1}{1+e_0} \int_{H_i}^{H_f} e_0 - A(\gamma'z)^{-\beta} dz$$

where  $H_i$  = top of pond depth corresponding to stress at  $e_0$  and  $H_f = H_i +$   
depth of clay,  $D_c$ , in the pond

$$\text{Integrating, } \Delta H = \frac{1}{1+e_0} \left[ e_0 z - \frac{A\gamma'^{1-\beta} z^{1-\beta} (1-\beta)^{H_f}}{1-\beta} \right]_{H_i} =$$

$$\frac{1}{1+e_0} \left[ e_0 (H_f - H_i) - \frac{A\gamma'^{1-\beta}}{1-\beta} \{ H_f^{1-\beta} - H_i^{1-\beta} \} \right]$$

In the case of a capped pond, we can treat the cap as a surcharge and

$\bar{\sigma} = q + \gamma'_c z_c$ , where  $q = \gamma'_{cap} z_{cap}$  and  $\gamma'_c, z_c$  are the buoyant unit weight and depth of clay respectively.

$$\text{Then } \Delta e = e_0 - A(q + \gamma'_c z)^{-\beta} \quad \text{and} \quad \Delta H = \frac{1}{1+e_0} \int_{z_i}^{z_c} e_0 - A(q + \gamma'_c z)^{-\beta} dz$$

where  $z_i$  = surface elevation of clay beneath cap  
and  $z_c = z_i +$  depth of clay in pond.

Remembering that  $\int (ax + b)^n dx = \frac{1}{a(n+1)} (ax + b)^{n+1}$ ,  $n \neq -1$ , then

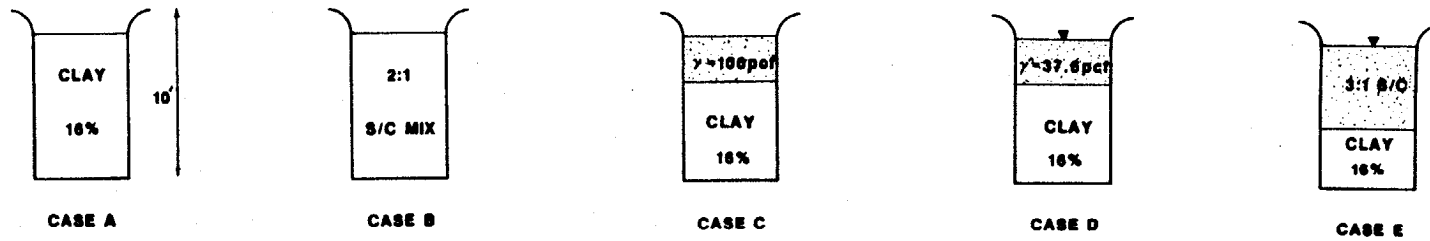
$$\begin{aligned} \Delta H &= \frac{1}{1+e_0} \int_{z_i}^{z_c} e_0 dz - \frac{A}{1+e_0} \int_{z_i}^{z_c} (\gamma_c z + q)^{-\beta} dz = \\ &= \frac{1}{1+e_0} [e_0 z]_{z_i}^{z_c} - \frac{A}{1+e_0} \left[ \frac{(\gamma_c z + q)^{-\beta}}{\gamma_c (1-\beta)} \right]_{z_i}^{z_c} \\ \therefore \Delta H &= \frac{1}{1+e_0} [e_0 (z_c - z_i)] - \frac{A}{\gamma_c (1-\beta)(1+e_0)} \left[ (\gamma_c z_c + q)^{1-\beta} - (\gamma_c z_i + q)^{1-\beta} \right] \end{aligned}$$

**Table 11 presents a comparison of consolidation magnitude using these equations for Cases A through E with supporting calculations in Appendix C. These calculations are based upon the assumption that the constitutive relationship  $e = A\bar{\gamma}^{-\beta}$  is the same for both waste clay and sand/clay mix. For Cases C and D, the sand cap is assumed as an incompressible surcharge, while for Case E, the s/c cap compressibility is calculated.**

**The use of the constitutive equation  $e = A\bar{\gamma}^{-\beta}$  implies that an effective stress,  $\bar{\gamma}$ , must exist for each  $e$  (or solids content) even though the effective stress at the top of the pond is zero. Accordingly, fictitious top of pond heights,  $H_f$  and  $H_i$ , are used by determining the effective stress,  $\bar{\sigma}$ , corresponding to the initial void ratio,  $e_0$ , and dividing by the buoyant unit weight,  $\gamma$ , of that void ratio. This procedure is straightforward, except for s/c mix cases, where several interpretations are possible. One interpretation uses the relationship  $e_t = A\bar{\sigma}^{-\beta}$  another  $e_t = e_c/(1+SCR)$  and  $e_t = A\bar{\sigma}^{-\beta}/(1+SCR)$ ; and lastly  $e_c = A\bar{\sigma}^{-\beta}$  and the sand is only considered to increase the buoyant**

Table 11

Comparison of Consolidation Magnitudes for S/C Mix and Capped Waste Ponds



Case	Description (a)	Initial Void Ratio, $e_0$ (b)	Unit Wt. clay, $\gamma'_c$ pcf (c)	Unit Wt. cap, $\gamma'$ pcf (d)	Depth of clay, $D_c$ (ft)	Initial Ht. $H_i$ (ft) (e)	Final Ht. $H_f$ (ft)	Surcharge $q$ (psf)	Consolidation $\Delta H$ (ft)	Final Pond Ht (ft)
A	Homogeneous clay $S_0 = 16\%$	13.91	6.90	-	10.0	1.433	11.433	--	2.20	7.80
B <sub>1</sub>	2:1 S/C	4.63	18.26	-	10.0	131.7	141.7	-	0.05	9.95
B <sub>2</sub>	2:1 S/C sand removed	13.91	18.26	-	8.82	0.542	9.362	-	2.68	7.31
B <sub>3</sub>	2:1 S/C $e_t$ used	4.63	18.26	-	10.0	0.546	10.546	-	2.80	7.20
C	Sand Cap	13.91	6.90	100	8.04	1.433	9.473	196	3.51	6.49
D	Sand Cap (submerged)	13.91	6.90	37.6	8.04	1.433	9.473	73.7	2.87	7.13
E <sub>1</sub>	3:1 S/C cap	3.48	-	22.99	7.06 (f)	440.8	447.86	-	0.013	7.05 (f)
E <sub>2</sub>	3:1 S/C sand removed	13.91	-	22.99	5.88 (f)	0.43	6.31	-	2.09	5.40 (f)
E <sub>3</sub>	3:1 S/C $e_t$ used	3.48	-	22.99	7.06 (f)	0.43	7.49	-	1.80	5.26 (f)
E <sub>4</sub>	Clay	13.91	6.90	-	2.94	1.433	4.37	162.3	1.21	1.73 (g)
E	3:1 S/C cap								1.80+1.21	6.99

(a)  $S_0$  clay = 16%,  $G = 2.65$  (b)  $e = (1-S)G/S$  (c)  $\gamma' = S\gamma_w(G-1)/[S(1-G) + G]$  (d)  $\gamma' = S\gamma_w(SCR + 1)(G-1)/[G(1-S) + S(1+SCR)]$

(e)  $H_i = \bar{\sigma}/\gamma'$ ,  $\bar{\sigma} = (e/A)** 1/\beta$ ,  $A = 22$ ,  $\beta = -0.2$  (f) S/C cap only (g) Clay only

unit weight. The last two interpretations are in close agreement for  $\Delta H$  calculations. Hence the  $e_t = A\bar{\sigma}^B/(1+SCR)$  interpretation, because of its computational ease is preferred. However, additional research on the compressibility and permeability of s/c mixes is needed.

An examination of Table 11 reveals a clearer hierarchy of consolidation magnitudes than does the effective stress profiles and suggests that capping even when submerged provides a greater consolidation than a s/c mix.

#### FLOCCOLANT TREATMENT OF NORALYN CLAY (Bloomquist, 1982)

The use of flocculants to enhance sedimentation and/or rapidly achieve solids contents capable of supporting a surcharging cap is an alternative consideration for waste clay disposal schemes. Although these centrifugal model tests were performed on Noralyn clays instead of Kingsford clays as reported previously in this report, these data are included for completeness (Bloomquist, 1982). The objectives of these model tests were to: (a) determine the effect of flocculant dosage, (b) evaluate the effectiveness of various flocculants, (c) examine the feasibility of capping flocculated clay and (d) study flocculated clay/sand mix performance. Table 12 summarizes the results of these model tests.

#### Optimum Flocculant Dosage

Table 13 lists the optimum dosage based upon 1 g bench tests for various flocculants. These values are based upon settling rates. Figure 48 shows the effects of Polyhall 1082 dosage level versus time. The approximate optimum dosage for this reagent was 0.60 kilograms of flocculant metric ton (kg/mt) of dry clay. As illustrated by the curves, as the flocculant dosage is increased, the initial rate of



Table 12  
Evaluation of Flocculants by Centrifugal Models

Test # & Clay	Flocculant	Dosage	Initial Model Condition		Acceler- ation level, g's	Dura- tion min.	Final Model Conditions		Prototype Conditions	
			Solids Contents %	Model Ht. cm			Solids Content %	Model Ht. cm	Initial Ht. m	Final Ht. m
Noralyn SD-2	-	-	4.3	10	60	600	24.1	1.55	6.0	0.93
SDF3	PAM	.25 kg/m <sup>T</sup>	4.3	10	60	600	22.7	1.66	6.0	1.00
SDF2	P'Ha11 1082	.50 kg/m <sup>T</sup>	4.3	10	60	600	21.2	1.80	6.0	1.08
SDF4	P' Ha11 1082	.60 kg/m <sup>T</sup>	4.3	10	60	550	21.4	1.78	6.0	1.07
SDF5	P' Ha11 1082	1.00 kg/m <sup>T</sup>	4.3	10	60	550	20.5	1.87	6.0	1.12
SDF6	P' Ha11 1082	3.00 kg/m <sup>t</sup>	4.3	10	60	550	19.1	2.03	6.0	1.22
SF7	Jaguar C-13-5	1.25 kg/m <sup>t</sup>	4.3	10	60	500	20.4	1.88	6.0	1.13
SF9	PEO	1.25/kg/m <sup>t</sup>	4.3	10	60	500	20.9	1.83	6.0	1.10
SF9	Percol 919-2	0.75 kg/m <sup>t</sup>	4.3	10	60	500	21.7	1.75	6.0	1.05
SF10	P'Ha11 402C	0.75 kg/m <sup>t</sup>	4.3	10	60	500	21.3	1.79	6.0	1.07
SF11	Percol 351	1.00 kg/m <sup>t</sup>	4.3	10	60	500	21.5	1.77	6.0	1.07
SF12	Percol 455	0.50 kg/m <sup>t</sup>	4.3	10	60	500	20.8	1.84	6.0	1.10
SF13	P'Ha11 1082	0.60 kg/m <sup>T</sup>	4.3	10	60	18	15.0	2.66	6.0	1.60
	+ 134 gm Sand		15.0	2.66	60	600	32.6	1.07	1.6	0.62
SF14	P'Ha11 1082	0.60 kg/m <sup>T</sup>	4.3	10	60	200	18.5	2.10	6.0	1.26
	+ 134 gm Sand		18.5	2.10	60	900	34.5	1.00	1.26	0.60
SF15	P'Ha11 1082	0.60 kg/m <sup>T</sup>	4.3	10	60	600	21.9	1.73	6.0	1.04
	+ 134 gm Sand									

Table 13

Approximate Optimum Dosages for Reagents Tested.

REAGENT NAME	TYPE	CHARGE	OPTIMUM DOSAGE KG/MT
POLYHALL 1082	POLYACRYLAMIDE	ANIONIC	0.60
POLYHALL 402c	POLYACRYLAMIDE	NONIONIC	0.75
PERCOL 455	POLYACRYLAMIDE	CATIONIC	0.50
PERCOL 351	POLYACRYLAMIDE	NONIONIC	1.00
PERCOL 919-2	POLYACRYLAMIDE	ANIONIC	0.75
PEO	POLYETHYLENE OXIDE	NONIONIC	1.25
JAGUAR c-13-s	GUAR GUM	CATIONIC	1.25

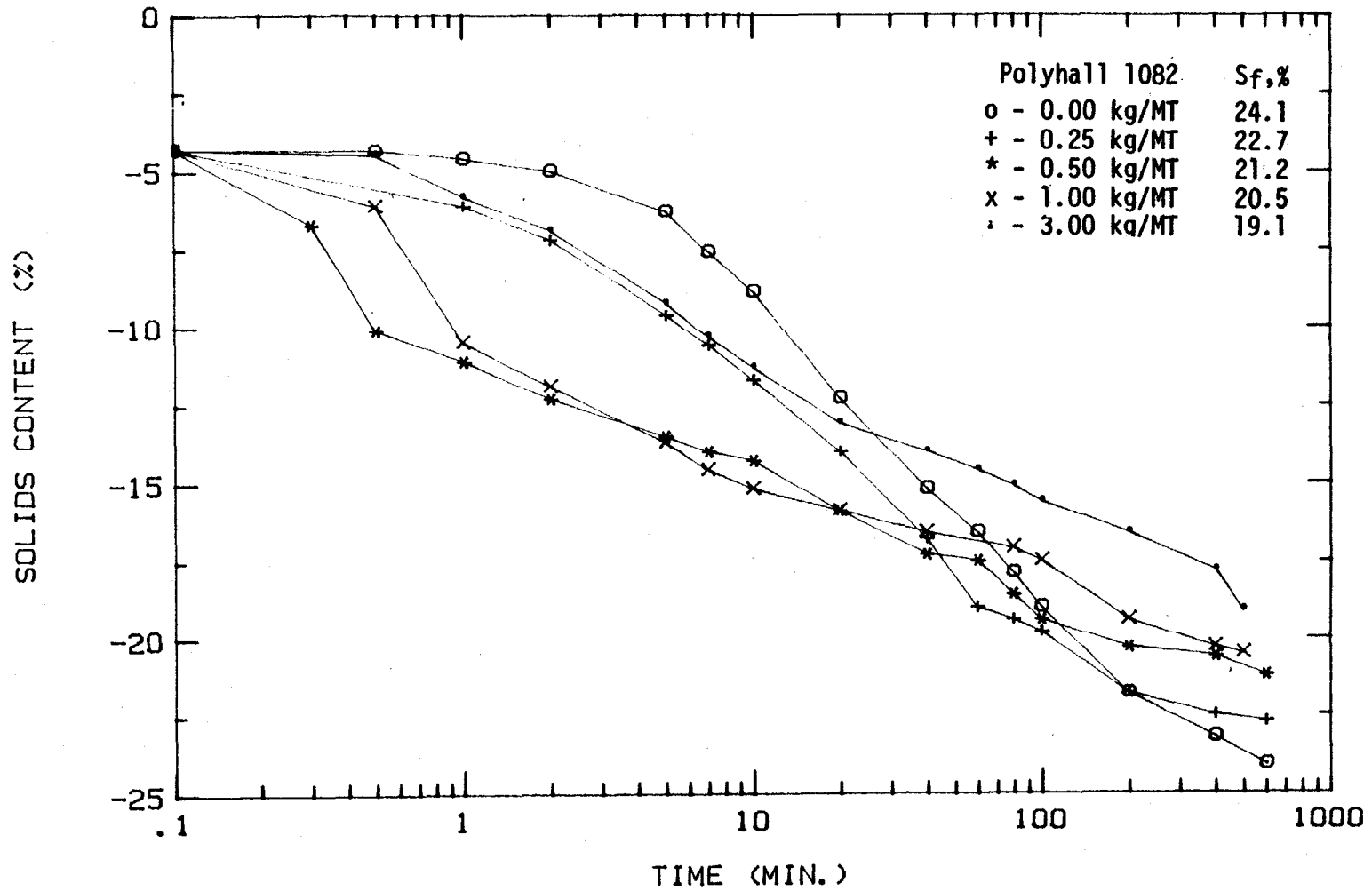


Figure 48: Effect of Dosage on Sedimentation/Consolidation for Noralyn Clay

settlement is substantially improved. However, as the dosage level increased beyond optimum, the settlement rate declined. At an extremely high dosage; i. e., 3 kg/mt, the benefits derived from the flocculant are reduced considerably.

Figure 48 also demonstrates the effect of flocculant over non-treatment on the final solids content. Although routine bench tests (1 g) have suggested that the final solids content achieved is reduced due to the larger flocs, (Bloomquist, 1982) the centrifugal tests belie this conclusion and show final solids contents of flocculated models only slightly lower than non-flocculated models. When the flocculated clay is subjected to field stress conditions, as provided in the centrifuge the agglomerated flocs collapse to these higher solids content. Nevertheless, in no model did the final solids content of a flocculated clay equal or surpass that of untreated clay which means that flocculants have a sedimentation rate advantage at the expense of a lower final solids content.

#### Flocculant Agent Effectiveness

Figures 49 and 50 evaluate various flocculating agents at their optimum dosages as determined from settling rates on 1-g bench tests. These results suggest that the polyacrylamides (PAM), Polyhall and Percol, were the most effective flocculant followed by polyethylene oxide (PEO) and guar gum. These results (Table 11) also show that anionic flocculants are the most effective, followed by nonionics and lastly cationic reagents. However the difference between flocculants is quite small. Polyhall 1082 and Percol 91, the anionics achieved final solids contents of 21.4 and 21.7%, respectively. The nonionics, Percol 351 and PEO achieved final solids contents of 21.5 and 20.9%,

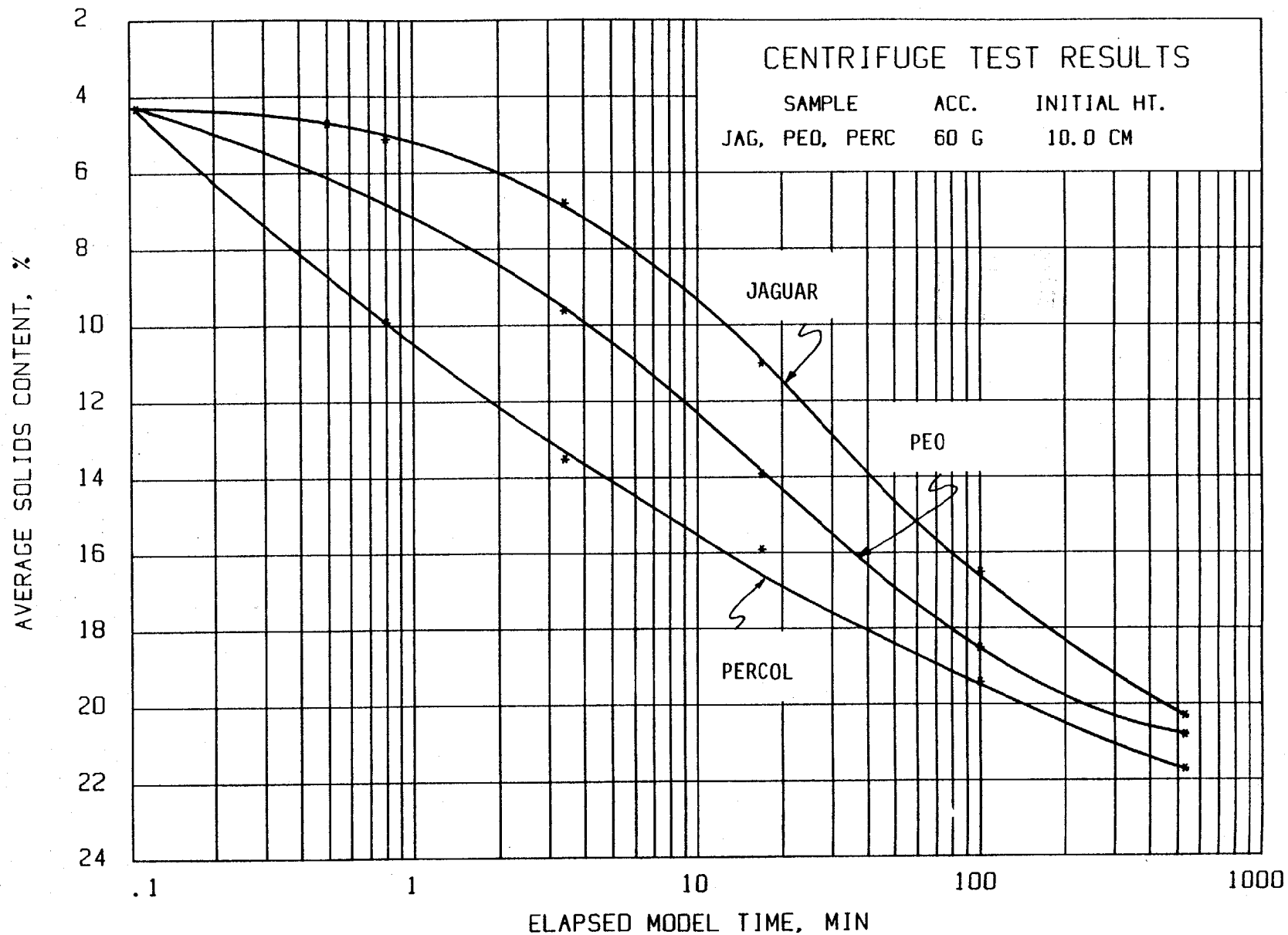


Figure 49: Average Solids Content Versus Time for Several Flocculated Specimens

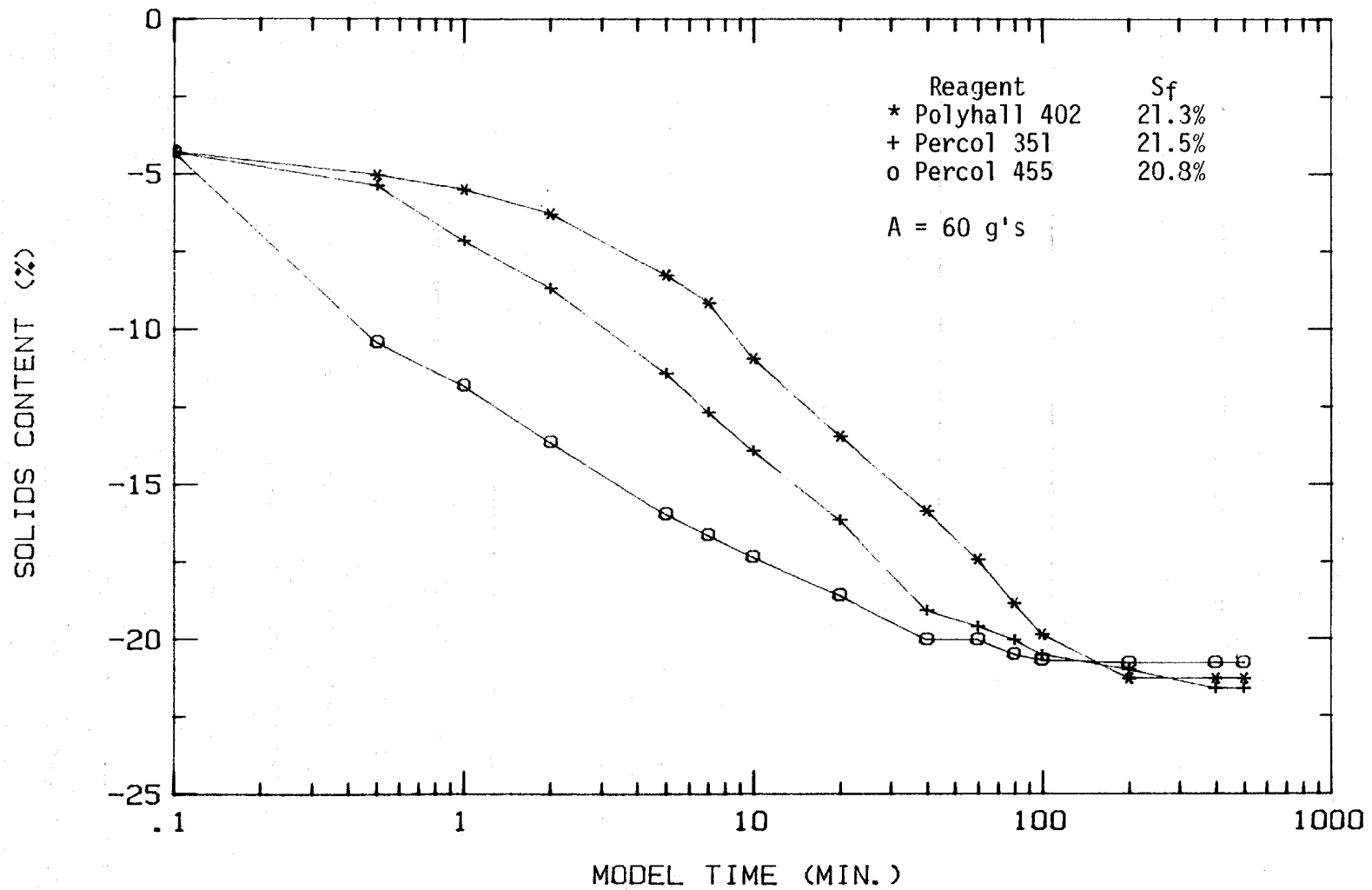


Figure 50: Effect of Flocculant on Sedimentation/Consolidation for Noralyh Clay

respectively. Percol 455 and Jaguar C-13-5, cationic reagents achieved final solids contents of 20.8 and 20.4, respectively.

### Flocculant/Sand Capping

Since capping low solids content clays (<15%) is unlikely due to bearing capacity failures, a model series investigated the concept of using flocculants to achieve rapidly a solids content capable of supporting a subsequently placed sand cap. These results are presented in Figure 51, which presents the results of two sand capping additions. In one test a cap of 134 grams (equivalent sand for a 2:1 SCR if mixed) was placed on the clay surface as soon as a solids content of 15 percent was achieved. In another test, the sand cap was added much later. As shown, the time of capping had only a minor effect final solids content. Although some mixing of sand and clay occurred at the interface, capping produced higher final solids contents than virgin or treated lay without capping.

### Flocculant/Sand Mixing

The concept of simultaneously mixing sand and clays to create a s/c mix is a viable disposal technique, provided the clays are at a solids content sufficient to entrap the sand and prevent segregation of the sand from merely settling to the bottom. In this context, flocculants can be used to achieve rapidly a clay solids content sufficient to entrap the sand. Accordingly, Figure 52 provides a comparison between non-flocculated, flocculated, and flocculated-sand entrapped waste clays. As shown, no benefit in final solids content was derived by mixing sand with flocculant treated clay. However, this scenario provides simultaneous disposal of sand tailings and waste clay, while the flocculant provides an additional time advantage.

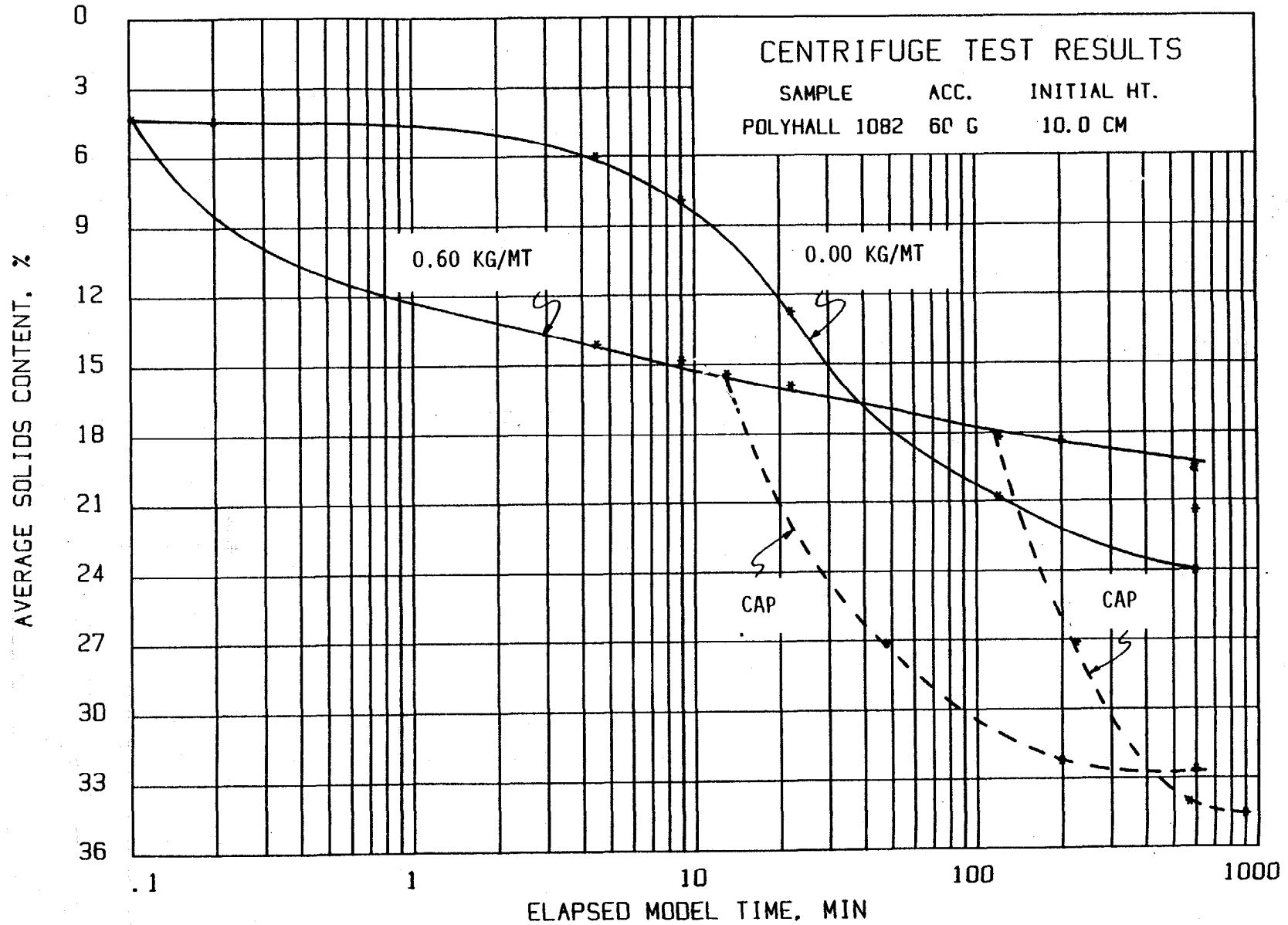


Figure 51: Results of Flocculants Plus Sand Cap Treatment



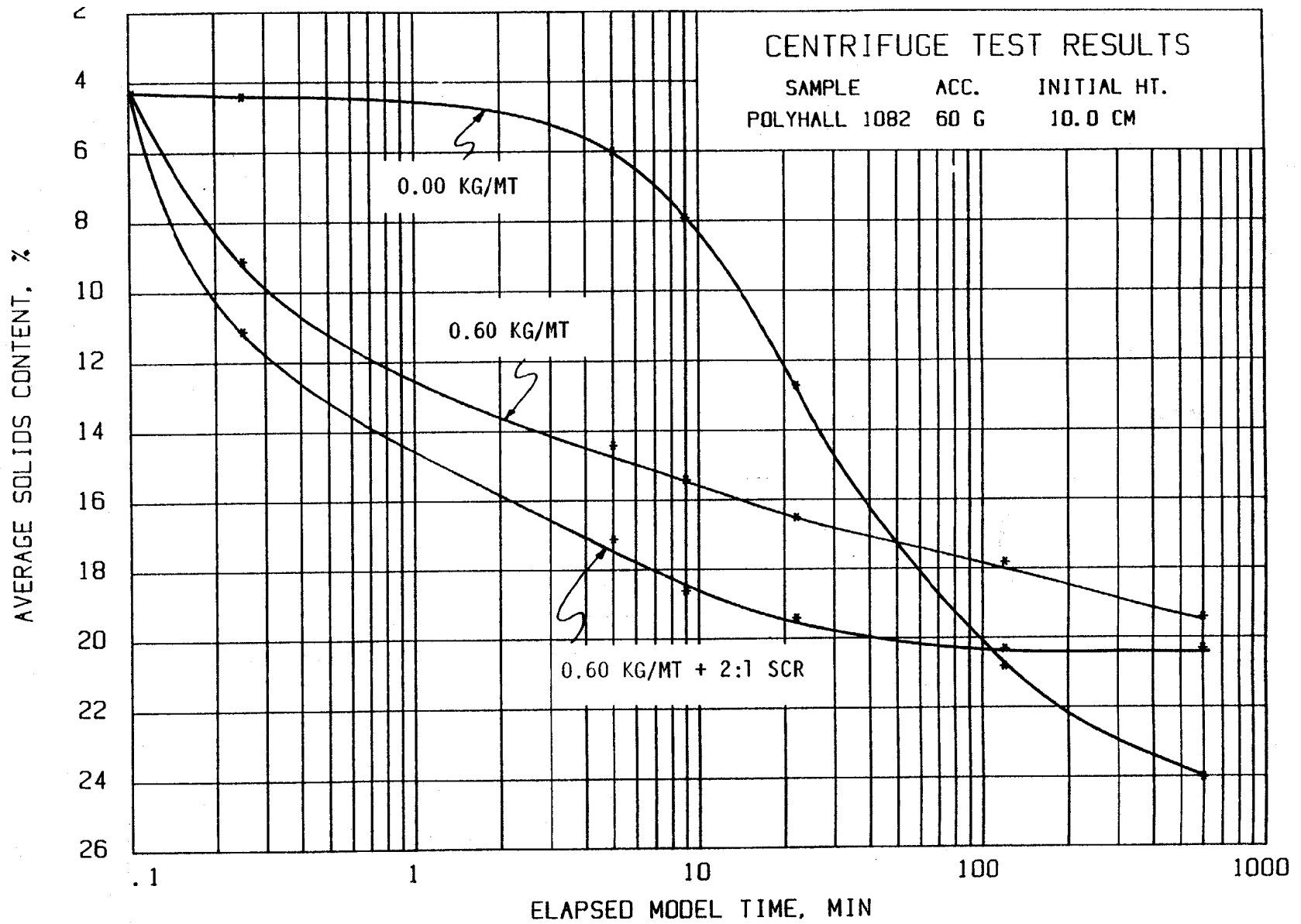


Figure 52: Results of Flocculant Plus Sand Mix

## CHAPTER V CONCLUSIONS

Based upon the testing methods and equipment, and soils tested, the following conclusions are made:

- 1) Centrifugal modelling is a viable technique for examining prototype waste clay disposal schemes. However, modelling of models is essential for determining time scaling exponents, and segregation potential must be evaluated in s/c mixes.
- 2) The time scaling exponent based upon modelling of models for Kingsford clay is a function of clay solids content, and increases from 1.6 at solids contents from 14 to 17%, to 2.0 at 20% solids.
- 3) Segregation of sand is not a major problem with s/c mixes when clay solids contents >16 percent. This is true for s/c mix ratios ranging from 1:1 to 6:1.
- 4) The descending order of disposal technique effectiveness in achieving the highest final clay solids content is:
  - (a) Sand capping (staged)
  - (b) S/c mix capping
  - (c) S/c mix, 1:1 to 2:1
  - (d) Flocculants or untreated clay

However, the time required is in proportion to the final solids content; e.g., highest solids contents require longest times.

- 5) When homogeneous s/c mixes are compared with untreated waste clays, the greatest reductions in interface height are achieved with the s/c ratio approximately 1:1. At s/c mix ratios exceeding 3:1, the final interface height will be above that for comparable untreated clay.

- 6) At low (1:1) s/c mix ratios, grain size has little effect on the final interface height. At high (6:1) s/c mix ratios, the greatest interface reduction is achieved with increasing grain sizes.
- 7) A threshold solids content exists below which the surface bearing capacity is insufficient to support a cap. Remolding of the underlying clay prior to cap placement has a detrimental effect on the success of capping.
- 8) Reduction in interface height appear to be independent of the s/c mix ratio. However, higher s/c ratios did produce higher clay solids in the underlying clay layer.
- 9) Closed-form solutions for calculating final consolidation heights were developed for quiescent clay ponds with and without a surcharging cap.
- 10) The primary benefit of flocculants is increasing the rate of sedimentation. Under prototype stress conditions, flocculated clay achieves a final solids content slightly lower than untreated clay. Capping flocculated clays produces major benefits, while flocculated clay/sand mixes provided only a marginal benefit.

## References

- Ardaman & Associates (1982), "Evaluation of Phosphatic Clay - Disposal and Reclamation Methods; Vol. 1: Index Properties of Phosphatic Clays; Vol. 2: Mineralogy of Phosphatic Clays," FIPR Publication Nos. 02-002-003, 02-002-004, Bartow, Florida.**
- Araman & Associates (1984), "Laboratory Testing of Phosphatic Clays for Reclamation of Phosphatic Waste Clay Pond by Capping - IMC Test Pit 3," Report to University of Florida.**
- Barwood, H. L. (1962), "Mineralogy and Chemistry of the Clays," Phos. Clay Workshop FIPR Publ. 02-020-012.**
- Bloomquist, D. (1982), "Centrifuge Modelling of Large Strain Consolidation Phenomena in Phosphatic Clay Retention Ponds." Ph. D dissertation, University of Florida, Gainesville.**
- Bloomquist, D. G., Davidson, J. L., and Townsend, F. C., "Platform Orientation and Start-up Time During Centrifuge Testing," Geotechnical Testing Journal, GTJ00J, Vol. 7, No. 4, December 1984, pp. 195-199.**
- Bromwell, L. G. and Oxford, T. P. (1977), "Waste Clay Dewatering and Disposal," ASCE Spec. Conf. on Geotechnical Practice for Disposal of Solid Waste Materials, Ann Arbor, Michigan.**
- Cardwell, W. T. (1941), "Drilling Fluid Viscosity," API Drilling & Production Practice [From Morgenstern, N. 1965 ] "The Stability of a Slurry Trench in Cohesionless Soils," Geotechnique, Vol. 15, No. 4, December**
- Croce, P. (1982), "Evaluation of Consolidation Theories by Centrifuge Model Tests," MSc Thesis, University of Colorado, Boulder.**
- D'Appolonia, D. J. (1980), "Soil-Bentonite Slurry Trench Cutoffs," ASCE GED Jrn. Vol. 106 No. GT4, April.**
- Davidson, J. L. and Bloomquist, D. (1980), "Centrifuge Modelling of the Consolidation/Sedimentation Process in Phosphatic Clays," EIES Rpt. 245-W65, University of Florida.**
- Keen, P. W. (1982), "C F Industries, Inc. Sand/Clay Mix Experiment," Phos. Clay Workshop FIPR Publ. No. 02-020-012.**
- Lawler, J. E. (1982), "Progress Report No. 6: IMC-Agrico-Mobil Slime Consolidation and Land Reclamation Study," IMC, Bartow, Florida.**
- Lawler, J. E. and Olson, S. I. (1982), "IMC-Agrico-Mobil Sand Capping for Waste Clay Consolidation," Phos. Clay Workshop FIPR Publ. No. 02-020-012.**

- Leitzman, R. A. (1982), "Brewster Phosphates Sand-Clay Reclamation Method," Phos. Clay Workshop FIPR Publ. No. 02-020-012.**
- McClimans, S.A. (1984), "Centrifugal Model Evaluation of the Consolidation - Behavior of Sand/Phosphatic Clay Mixes," Master of Engineering Report, University of Florida, Department of Civil Engineering, Gainesville, Florida.**
- McVay, M C. (1984), Personal Communication, University of Florida, Gainesville, Florida.**
- McLandon, J. T., Boyle, J. R. and Sweeney, J. W (1983), "State-of-the-Art of Phosphatic Clay Dewatering Technology and Disposal Techniques," Vol. 2 FIPR Grant 81-02-017.**
- Martin, R. T., Bromwell, L. G. and Sholine, J. H (1977), "Field Tests of Phosphatic Clay Dewatering," ASCE Spec. Conf. in Geotechnical Practice for Disposal of Solid Waste Materials, Ann Arbor, Michigan.**
- Mkasa, M and Takada, N. (1973), "Significance of Centrifugal Model Tests in Soil Mechanics," 8th ICSMFE Vol. 1, p 273.**
- Onoda, G (1977), "The Mechanism of Flocculation of Phosphatic Slimes," Res. Rpt. to NSF Grant AER 76-24676.**
- Raden, D. J. (1982), "Estech, Inc. Plant Scale Disposal of Phosphatic Clay - Flocculation With Sand Mix," Phos. Clay Workshop, FIPR Publ. No. 02-020-012.**
- Smelley, A. G. and Feld, F. L. (1979), "Flocculation Dewatering of Florida Phosphatic Clay Waste," USBM RI 8349.**
- Somogyi, F. (1979), "Analysis and Prediction of Phosphatic Clay Consolidation: Implementation Package," Bromwell Engr. Inc., Lakeland, Florida.**
- Weiss. F. (1967). "Die Standicherheit Flüssigkeitsgestutzter Erwände, "Bauingenieur-Parxis," Heft 70, Ernst, Berlin and Munich, [from Xanthakos, Petros (1979, Slurry Walls, McGraw-Hill, New York, p. 67].**

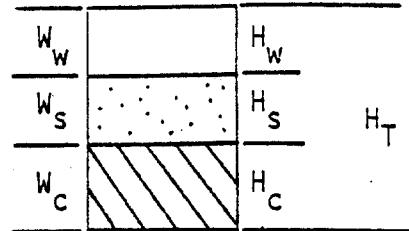
APPENDIX A

TOTAL SOLIDS CONTENT

$W_W$  = weight of water

$W_S$  = weight of sand

$W_C$  = weight of clay



$H_W$  = height of water

$$W_T = \text{total weight} = W_W + W_S + W_C$$

$H_S$  = height of sand

$H_C$  = height of clay

$$H_T = \text{total height} = H_W + H_S + H_C$$

definition of intermediate solids content

$$\frac{\text{weight of solids}}{\text{weight of solids} + \text{weight of interstitial water} - \text{weight of water above interface}}$$

$$S_{it} = \frac{W_C + W_S}{W_C + W_S + W_W - W_i} \quad (A-1)$$

initial clay solids content,  $S_0 = \frac{W_C}{W_C + W_W}$

solving for  $W_W$ :

$$W_C S_0 + W_W S_0 = W_C$$

$$W_W = \frac{(1-S_0)}{S_0} W_C \quad (A-2)$$

sand/clay ratio,  $SCR = \frac{W_S}{W_C}$

solving for  $W_S$ :

$$W_C SCR = W_S \quad (A-3)$$

weight of water above interface,  $W_i = \Delta G (A) \gamma_W$

assuming a unit area  $(A) = 1$ ,  $W_i = \Delta H \gamma_W \quad (A-4)$

substituting A-2, A-3, and A-4 into A-1

$$S_{it} = \frac{W_c + SCR \cdot W_c}{W_c + SCR \cdot W_c + \frac{(1-S_o)}{S_o} - \Delta H \gamma_w} \quad (A-5)$$

divide through by  $W_c$ :

$$S_{it} = \frac{1 + SCR}{1 + SCR + \frac{(1-S_o)}{S_o} - \Delta H \frac{\gamma_w}{W_c}} \quad (A-6)$$

$W_c$  is not known, but

$$\begin{aligned} W_T &= W_c + W_s + W_w \\ &= W_c + SCR \cdot W_c + \frac{(1-S_o)}{S_o} W_c \end{aligned}$$

and

$$\begin{aligned} H_T &= H_c + H_s + H_w \\ &= \frac{W_c}{\gamma_w G_c} + \frac{SCR \cdot W_c}{\gamma_w \cdot G_s} + \frac{(1-S_o)W_c}{S_o \gamma_w} \\ &= \frac{W_c}{\gamma_w} \left( \frac{1}{G_c} + \frac{SCR}{G_s} + \frac{(1-S_o)}{S_o} \right) \end{aligned}$$

where  $G_c$  = specific gravity, clay

$G_s$  = specific gravity, sand

rearranging

$$W_c = \frac{H_T \cdot \gamma_w}{\left( \frac{1}{G_c} + \frac{SCR}{G_s} + \frac{(1-S_o)}{S_o} \right)} \quad (A-7)$$

substituting A-7 into A-6:

$$S_{it} = \frac{1 + SCR}{1 + SCR + \frac{(1-S_o)}{S_o} - \frac{\Delta H \gamma_w}{H_T \gamma_w} \left( \frac{1}{G_c} + \frac{SCR}{G_s} + \frac{(1-S_o)}{S_o} \right)}$$

rearranging and defining  $\epsilon H = \frac{\Delta H}{H_T}$

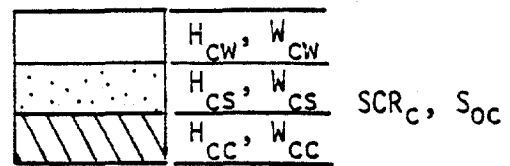
$$S_{it} = \frac{1 + SCR}{1 + SCR + \frac{(1-S_o)}{S_o} - \epsilon H \left[ \frac{1}{G_c} + \frac{1}{G_s} + \frac{(1-S_o)}{S_o} \right]}$$

simplifying and combining terms

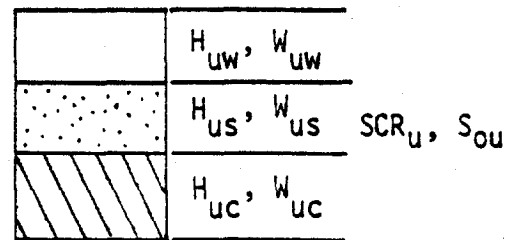
$$S_{it} = \frac{1 + SCR}{1 + SCR + (1-\epsilon H) \frac{(1-S_0)}{S_0} - \epsilon H \left[ \frac{1}{G_c} + \frac{SCR}{G_s} \right]} \quad (A-8)$$

This equation may be used when the initial clay solids content,  $S_0$ , is the same for both the sand/clay cap (if one exists) and the underlying clay slurry. When the initial clay solids contents are different, a more general equation may be found.

sand/clay cap



underlying clay  
layer (may also  
include sand)



height of cap,  $H_c = H_{cw} + H_{cs} + H_{cc}$

height of underlying layer,  $H_u = H_{uw} + H_{us} + H_{uc}$

total model height,  $H_T = H_c + H_u$

$$H_c = H_{cw} + H_{cs} + H_{cc} = \frac{W_{cc}}{\gamma_w G_c} + \frac{W_{cc} \cdot SCR_c}{\gamma_w \cdot G_s} + \frac{(1-S_{oc})W_{cc}}{S_{oc} \gamma_w}$$

$$= \frac{W_{cc}}{\gamma_w} \left[ \frac{1}{G_c} + \frac{SCR_c}{G_s} + \frac{(1-S_{oc})}{S_{oc}} \right] \quad (A-9)$$

$$H_u = H_{uw} + H_{us} + H_{uc} = \frac{W_{uc}}{\gamma_w G_c} + \frac{W_{uc} \cdot SCR_u}{\gamma_w \cdot G_s} + \frac{(1-S_{ou})W_{uc}}{S_{ou} \gamma_w}$$

$$= \frac{W_{uc}}{\gamma_w} \left[ \frac{1}{G_c} + \frac{SCR_u}{G_s} + \frac{(1-S_{ou})}{S_{ou}} \right] \quad (A-10)$$



rearranging A-9 and A-10

$$W_{cc} = \frac{H_c \cdot \gamma_w}{\frac{1}{G_c} + \frac{SCR_c}{G_s} + \frac{(1-S_{oc})}{S_{oc}}} \quad (A-11)$$

and

$$W_{uc} = \frac{H_u \cdot \gamma_w}{\frac{1}{G_c} + \frac{SCR_u}{G_s} + \frac{(1-S_{uc})}{S_{uc}}} \quad (A-12)$$

referring to A-1

$$S_i = \frac{W_c + W_s}{W_c + W_s + W_w - W_i}$$

substituting  $W_{cc}$ ,  $W_{uc}$ ,  $S_{oc}$ ,  $S_{uc}$ ,  $SCR_c$ , and  $SCR_u$

$$S_i = \frac{W_{cc} + W_{uc} + SCR_c W_{cc} + SCR_u W_{uc}}{W_{cc} + W_{uc} + SCR_c W_{cc} + SCR_u W_{uc} + \frac{(1-S_{oc})}{S_{oc}} W_{cc} + \frac{(1-S_{ou})}{S_{ou}} W_{uc} - \Delta H \cdot \gamma_w} \quad (A-13)$$

defining  $\alpha = \frac{1}{G_c} + \frac{SCR_c}{G_s} + \frac{1-S_{oc}}{S_{oc}}$

and

$$\beta = \frac{1}{G_c} + \frac{SCR_u}{G_s} + \frac{1-S_{ou}}{S_{ou}}$$

and substituting into A-13:

$$S_i = \frac{\frac{H_c \cdot \gamma_w}{\alpha} + \frac{H_u \cdot \gamma_w}{\beta} + SCR_c \frac{H_c \cdot \gamma_w}{\alpha} + SCR_u \frac{H_u \cdot \gamma_w}{\beta}}{\frac{H_c \cdot \gamma_w}{\alpha} + \frac{H_u \cdot \gamma_w}{\beta} + SCR_c \frac{H_c \cdot \gamma_w}{\alpha} + SCR_u \frac{H_u \cdot \gamma_w}{\beta} + \frac{(1-S_{oc})}{S_{oc}} \frac{H_c \cdot \gamma_w}{\alpha} + \frac{(1-S_{ou})}{S_{ou}} \frac{H_u \cdot \gamma_w}{\beta} - \Delta H \gamma_w}$$

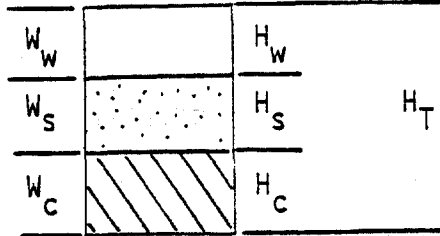
cancelling terms and rearranging:

$$S_i = \frac{(1+SCR_c) \frac{H_c}{\alpha} + (1+SCR_u) \frac{H_u}{\beta}}{\left(1+SCR_c + \frac{1-S_{oc}}{S_{oc}}\right) \frac{H_c}{\alpha} + \left(1+SCR_u - \frac{1-S_{ou}}{S_{ou}}\right) \frac{H_u}{\beta} - \Delta H} \quad (A-14)$$

where  $\alpha = \frac{1}{G_c} + \frac{SCR_c}{G_s} + \frac{1-S_{oc}}{S_{oc}}$  (cap)

$$\beta = \frac{1}{G_c} + \frac{SCR_u}{G_s} + \frac{1-S_{ou}}{S_{ou}} \quad (\text{underlying clay})$$

EFFECTIVE CLAY SOLIDS CONTENT



definition of intermediate effective clay solids content:

$$S_{ie} = \frac{\text{weight of clay}}{\text{weight of clay + weight of interstitial water - weight of water above interface}} = \frac{W_c}{W_c + \frac{W_c}{S_o} - \Delta H \cdot \gamma_w} \quad (\text{A-15})$$

dividing through by  $W_c$ :

$$S_{ie} = \frac{1}{1 + \frac{(1-S_o)}{S_o} - \frac{\Delta H \cdot \gamma_w}{W_c}} \quad (\text{A-16})$$

referring to A-7

$$W_c = \frac{H_T \cdot \gamma_w}{\left( \frac{1}{G_c} + \frac{SCR}{G_s} + \frac{(1-S_o)}{S_o} \right)}$$

substituting into A-16

$$S_{ie} = \frac{1}{1 + \frac{(1-S_o)}{S_o} + \frac{\Delta H \cdot \gamma_w}{H_T \cdot \gamma_w} \left( \frac{1}{G_c} + \frac{SCR}{G_s} + \frac{(1-S_o)}{S_o} \right)}$$

cancelling terms and rearranging

$$S_{ie} = \frac{1}{1 + \frac{(1-S_o)}{S_o} - \epsilon H \left( \frac{1}{G_c} + \frac{SCR}{G_s} + \frac{(1-S_o)}{S_o} \right)}$$

rearranging further:

$$S_{ie} = \frac{1}{1 + \frac{(1-S_0)}{S_0} (1-\epsilon H) - \epsilon H \left( \frac{1}{G_c} + \frac{SCR}{G_s} + \frac{(1-S_0)}{S_0} \right)} \quad (A-17)$$

Again, this assumes that the initial clay solids content is the same for the sand/clay cap and the underlying clay slurry. A more general solution (similar to A-14) could be derived for the effective clay solids content as well.

(For capped samples, an effective SCR should be calculated and used in equations A-8 and A-17

$$SCR_{AVE} = \frac{SCR_{CAP} \cdot H_{CAP}}{H_{CAP} + H_{UNDERLYING CLAY}}$$

During a post-test analysis, the sample is cored and a relationship may be determined between solids content and depth. If the total solids content and SCR is known at a particular depth, the effective clay solids content may also be calculated.

$$S_t = \frac{W_s + W_c}{W_s + W_c + W_w}$$

and

$$S_e = \frac{W_c}{W_c + W_w}$$

rearranging

$$S_t = \frac{SCR \cdot W_c + W_c}{SCR \cdot W_c + W_c + W_w} = \frac{SCR + 1}{SCR + 1 + \frac{W_w}{W_c}} \quad (A-18)$$

$$S_e = \frac{W_c}{W_c + W_w} \rightarrow \frac{W_w}{W_c} = \frac{1}{S_e} - 1 \quad (A-19)$$

substituting A-19 into A-18

$$S_t = \frac{SCR + 1}{SCR + 1 + \left( \frac{1}{S_e} - 1 \right)}$$

solving for  $S_e$

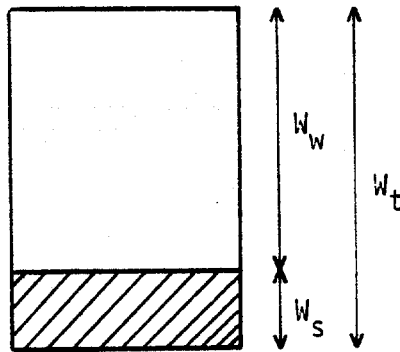
$$S_e = \frac{1}{\frac{1}{S_t} (SCR + 1) - SCR}$$

combining terms and rearranging

$$S_e = \frac{1}{1 + (1 + SCR) \left(\frac{1}{S_t} - 1\right)}$$

## APPENDIX B

A slurry of some known initial concentration  $S_0$  is placed in the Plexiglas container. An interface between the supernatant water and the slurry surface develops and with time lowers. At any time, within the container, there are two phases, solid and liquid. These may be hypothetically separated for analysis.



$$W_T = W_w + W_s$$

Where  $W_T$  = Total weight of material in container  
 $W_w$  = Weight of water in container  
 $W_s$  = Weight of solids in container

The % solids by weight is defined as

$$S_o = \frac{W_s}{W_t} \times 100$$

Where  $S_o$  = initial solid concentration

so

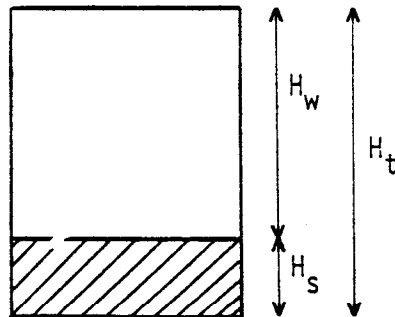
$$S_o = \frac{W_s}{W_s + W_w}$$

Solving for  $W_w$

$$W_s S_o + W_w S_o = W_s$$

$$W_w = \frac{W_s (1 - S_o)}{S_o} \quad (1)$$

The same analogy may be used in dealing with volumes rather than weights. Since the area of the container A is constant, the volumes may be divided by the container area to obtain heights. Thus;  $H_t = H_w + H_s$



where  $H_t$  = Total height of sample in container  
 $H_w$  = Height of water in container  
 $H_s$  = Height of solid in container

$$\frac{H_s}{H_w} = \frac{H_s \cdot A}{H_w \cdot A} = \frac{V_s}{V_w}$$

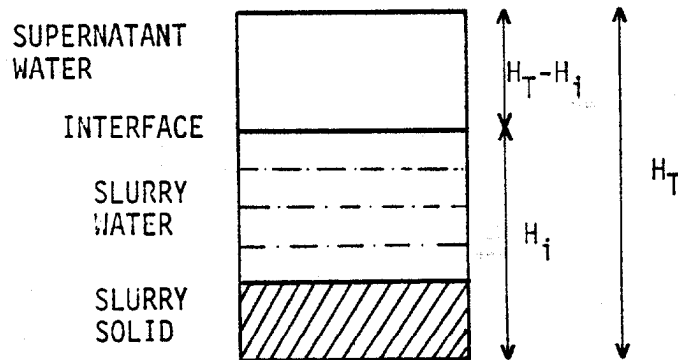
since in general  $\gamma_x = \frac{W_x}{V_x}$  or  $V_x = \frac{W_x}{\gamma_x}$

$$\frac{H_s}{H_w} = \frac{W_s}{\gamma_s} \cdot \frac{\gamma_w}{W_w} = \frac{W_s}{W_w} \cdot G \quad (2)$$

where  $G$ , the specific gravity of the solids is defined by

$$G = \gamma_s / \gamma_w$$

Next, the effect of the supernatant water is included in the phase diagram. At any time interval  $i$ , we have



where

$H_i$  = height of interface at any time interval  $i$

Since the supernatant is devoid of solids, we may write

$$S_i = \frac{W_s}{W_s + W_{w_i}} \quad (3)$$

where  $S_i$  = solid concentration of the slurry at time  $i$   
 $W_{wi}$  = weight of water below interface at time  $i$

Solving for  $W_{wi}$  we have

$$W_{wi} = W_w - (H_T - H_i) A \gamma_w$$

Substituting Equation 1 into the above yields;

$$W_{wi} = \frac{W_s (1 - S_0)}{S_0} - (H_T - H_i) A \gamma_w$$

$$G = \frac{\gamma_s}{\gamma_w} = \frac{W_s}{H_s A \gamma_w}$$

$$\gamma_w = \frac{W_s}{H_s A G}$$

$$W_{wi} = \frac{W_s (1 - S_0)}{S_0} - (H_T - H_i) A \frac{W_s}{H_s A G}$$

$$W_{wi} = \frac{W_s (1 - S_0)}{S_0} - \frac{(H_T - H_i) W_s}{H_s G}$$

Substituting this into equation (3)

$$S_i = \frac{\frac{W_s (1 - S_0)}{S_0} - \frac{(H_T - H_i) W_s}{H_s G}}{W_s} + W_s$$

Cancelling  $W_s$  yields

$$S_i = \frac{1}{\frac{1 - S_0}{S_0} - \frac{H_T - H_i}{H_s G} + 1} \quad (4)$$



It is now desirable to remove  $H_S$  from the equation. Recalling that:

$$H_S = H_T - H_W$$

and

$$H_W = \frac{H_S W_W G}{W_S}$$

we have

$$H_S = H_T - \frac{H_S W_W G}{W_S}$$

$$H_T = H_S + \frac{H_S W_W G}{W_S}$$

$$= H_S \left( 1 + \frac{W_W G}{W_S} \right)$$

Also from before,

$$W_W = \frac{W_S (1 - S_0)}{S_0}$$

Inserting this into the above,

$$H_T = H_S \left[ 1 + \frac{W_S (1 - S_0)}{S_0} \left( \frac{G}{W_S} \right) \right]$$

or

$$H_S = \frac{H_T}{\frac{1 + G(1 - S_0)}{S_0}} \quad (5)$$

Substituting equation 5 into equation 4

$$S_i = \frac{1}{\left[ \frac{1 - S_0}{S_0} - \frac{H_T - H_i}{G H_T} \frac{1 + G(1 - S_0)}{S_0} \right] + 1}$$

rearranging this

$$S_i = \frac{1}{\left[ \frac{1 - S_0}{S_0} - \frac{(H_T - H_i)}{H_T G} \left( 1 + G \left( \frac{1 - S_0}{S_0} \right) \right) \right] + 1}$$

$$= \frac{1}{\left[ \frac{1 - S_0}{S_0} \left( 1 - \frac{H_T - H_i}{H_T} \right) - \frac{H_T - H_i}{H_T G} \right] + 1}$$

Multiplying top and bottom by  $S_0$

$$S_i = \frac{S_0}{S_0 \left( \frac{1 - S_0}{S_0} \left[ 1 - \frac{H_T - H_i}{H_T} \right] - \frac{H_T - H_i}{H_T G} \right) + S_0}$$

Expanding terms

$$S_i = \frac{S_0}{1 - S_0 - \frac{H_T - H_i}{H_T} + S_0 \left[ \frac{H_T - H_i}{H_T} \right] - S_0 \left[ \frac{H_T - H_i}{H_T} \right] + S_0}$$

$$S_i = \frac{S_o}{1 - \frac{H_T - H_i}{H_T} \left[ 1 - S_o + \frac{S_o}{G} \right]}$$

Rearranging yields a final form

$$S_i = \frac{S_o}{1 - \frac{H_T - H_i}{H_T} \left[ 1 - S_o \left( \frac{G - 1}{G} \right) \right]}$$

**This form is convenient to use, since the bracketed quantity is a constant for a given test.**

**By knowing the initial concentration,  $S_o$ , the initial height of slurry,  $H_T$ , and the specific gravity of the solids,  $G$ , the solids content,  $S_i$ , when the interface is at height  $H_i$  may be determined.**

**Another useful relationship involves the void ratio and the percent solids. All definitions and symbols refer to the portion of slurry below the supernatant interface. By definition**

$$e = \frac{V_v}{V_s}$$

where  $e$  = void ratio

$V_v$  = volume of voids

$V_s$  = volume of solids

Since the slurry is saturated, no air voids exist, and the volume of voids equals the volume of water, or;

$$e = \frac{V_v}{V_s} = \frac{V_w}{V_s}$$

$$= \frac{\gamma_s}{\gamma_w} \cdot \frac{W_w}{W_s} = G \frac{W_w}{W_s}$$

$$e = G \frac{(1 - s)}{s} \quad \text{from equation (1)}$$

Knowing the specific gravity and the percent solids at any time, the void ratio can be computed.

## Appendix C

### Deviation of Unit Weights for Waste Clays and Sand/Clay Mixes

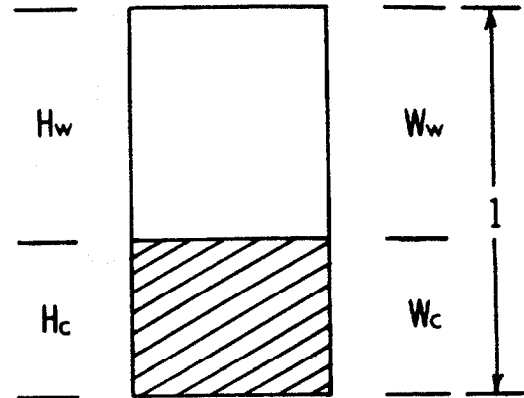
1) Unit weight of clay in terms of solids content

$H_w$  = Height of water

$H_c$  = Height of clay

$W_w$  = Weight of water

$W_c$  = Weight of clay



Definition  $S = \frac{W_c}{W_w + W_c}$  Assumption  $W_w + W_c = 1 \therefore S = W_c$  &  $W_w = 1 - S$

$$H_w = (1 - S) / \gamma_w$$

$$H_c = \frac{S}{\gamma_w G_s}$$

Definition: 
$$\gamma_t = \frac{W_w + W_c}{V_t} = \frac{(1 - S) + S}{\frac{(1 - S)}{\gamma_w} + \frac{S}{\gamma_w G_s}} = \frac{\gamma_w G_s}{(1 - S) G_s + S}$$

$$= \frac{\gamma_w G_s}{S(1 - G_s) + G_s}$$

$$\gamma' = \gamma_t - \gamma_w = \frac{\gamma_w G_s}{S(1 - G_s) + G_s} - \gamma_w = \frac{\gamma_w G_s - S \gamma_w (1 - G_s) - G_s \gamma_w}{S(1 - G_s) + G_s} = \frac{S \gamma_w (G_s - 1)}{S(1 - G_s) + G_s}$$

Equation C-1

2) Unit weight of sand/clay mix in terms of SCR

$H_w, H_s, H_c$  = height of water, sand, clay

$W_w, W_s, W_c$  = weight of water, sand clay

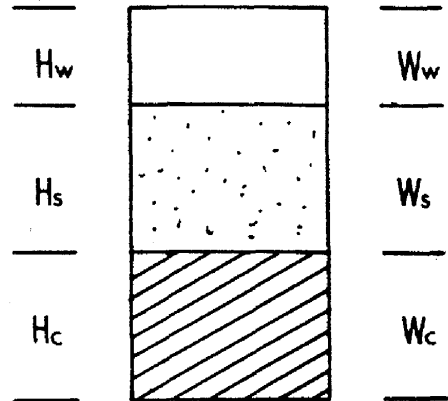
Definition:  $SCR = W_s/W_c$

$$S = W_c/W_c + W_w$$

Assume:  $G_{sand} = G_{clay}$

$$W_c = 1, \therefore H_c = W_c/G\gamma_w$$

$$W_s = SCR \cdot H_s = SCR/G\gamma_w$$



$$S = 1/(1 + W_w)$$

$$S + SW_w = 1$$

$$W_w = (1-S)/S \quad \therefore H_w = (1-S)/\gamma_w S$$

Definition: 
$$\gamma_t = \frac{W_w + W_s + W_c}{V_t} = \frac{(1-S)/S + SCR + 1}{\frac{(1-S)}{\gamma_w S} + \frac{SCR}{G\gamma_w} + \frac{1}{G\gamma_w}}$$

$$\gamma_t = \frac{(1+S \cdot SCR)\gamma_w G}{G(1-S) + S(1+SCR)}$$

$$\gamma' = \gamma_t - \gamma_w$$

$$= \frac{S\gamma_w (SCR + 1)(G-1)}{G(1-S) + S(1+SCR)}$$

Equation C-2

3) Determination of Heights and Weights of sand, clay, and water in a s/c mix

$$S = W_c/(W_c + W_w) \rightarrow W_w = W_c (1-S)/S$$

$$SCR = W_s/W_c \rightarrow W_s = W_c \cdot SCR$$

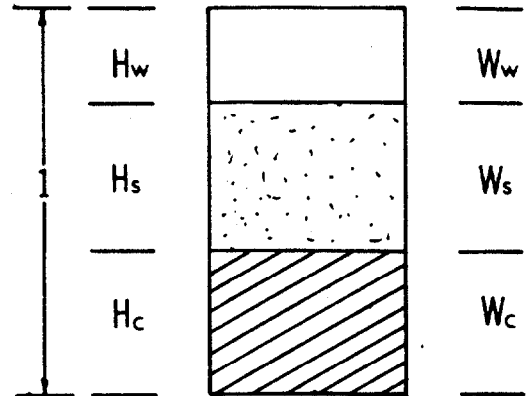
Assume  $G_{sand} = G_{clay}$

$$1 = H_w + H_s + H_c$$

$$= \frac{W_w}{\gamma_w} + \frac{W_s}{G_s \gamma_w} + \frac{W_c}{G_s \gamma_w}$$

$$= \frac{W_c(1-S)}{S \gamma_w} + \frac{W_c \cdot SCR}{G_s \gamma_w} + \frac{W_c}{G_s \gamma_w}$$

$$= \frac{W_c(1-S)G + W_c \cdot SCR \cdot S + W_c \cdot S}{S \gamma_w G}$$



$$\therefore W_c = \frac{S \gamma_w G}{G(1-S) + S(1+SCR)} \quad \& \quad W_s = \frac{S \gamma_w G \cdot SCR}{G(1-S) + S(1+SCR)} \quad \& \quad W_w = \frac{\gamma_w G(1-S)}{G(1-S) + S(1+SCR)}$$

$$\therefore W_c = \frac{S \gamma_w G}{G(1-S) + S(1+SCR)} \quad \& \quad W_s = \frac{S \gamma_w G \cdot SCR}{G(1-S) + S(1+SCR)} \quad \& \quad W_w = \frac{\gamma_w G(1-S)}{G(1-S) + S(1+SCR)}$$

Equation C-3

Since height =  $W/G_s \gamma_w$ , then

$$H_w = \frac{(1-S)G}{G(1-S) + S(1+SCR)} \quad \& \quad H_s = \frac{S \cdot SCR}{G(1-S) + S(1+SCR)} \quad \& \quad H_c = \frac{S}{G(1-S) + S(1+SCR)}$$

Equation C-4

### Calculation of Effective Stress Profile

Table C-1 presents the calculations of the effective stress profiles for Cases A through E. These cases assume a waste pond of unit depth, with an unlimited supply of waste clays. However, the sand used in s/c mixes and caps is equal for all cases where appropriate.

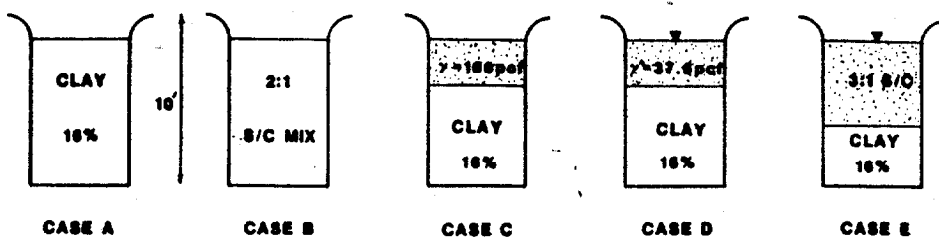
**Example:** Determine the effective stress profile for 5 cases of a unit deep pond

A) untreated clay, 0:1 SCR  $S_0 = 16\%$

B) 2:1 s/c mix  $S_0 = 16\%$

Table C-1

Effective Stress Profiles for Case A through E



$\sigma'$  (psf) @ z, ft

Case	$\gamma'_{\text{clay}}$ pcf	$\gamma'_{\text{cap}}$ pcf	$D_{\text{clay}}$ ft	$H_{\text{cap}}$ ft	0	$H_c$	0.5	1.0
A	6.90	-	1.0	-	0	-	3.45	6.90
B	18.26	-	1.0	-	0	-	9.13	18.26
C	6.90	100	0.804	0.196	0	19.60	21.70	25.15
D	6.90	37.6	0.804	0.196	0	7.37	9.47	12.92
E	6.90	22.99	0.2937	0.7063	0	16.24	11.49	18.26

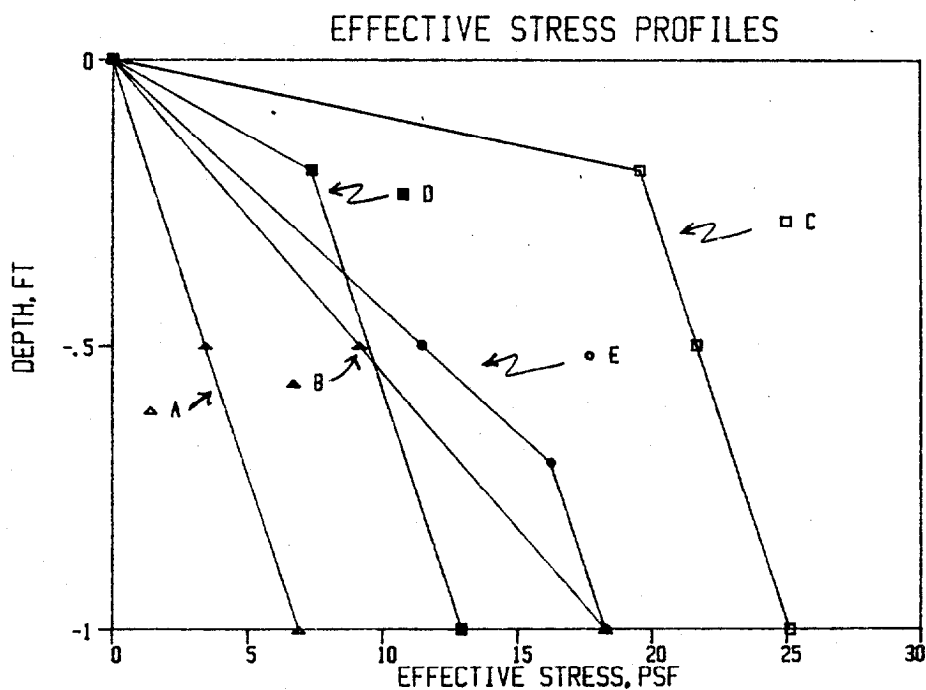


Figure C-1 Comparison of Effective Stress Profiles for Cases A through E

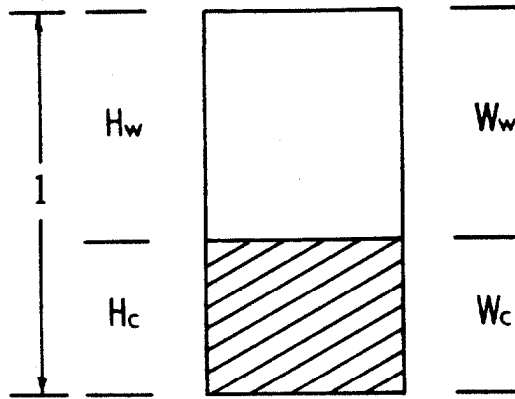


C) sand cap where  $W_s$  in cap =  $W_s$  in 2:1 s/c mix (Case B)  
and  $\gamma_s = 100$  pcf

D) same as Case C, but sand cap becomes saturated,  
 $\gamma'_s = 37.6$  pcf

E) 3:1 s/c mix cap  $S_0 = 16\%$  using equal sand and clay  
quantities as Case B

Case A



Definitions

$$S = W_c / (W_c + W_s)$$

$$H_c + H_w = 1$$

$$1) \quad H_w = W_w / \gamma_w \rightarrow W_w = H_w \gamma_w$$

$$2) \quad H_c = W_c / G \gamma_w \rightarrow W_c = H_c G \gamma_w$$

$$3) \quad H_w = 1 - H_c \therefore W_w = (1 - H_c) \gamma_w$$

$$4) \quad S = \frac{H_c G \gamma_w}{H_c G \gamma_w + (1 - H_c) \gamma_w} = \frac{H_c G}{H_c G + 1 - H_c}$$

$$S H_c G + S - S H_c = H_c G$$

$$S = H_c G - S H_c G + S H_c$$

$$5) \quad H_c = \frac{S}{G(1-S) + S} \quad \& \quad H_w = 1 - H_c = \frac{G(1-S) + S - S}{G(1-S) + S} = \frac{G(1-S)}{G(1-S) + S}$$

$$6) \quad H_c = \frac{0.16}{2.65(1-0.16) + 0.16} = 0.067$$

$$H_w = \frac{2.65(1-0.16)}{2.65(1-0.16) + 0.16} = 0.933$$

$$7) \quad W_c = H_c G \gamma_w = (0.067)(2.65)(62.4) = 11.08$$

$$W_w = H_w \gamma_w = (0.933)(62.4) = 58.22$$


---


$$69.30$$

$$8) \quad \gamma_t = 69.3/1 = 69.3 \text{ pcf}$$

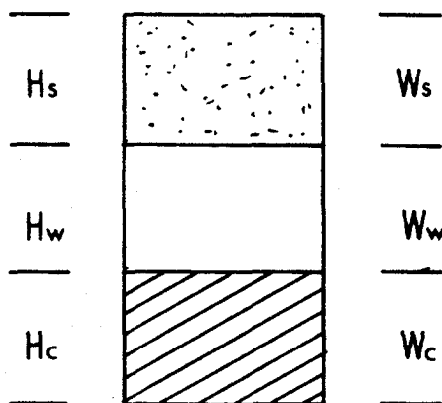
$$\gamma' = \gamma_t - \gamma_w = 69.3 - 62.4 = 6.90 \text{ pcf}$$

$$9) \quad \gamma' = S \gamma_w (G-1) / [S(1-G) + G] = \frac{(0.16)(62.4)(2.65 - 1)}{0.16(1-2.65)+2.65}$$

$$= 6.90 \text{ pcf}$$

Case B SCR = 2:1

Definition



$$W_s = (SCR)(W_c) = 2W_c$$

$$H_s + H_c + H_w = 1.0$$

$$S = W_c / (W_c + W_w) = 16\%$$

$$G (\text{clay}) = G (\text{sand})$$

$$1) \quad H_s = W_s / G \gamma_w, \quad H_c = W_c / G \gamma_w, \quad H_w = W_w / \gamma_w$$

$$2) \quad H_s = (W_c)(SCR) / G \gamma_w$$

$$3) \quad 1 = \frac{(W_c)(SCR) + \frac{W_c}{G\gamma_w} + \frac{W_w G}{\gamma_w G}}{G\gamma_w} = \frac{W_c(SCR) + W_c + GW_w}{G\gamma_w} = \frac{W_c(1+SCR) + GW_w}{G\gamma_w}$$

$$G\gamma_w - W_c(1+SCR) = GW_w$$

$$\therefore W_w = \frac{G\gamma_w - W_c(1+SCR)}{G}$$

$$4) \quad S = \frac{W_c}{(W_c + W_w)} = \frac{W_c}{\frac{W_c + G\gamma_w - W_c(1+SCR)}{G}} = \frac{W_c G}{W_c G + G\gamma_w - W_c - W_c(SCR)}$$

$$SW_c G + SG\gamma_w - SW_c - SW_c(SCR) = W_c G$$

$$W_c G - SW_c G + SW_c + SW_c(SCR) = SG\gamma_w$$

$$W_c = \frac{SG\gamma_w}{S(SCR+1-G) + G}$$

$$5) \quad W_s = W_c \times SCR = \frac{SG\gamma_w \times SCR}{S(SCR+1-G) + G}$$

$$6) \quad W_w = \frac{G\gamma_w - W_c(1+SCR)}{G}$$

$$7) \quad W_c = \frac{(0.16)(2.65)(62.4)}{(0.16)(2+1 - 2.65) + 2.65} = 9.78 \text{ lbs.}$$

$$H_c = 9.78/2.65 (62.4) = 0.059$$

$$W_s = W_c \times SCR = (9.78)(2) = 19.56 \text{ lbs}$$

$$H_s = 19.56/2.65(62.4) = 0.118$$

$$W_w = \frac{(2.65)(62.4) - 9.78(1+2)}{2.65} = 51.33 \text{ lbs}$$

$$H_w = 51.33/62.4 = 0.823$$

$$8) \quad \text{Total } W = W_c + W_s + W_w = 80.67 \text{ lbs}$$

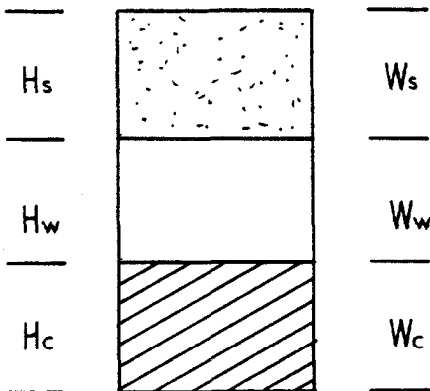
$$\text{Total } V = H_c + H_s + H_w = 1.00$$

$$\gamma_t = W/v = 80.67/1 = 80.67 \text{ pcf}$$

$$\gamma' = \gamma_z - \gamma_w = 80.67 - 62.4 = 18.27 \text{ pcf}$$

$$9) \quad \gamma' = \frac{S\gamma_w(SCR+1)(G-1)}{G(1-S) + S(1+SCR)} = \frac{(0.16)(62.4)(2+1)(2.65-1)}{2.65(1-0.16) + 0.16(1+2)} = 18.26 \text{ pcf}$$

Case C & D



Given:

$$H_s + H_w + H_c = 1$$

$$W_s = (SCR)(W_c) = 2 \times W_c$$

$$H_s = W_s/\gamma_s = W_s/100$$

$$\text{From Case B, } W_s = 19.56 \text{ lbs.}$$

$$S = W_c/(W_w + W_c) = 16\%$$

$$1) \quad H_s = W_s/\gamma_s, \quad H_c = W_c/G\gamma_w, \quad H_w = W_w/\gamma_w$$

$$2) \quad 1 = \frac{H_s + \frac{W_c}{G\gamma_w} + \frac{W_w}{\gamma_w}}{G\gamma_w} = \frac{H_s G\gamma_w + W_c + W_w G}{G\gamma_w}$$

$$G\gamma_w - H_s G\gamma_w - W_w G = W_c$$

$$W_c = G\gamma_w(1-H_s) - W_w G$$

$$3) \quad S = \frac{G\gamma_w(1-H_s) - W_w G + SW_w(1-G) + SG\gamma_w(1-H_s)}{W_w + G\gamma_w(1-H_s) - W_w G} = G\gamma_w(1-H_s) - W_w G$$

$$SW_w(1-G) + W_w G = G\gamma_w(1-H_s) - SG\gamma_w(1-H_s)$$

$$W_w = \frac{G\gamma_w(1-H_s)(1-S)}{S(1-G) + G}$$

$$4) \quad H_s = 19.56/100 = 0.196$$

$$W_w = \frac{(2.65)(62.4)(1-0.196)(1-0.16)}{0.16(1-2.65) + 2.65} = 46.81 \text{ lbs}$$

$$H_w = 46.81/62.4 = 0.750$$

$$5) \quad W_c = G\gamma_w(1-H_s) - W_w G$$

$$W_c = 2.65(62.4)(1-0.196) - 46.81(2.65) = 8.91 \text{ lbs}$$

$$H_c = 8.91/2.65 \cdot 62.4 = 0.054$$

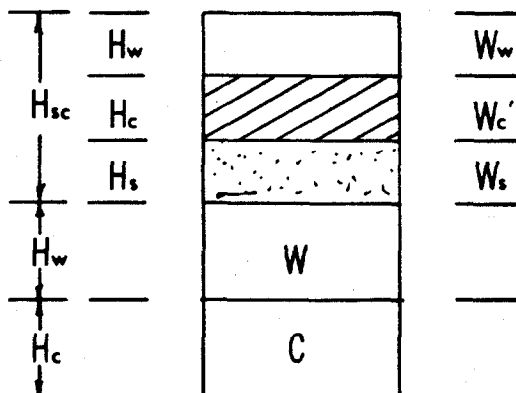
$$\text{Total } V = H_s + H_w + H_c = 0.999$$

$$6) \quad \text{clay } \gamma_t = (W_w + W_c)/(H_w + H_c)(46.81 + 8.91)/(0.750 + 0.054)$$

$$= 69.30 \text{ pcf}$$

$$\text{clay } \gamma' = \gamma_t - \gamma_w = 69.30 - 62.4 = 6.90 \text{ pcf}$$

Case E



Given:

$$H_{sc} + H_w + H_c = 1$$

$$\text{Cap SCR} = 3:1 = W_s/W_c$$

$$\text{From Case B } W_s \text{ in cap} = 19.56$$

$$S = W_c/(W_w + W_c) \text{ both cap \& underlying clay}$$

$$= 16\%$$

$$G(\text{clay}) = G(\text{sand})$$

$$1) \quad H_{SC} + H_W + H_C = 1$$

$$2) \quad H_{SC} = H_W + H_C + H_S, \quad H_W = W_W / \gamma_W, \quad H_S = W_S / \gamma_W G,$$

$$H_C = W_C' / \gamma_W G$$

$$W_S = (W_C') (SCRC)$$

$$S = W_C' / (W_W + W_C) \rightarrow SW_W' + SW_C' = W_C' \therefore W_W' = W_C' (1-S) / S$$

$$\begin{aligned} 3) \quad H_{SC} &= \frac{W_C' (1-S)}{S \gamma_W} + \frac{W_C'}{G \gamma_W} + \frac{W_C' (SCRC)}{G \gamma_W} \\ &= \frac{W_C' (1-S)(G) + W_C' S + W_C' (SCRC)(S)}{S G \gamma_W} \\ &= \frac{W_C' G - W_C' S G + W_C' S + W_C' SCRC(S)}{S G \gamma_W} \\ &= \frac{W_C' G (1-S) + W_C' S (1+SCRC)}{S G \gamma_W} \end{aligned}$$

$$4) \quad H_W + H_C = (1 - H_{SC})$$

$$\frac{W_W}{\gamma_W} + \frac{W_C}{G \gamma_W} = (1 - H_{SC}), \quad \text{From (2) } W_W = W_C (1-S) / S$$

$$\frac{W_C (1-S)}{S \gamma_W} + \frac{W_C}{G \gamma_W} = 1 - H_{SC} \rightarrow \frac{G W_C (1-S) + W_C S}{G S \gamma_W} = 1 - H_{SC}$$

5) Combining (3) and (4)

$$\frac{G W_C (1-S) + W_C S}{G S \gamma_W} = 1 - \frac{W_C' G (1-S) + W_C' S (1+SCRC)}{S G \gamma_W}$$

$$G W_C - S G W_C + W_C S = S G \gamma_W - W_C' G (1-S) - W_C' S (1+SCRC)$$

$$W_C [G(1-S) + S] = SG\gamma_W - W_C' [S(1+SCRC) + G(1-S)]$$

$$\therefore W_C = \frac{SG\gamma_W - W_C' [S(1+SCRC) + G(1-S)]}{G(1-S) + S}$$

6)  $W_C' = 19.56/3 = 6.52 \text{ lbs} \dots H_C' = 6.52/2.65(62.4) = 0.0394$

$$W_C = \frac{(0.16)(2.65)(62.4) - 6.52 [0.16(1+3)+2.65(1-.16)]}{2.65(1-.16)+0.16}$$

$$= 3.26 \text{ lbs}$$

$$\therefore H_C = 3.26/2.65(62.4) = .0197$$

$$W_W' = W_C' (1-S)/S = 6.52(1-.16)/.16 = 34.23 \text{ lbs}$$

$$H_W' = 34.23/62.4 = 0.5486$$

$$W_S' = 19.56 \quad \therefore H_S = 19.56/2.65(62.4) = 0.1183$$

$$W_W = W_C (1-S)/S = 3.26(1-.16)/.16 = 17.10$$

$$H_W = 17.10/62.4 = 0.2740$$

$$\Sigma H = .0394 + .5486 + .1183 + .0197 + .2740 = 1.0000$$

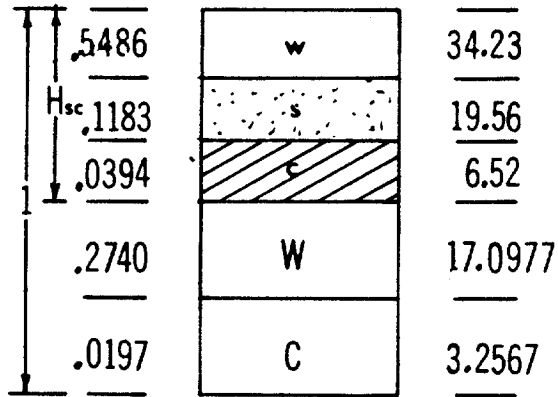
$$H_{SC} = 0.7063$$

7)  $\gamma' \text{ cap} = (6.52 + 34.23 + 19.56)/.7063 - \gamma_W$

$$= 85.39 - 62.4 = 22.99 \text{ pcf}$$

$$\gamma' \text{ clay from Case A} = 6.90 \text{ pcf}$$

Case E



Given:

$$H_{sc} + H_w + H_c = 1$$

$$\text{Cap SCR} = 3:1 = W_s/W_c$$

From Case B,

$$W_s \text{ in Cap} = 19.56 \text{ lbs}$$

$$S = W_c/(W_c + W_w) = 16\%$$

both cap & underlying clay

$$G(\text{clay}) = G(\text{sand}) = 2.65$$

$$1) \quad S = W_c'/(W_w + W_c), \therefore W_w = W_c'(1-S)/S$$

$$= 6.52(1-.16)/.16 = 34.23$$

$$2) \quad H_{sc} = \frac{W_c'G(1-S) + W_c'S(1+SCR)}{SG\gamma_w}$$

$$= \frac{6.52(2.65)(.84) + 6.52(.16)(4)}{(.16)(2.65)(62.4)}$$

$$= 0.7063 \text{ vs } .7063$$

$$3) \quad H_w + H_c = 1 - H_{sc} = 0.2937$$

$$\frac{W_c}{G\gamma_w} + \frac{W_w}{\gamma_w} = 0.2937 \quad W_w = W_c(1-S)/S$$

$$\frac{W_c}{G\gamma_w} + \frac{W_c(1-S)}{S\gamma_w} = 0.2937$$



$$W_C S + W_C G(1-S) = .2937 (SG\gamma_w)$$

$$W_C [S + G(1-S)] = .2937 (SG\gamma_w)$$

$$W_C = \frac{.2937(.16)(2.65)(62.4)}{.16 + 2.65 (.84)} = 3.2567$$

$$H_C = 3.2567/62.4 = .0197$$

$$4) \quad W_W = W_C(1-S)/S = 3.2567(.84)/.16 = 17.0977$$

$$H_W = 17.0977/62.4 = 0.2740$$

Since a comparison between Case B (s/c mix) and Case C' (submerged cap) reveals higher effective stresses at the surface for Case C' but lower at the bottom, one might ask, which case causes the greater settlement?

Assuming the following model describes the effective stress/void ratio relationship, calculate the total settlement

$$e = (1-S)G_s/S$$

$$\text{Let } A = 22, \text{ and } \beta = 0.2$$

In the case of a s/c mix:

$$\frac{\Delta e}{1+e_0} \frac{1}{H_0} \rightarrow \Delta H = H_0 \frac{\Delta e}{1+e_0} \quad \text{or} \quad \Delta H = \int_{H_i}^{H_f} \frac{\Delta e}{1+e_0} dz$$

$$\text{If } \Delta e = e_0 - e_f \text{ and } e_f = A\bar{\sigma}^{-\beta} \text{ then } \Delta e = e_0 - A\bar{\sigma}^{-\beta}$$

Since  $\bar{\sigma} = \gamma'z$ , then  $\Delta e = e_0 - A(\gamma'z)^{-\beta}$

$$\text{Finally, } \Delta H = \int_{H_i}^{H_f} \frac{e_0 - A(\gamma'z)^{-\beta}}{1+e_0} dz = \frac{1}{1+e_0} \int_{H_i}^{H_f} e_0 - A(\gamma'z)^{-\beta} dz$$

$$\begin{aligned} \Delta H &= \frac{1}{1+e_0} \left[ e_0 z - \frac{A\gamma'^{-\beta} z^{1-\beta}}{1-\beta} \right]_{H_i}^{H_f} \\ &= \frac{1}{1+e_0} \left( e_0(H_f - H_i) - \frac{A\gamma'^{-\beta}}{1-\beta} [H_f^{1-\beta} - H_i^{1-\beta}] \right) \end{aligned}$$

In the case of the sand cap, we can treat the sand cap as a surcharge, and

$$\bar{\sigma} = q + \gamma' z_c, \text{ where } q = \gamma'_s z_s \text{ and } z_c = \text{depth of clay } (H - z_s)$$

then,  $\Delta e = e_0 - A(q + \gamma' z_c)^{-\beta}$  and

$$\Delta H = \frac{1}{1+e_0} \int_{z_i}^{z_c} e_0 - A(q + \gamma' z)^{-\beta} dz$$

Remembering that  $\int (ax+b)^n dx = \frac{1}{a(n+1)} (ax+b)^{n+1}$ ,  $n \neq -1$ , then

$$\begin{aligned} \Delta H &= \frac{1}{1+e_0} \int_{z_i}^{z_c} e_0 dz - \frac{A}{1+e_0} \int_{z_i}^{z_c} (\gamma' z + q)^{-\beta} dz \\ &= \frac{1}{1+e_0} [e_0 z]_{z_i}^{z_c} - \frac{A}{1+e_0} \left[ \frac{(\gamma' z + q)^{1-\beta}}{\gamma'(1-\beta)} \right]_{z_i}^{z_c} \end{aligned}$$

$$\Delta H = \frac{1}{1+e_0} [e_0(z_c - z_i)] - \frac{A}{\gamma'(1-\beta)(1+e_0)} \times$$

$$[(\gamma' z_c + q)^{1-\beta} - (\gamma' z_i + q)^{1-\beta}]$$

## Calculations of Consolidation Magnitudes

From the previous equation we can calculate the consolidation magnitude for s/c mix and capped waste ponds as presented in Table C-2. These calculations are based upon the assumption that the constitutive relationship  $e = A \bar{\sigma}^{-\beta}$  is the same for s/c mix and waste clay. For Cases C and D the sand surcharge,  $q$ , is incompressible, while for Case E, the s/c mix cap compressibility is calculated. The use of the constitutive equation  $e = A \bar{\sigma}^{-\beta}$  implies an effective stress exists for all void ratios, although the effective stress at the pond top is zero. Accordingly a fictitious initial pond height,  $H_i$ , is used by determining the effective stress,  $\bar{\sigma}$ , corresponding to  $e_0$  and dividing by the buoyant unit weight of that void ratio.

Case A Homogeneous 10 ft. deep clay pond  $S_o = 16\%$   $G = 2.65$

Since  $e = A \bar{\sigma}^{-\beta}$ , then  $\bar{\sigma} = (e/A)^{1/\beta} = (13.91/22)^{1/0.2}$

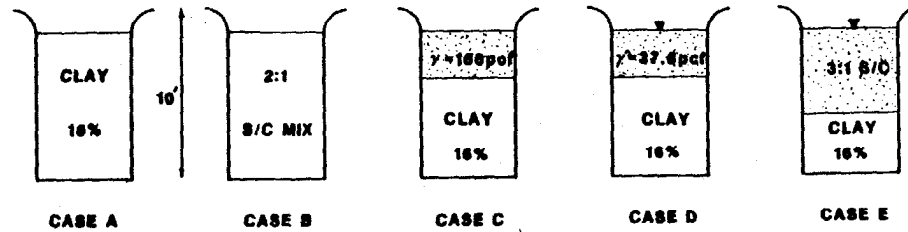
$= 9.89$  psf. Thus  $H_i = \bar{\sigma}/\gamma' = 9.89/6.9 = 1.433$  ft and

$H_f = H_i + D_c = 1.433 + 10 = 11.433$  ft. Accordingly

$$\Delta H = \frac{1}{1+e_0} \left( e_0 (H_f - H_i) - \frac{A \gamma'^{-\beta}}{(1-\beta)} [H_f^\beta - H_i^\beta] \right)$$

$$= \frac{1}{1+13.91} \left( 13.91(11.433-1.433) - \frac{22(6.9)^{-0.2}}{(1-0.2)} [11.433^{0.8} - 1.433^{0.8}] \right) = 2.20 \text{ ft}$$

Table C-2  
Calculation of Consolidation Magnitudes for S/C Mix and Capped Waste Ponds



Case	Description	Initial Void Ratio, $e_0$ (a)	Unit Wt. clay, $\gamma'_C$ pcf (b)	Unit Wt. cap, $\gamma'$ pcf (c)	Depth of clay, $D_C$ (ft)	Initial Ht. $H_i$ (ft) (d)	Final Ht. $H_f$ (ft)	Surcharge $q$ psf	Consolidation $\Delta H$ (ft)
A	Homogeneous clay $S_o = 16\%$ , $G = 2.65$	13.91	6.90	-	10.0	1.433	11.433	-	2.20
B	2:1 S/C	4.63	18.26	-	10.0	131.7	141.7	-	0.05
B	2:1 S/C sand removed	13.91	18.26	-	8.82	0.542	9.362	-	2.68
B	2:1 S/C $e_t$ used	4.63	18.26	-	10.0	0.546	10.546	-	2.80
C	Sand Cap	13.91	6.90	100	8.04	1.433	9.473	196.0	3.51
D	Sand Cap (submerged)	13.91	6.90	37.6	8.04	1.433	9.473	73.7	2.87
E	Clay under S/C cap	13.91	6.90	22.99	2.94	1.433	4.37	162.3	1.21
E	3:1 S/C cap	3.48	-	22.99	7.06 (e)	440.8	447.86	-	0.013
E	3:1 S/C sand removed	13.91	-	22.99	5.88 (e)	0.43	6.31	-	2.09
E	3:1 S/C $e_t$ used	3.48	-	22.99	7.06 (e)	0.43	7.49	-	1.80

(a)  $e = (1-S)G/S$  (b)  $\gamma' = S\gamma_w(G-1)/[S(1-G)+G]$  (c)  $\gamma' = S\gamma_w(SCR+1)(G-1)/[G(1-S)+S(1+SCR)]$

(d)  $H_i = \bar{\sigma}/\gamma'$   $\bar{\sigma} = (e_0/A)**1/B$ ,  $A = 22$ ,  $B = -0.2$  (e) S/C cap only

Final pond height = 10 - 2.20 = 7.80 ft. A computer analysis using Somogyi (1979) also calculated a final pond height = 7.80 ft, thus verifying the procedure.

Case B 2:1 S/C Mix  $S_c = 16\%$   $D_p = 10$  ft

For a s/c mix  $e_{total} = e_c / (1 + SCR)$ , thus  $e_t = 13.91 / (1 + 2) = 4.63$ .

Since  $\bar{\sigma} = (e/A)^{**} 1/B$ , then  $\bar{\sigma} = (4.63/22)^{**} - 1/.2 = 2404.8$  psf and

$H_i = 2404.8 / 18.26 = 131.7$  ft thus  $H_f = D_p + H_i = 10 + 131.7 = 141.7$  ft.

Accordingly

$$\Delta H = \frac{1}{1+4.63} \left( 4.63(141.7-131.7) - \frac{22(18.26)^{-2} [141.7^{0.8} - 131.7^{0.8}]}{1-0.2} \right)$$

$$= 0.049 \text{ ft.}$$

Final pond height = 10 - 0.049 = 9.95 ft.

Although the  $\Delta H = 0.049$  ft calculated above is quite correct, an alternate calculation assumes only the clay is compressible and the sand merely increases the buoyant unit weight,  $\gamma'$ . Thus instead of a 10' deep pond, a pond consisting of 8.82 ft. of clay and water having a  $\gamma' = 18.26$  pcf is considered and,

$$\bar{\sigma} = (13.91/22)^{**} - 1/.2 = 9.89 \text{ psf and } H_i = 9.89 / 18.26 = 0.542 \text{ ft.}$$

Thus  $H_f = 0.542 + 8.82 = 9.362$  ft. and;

$$\Delta H = \frac{1}{13.91+1} \left[ 13.91(9.362-0.542) - \frac{22(18.26)^{-2} (9.362^{0.8} - 0.542^{0.8})}{(1-0.2)} \right] = 2.68 \text{ ft}$$

The height of sand involved is 1.18 ft; hence the final pond height = 8.82-2.68+1.18 = 7.31 ft.

Lastly the procedure used by Somogyi (1979) redefines the constitutive relationship in terms of the total void ratio, i.e.,

$$e_t = e_c / (1+SCR). \quad \text{Thus} \quad e_t = \frac{A \bar{\sigma}^{-\beta}}{1+SCR} \quad \text{and} \quad \bar{\sigma} = \frac{[e_t(1+SCR)]^{** -1/\beta}}{A}$$

Hence, 
$$\bar{\sigma} = \frac{[4.63(1+2)]^{**(-1/0.2)}}{22} = 9.97 \text{ psf and } H_i = 9.97/18.26$$

$$= 0.546. \quad \text{Thus } H_f = H_i + D_p = 0.546+10 = 10.546 \text{ and}$$

$$\Delta H = \frac{1}{4.63+1} \left( 4.63(10.546-0.546) - \frac{22(18.26)^{-0.2}}{(1+2)(1-0.2)} \right) \times [10.546^{0.8} - 0.546^{0.8}] = 2.80 \text{ ft}$$

Therefore the final pond height = 10.0 - 2.80 = 7.20 ft, which was calculated using Smogyi's (1979) program.

### Case C Sand Cap

Since  $S_0 = 16\%$  of the underlying clays, then from Case A,  $e_0 = 13.91$ ,  $z_i = 1.433$  ft. However, since the sand cap for a 10' deep pond is 1.96 ft thick (Table (10)) then  $z_c = z_i + D_c = 1.433 + 8.04 = 9.473$  ft, and  $q = 196.0$  psf.

$$\Delta H = \frac{1}{1+e_0} \left[ e_0(z_c - z_i) \right] - \frac{A}{\gamma'(1-\beta)(1+e_0)} \times [(\gamma'z_c + q)^{1-\beta} - (\gamma'z_i + q)^{1-\beta}]$$

$$= \frac{1}{1+13.91} [13.91(9.473-1.433)] - \frac{22}{(6.9)(1-0.2)(1+13.91)}$$

$$[(6.9)(9.473) + 196.0]^{0.8} - [(6.9)(1.433) + 196.0]^{0.8} = 3.51 \text{ ft}$$

therefore the final pond height is  $8.04 - 3.51 + 1.96 = 6.49 \text{ ft}$ .

#### Case D - Submerged Sand Cap

Since Case D is identical to Case C with the exception that the sand cap has become submerged and thus  $q = 73.7 \text{ psf}$ , then:

$$\Delta H = \frac{1}{1+13.91} [13.91(9.473-1.433)] - \frac{22}{(6.9)(1-0.2)(1+13.91)}$$

$$[(6.9)(9.473)+73.7]^{1-0.2} - [(6.9)(1.433)+73.7]^{1-0.2} = 2.87$$

Therefore the final pond height is  $8.04-2.87+1.96 = 7.13 \text{ ft}$ .

#### Case E S/C Mix Cap 3:1

For Case E, we must consider the  $\Delta H$  of the s/c mix cap plus the  $\Delta H$  of the underlying clay, with account taken of the surcharge,  $q$ , imposed by the s/c mix cap on the clay. Likewise as in Case B, several alternatives are available for estimating  $e_0$  and  $H_i$  of the s/c mix.

For a s/c mix  $e_t = e_c/(1+SCR)$ , thus  $e_t = (13.91)/(1+3) = 3.48$ .  
 Since  $\bar{\sigma} = (e/A)**1/\beta$ , then  $\bar{\sigma} = (3.48/22)**(-1/0.2) = 10,134 \text{ psf}$ , and  $H_i = 10,134/22.99 = 440.8 \text{ ft}$ . thus  $H_f = H_i + D_{\text{cap}} = 440.6 + 7.06 = 447.86 \text{ ft}$   
 (see Table 11) accordingly,

$$\Delta H = \frac{1}{1+3.48} [3.48(447.86-440.8) - \frac{22(22.99)^{-0.2}}{(1-0.2)}]$$

$$[447.86^{0.8} - 440.8^{0.8}]$$

$$= 0.013 \text{ ft}$$

If we consider that only the clay is compressible and the sand merely occupies volume, then the 7.06 ft s/c mix cap consists of 0.39 ft of clay, 5.49 ft of water and 1.18 ft of sand, with a buoyant unit weight  $\gamma'$  of 22.99 pcf. Since the clay present in the s/c mix is at 16% solids, then  $\bar{\sigma} = (13.91/22)**(-1/0.2) = 9.89$  psf and  $H_i = 9.89/22.99$

$$= 0.43 \text{ ft and } H_f = 0.43 + 0.39 + 5.49 = 6.31 \text{ ft}$$

$$\begin{aligned} \text{thus } \Delta H &= \frac{1}{1+13.91} \left[ 13.91(6.31-0.43) - \frac{(22)(22.99)^{-0.2}}{(1-0.2)} \right. \\ &\quad \left. (6.31^{0.8} - 0.43^{0.8}) \right] \\ &= 2.09 \text{ ft} \end{aligned}$$

the final cap height will be  $6.31 - 2.09 + 1.18 = 5.40$  ft.

Alternatively, by considering the effective stress/void ratio relationship in terms of total void ratio, then

$$\bar{\sigma} = \frac{(e_t(1+SCR))^{**1/8}}{A} = \frac{(3.48(1+3))^{**(-1/.2)}}{22} = 9.89 \text{ psf.}$$

Thus  $H_i = 9.89/22.99 = 0.43$  ft, and  $H_f$  of the cap =  $0.43 + 7.06 = 7.49$  ft.

$$\begin{aligned} \text{Then } \Delta H &= \frac{1}{1+e_0} \left[ e_0(H_f - H_i) - \frac{A\gamma'^{-B}}{(1+SCR)(1-B)} (H_f^{1-B} - H_i^{1-B}) \right] \\ &= \frac{1}{1+3.48} \left[ 3.48(7.49-0.43) - \frac{22(22.99)^{-0.2}}{(1+3)(0.8)} (7.49^{0.8} - 0.43^{0.8}) \right] \\ &= 1.80 \text{ ft.} \end{aligned}$$

The final cap height will be  $7.06 - 1.80 = 5.26$  ft.

The clay underlying the s/c mix cap will be 2.94 ft thick at 16% solids content; thus  $\bar{\sigma} = (13.91/22)**(-1/.2) = 9.89$  psf and



$z_i = 9.89/6.90 = 1.433$  ft. The value for  $z_c$  will be  $1.433+2.94 = 4.37$  ft, with a 162.3 surcharge.

Accordingly,

$$\Delta H = \frac{1}{1+e_0} (e_0(z_c - z_i)) - \frac{A}{\gamma'(1-\beta)(1+e_0)} \times [(\gamma'z_c + q)^{1-\beta} - (\gamma'z_i + q)^{1-\beta}]$$

$$= \frac{1}{1+13.91} (13.91(4.37-1.43)) - \frac{22}{(6.9)(1-0.2)(1+13.91)} [(6.9(4.37)+162.3)^{0.8} - ((6.9)(1.43)+162.3)^{0.8}] = 1.21 \text{ ft.}$$

The final clay height will be  $2.94-1.21 = 1.73$  ft.

In summation, the final height of the pond will depend upon which  $\Delta H$  is selected for representing the s/c mix. Because the methods using the 3:1 s/c but with the sand removed or the 3:1 s/c  $e_t$  used are in close agreement,  $\Delta H$  s/c mix = 1.80 for the  $e_t = \frac{A}{(1+SCR)} \sigma^{-\beta}$  relationship is selected as being representative. Thus the final pond height will be  $\Delta H$  s/c mix = 1.80 +  $\Delta H$  clay = 1.21 = 3.01 ft; then the final pond height is 6.99 ft.